Rapid Isolation of Faults in Power Networks with Distributed Generators

by

Nuwan Perera

A Thesis

Submitted to the Faculty of Graduate Studies

In Partial Fulfillment of the Requirements

For the Degree of

Master of Science

The Department of Electrical and Computer Engineering

The University of Manitoba

Winnipeg, Manitoba, Canada

Rapid Isolation of Faults in Power Networks with Distributed Generators

BY

Nuwan Perera

A Thesis/Practicum submitted to the Faculty of Graduate Studies of The University of Manitoba in partial fulfillment of the requirement of the degree

Master of Science

To my loving parents

Acknowledgements

I would like to express my sincere thanks to Dr. Athula D. Rajapakse for his continuous advice, guidance and encouragement throughout the course of this work. I consider myself privileged to have had the opportunity to work under his guidance. I thank the members of my thesis examination committee, Prof. Aniruddha Gole and Dr. Nipon Rattanawangcharoen, for graciously accepting to review my thesis.

The financial support received from Manitoba Hydro, National Science and Engineering Research Council, Province of Manitoba in the form of Graduate Scholarship and Manitoba HVDC Research Centre is greatly appreciated. I must also express my gratitude to Mr. Todd E. Buchholzer of Manitoba Hydro for acting as the liaison officer and project consultant.

I would like to thank the staff and all of my friends in the Department of Electrical and Computer Engineering for their continuous encouragement and for making my years at the University of Manitoba a pleasant experience.

This acknowledgement will not be complete without thanking my family. I extend my heartfelt gratitude to my wife and parents. They were always understanding and encouraged me during my hard times. I would like to also thank my brother for all the love and support.

Nuwan Perera

May 2007

Summary

There are a number of technical issues that arise with increased penetration of Distributed Generation (DG) into distribution grids. Among them, foremost are the problems related to protection. With the interconnection of DG, distribution network protection systems may encounter situations which were unforeseen when they were originally designed and therefore fail to provide the required safety for the public, workers and equipment. Current DG operating practices overcomes these problems by disconnecting of all distributed generators when a fault occurs in the distribution network. This practice, though satisfies most of the safety related concerns, foregoes the opportunity for improving the power supply reliability using DG.

This thesis proposes an agent based protection scheme for distribution networks with distributed generators. The distribution network is divided into several network segments. The relay agents which are located at boundaries of these segments can determine the direction of fault currents using the transients, generated by the fault. Fault directions determined by the relay agents located at different points of the network are combined to determine the faulted segment. A fault direction identification technique which uses wavelet coefficient of the measured line currents was developed for relay agents. These relay agents are also capable of making the decisions based on the local information when they are unable to communicate with each other. A Decision Tree based transient classification scheme is proposed to distinguish the fault disturbances from non-fault disturbances which occur in the system. The operation of the proposed protection scheme was validated through extensive simulations.

List of Symbols

f_s	Sampling frequency
r	Correlation of coefficient
I_a	Current in Phase-A
I_b	Current in Phase-B
I_c	Current in Phase-C
I_α	Ground Clarke component
I_β	Alpha Clarke component
I_γ	Beta Clarke component
R_f	Fault Impendence
$H(n)$	High pass filter
$L(n)$	Low pass filter
$H'(n)$	Dual high pass filter
$L'(n)$	Dual low pass filter
nB	Calculation cycle
nX	Length of the input signal
l	Level
A	Approximation Wavelet Coefficients
D	Detail Wavelet Coefficients
EA	Approximation Wavelet Energy
ED	Detail Wavelet Energy

Acronyms

DG	Distributed Generation
DR	Distributed Resources
CHP	Combined Heat and Power
DER	Distributed Energy Resources
DP	Dispersed Power
EG	Embedded Generation
DA	Distribution Automation
MV	Medium Voltage
HV	High Voltage
FFT	Fast Fourier Transform
WFT	Windowed Fourier Transform
FIR	Finite Impulse Response
DWT	Discrete Wavelet Transform
WTC	Wavelet Transform Coefficients
CTs	Current Transformers
ROCOF	Rate of Change of Frequency
VVS	Voltage Vector Surge
PCC	Point of Common Coupling
EPS	Electrical Power System
DSP	Digital Signal Processors
CB	Circuit Breakers
ANNs	Artificial Neural Networks
DTW	Dynamic Time Warping
HIF	High Impedance Fault
EMTDC	Electromagnetic Transients including DC

Table of Contents

List of Figures

List of Tables

Chapter 1

Introduction

1.1 Background

The world's electricity demand is increasing rapidly. Distributed generation (DG) is projected to play a significant role in satisfying this increasing demand. The term Distributed Generation is referred to small scale power generation. DG is also refereed to as Distributed Resources (DR), Distributed Energy Resources (DER), Dispersed Power (DP) or Embedded Generation (EG). The portfolio of DG technologies includes reciprocating engines, micro-turbines, combustion gas turbines, fuel cells, photo-voltaic, small hydro turbines and wind turbines. Distributed Generators (DGs) are interconnected to the grid at substation,distribution feeder or customer load level. Grid interconnection of DG may be direct or inverter based. Technologies such as fuel cells and photo-voltaic use inverter based interconnection and turbine powered ac machines use direct interconnection. DC generators are sometimes used in DG. They also need inverter based interconnection[1].

There is a number of benefits associated with DG. When Renewable Energy Resources (RER) are used, DG can reduce the emissions due to power generation. DG is generally located near the loads. This results in reduced transmission and distribution losses. DG can improve the voltage profile along the distribution lines and increase the power quality[2]. DG can delay or eliminate the development of central power stations and transmission facilities. DG can potentially help to maintain the system stability and provide spinning reserve[3][4]. Due to those environmental and economical benefits DG is becoming popular all over the world.

1.2 Problem Definition

Although DG provides such benefits, interconnection of DG to distribution network results in several technical issues. The most problematic issue is related to network protection. This arises mainly due to the fact that the interconnection of DGs has not been taken into account when the protection system is initially designed. Traditionally, distribution networks have a radial structure and are protected using co-ordinated fuses and reclosers. The coordination between fuses and reclosers can change when DG is interconnected to the distribution grid depending on the size, type and location of distributed generators. This may lead to incorrect operation of protection, compromising the safety for the public, workers and equipment[1][2][3].

The other main protection issue related to DG is islanding, that is the operation of one or several generators isolated from the main grid. Islanding may results in abnormal variations in the system frequency and voltage, and may lead to form an ungrounded network that can be hazardous for equipment, users and maintenance crews. Thus current DG interconnection standard specify various requirements to prevent DGs from operating in islanded mode. Satisfaction of some interconnection criterion[5] results in isolation of DGs even for faults that happen in remote locations.Thus these practices, which are introduced to ensure safety, essentially restrict the potential of DGs to improve the power supply reliability.

1.3 Motivation Behind the Research

Disconnection of DGs for remote faults is a waste of the potential of DGs to improve the supply reliability. If the faulty segments in a network can be rapidly identified and isolated, disconnection of DGs for remote faults can be avoided. Further, if islanded operation of a single or group of DGs is enabled when safe, supply to the loads that are connected to the sections unaffected by the fault can be continued. A load shedding algorithm can be used to balance the load and generation in the island if necessary.

Such measures, which are often referred to as the intentional islanded operation, will enable the full utilization of the potential of DGs to improve the supply reliability. Researchers have attempted to address this issue using various protection strategies [7][8][9][10]. However further research is required to develop practical and cost effective protection solutions.

1.4 Objective of the Research

The overall objective of this research is to develop a protection solution for distribution networks with distributed generators. The protection scheme must ideally be able to locate and isolate faulty network segments without depending on the structure of the network and the present of DGs, and ultimately facilitate intentional islanded operation. The protection scheme should be economical to implement at distribution and sub-transmission levels.

This thesis proposes a current transients based protection scheme to identify and isolate the faulty segments in distribution network with distributed generators. It is also proposed to implement the protection scheme using co-operative relay agents located on strategic points of the network.The increased computational power of microprocessors and the availability of affordable, realizable and reliable telecommunication makes such a scheme practically realizable using today's technology.

The overall research goal is proposed to achieve by fulfilling the following specific objectives:

1. Development of a fault direction identification technique using transient currents originating from the fault. The technique proposed uses wavelet coefficients of transient currents for this purpose.

2. Development of an algorithm to utilize the fault direction information determined

in the first objective to locate and isolate a fault with minimum disruption to the network.

3. Development of transient classification scheme to differentiate non-faulty transients from faulty transients.

4. Testing and verification of the developed algorithm through time domain simulation of test networks. This thesis utilizes PSCAD/EMTDC for all simulations.

1.5 Thesis Overview

This chapter gives a basic introduction to the thesis, motivation behind the research and objective of the research.

Chapter 2 gives a literature survey on protection of networks with distributed generation. This includes introduction to distributed generation, protection of distribution networks, protection issues related to distributed generation and overview to the distributed generator interconnection standards. Furthermore this chapter describes recent research work related to protection of distribution networks with distributed generators and future trend towards distributed generation protection and control.

Analysis of transients in three-phase systems is presented in Chapter 3. This includes the basic concepts behind this thesis; use of Clarke components for analyzing three phase currents and transient analysis using wavelets. Furthermore, this chapter includes implementation of online discrete wavelet transformation in PSCAD/EMTDC environment.

Chapter 4 presents the proposed agent based protection scheme for locating the faults in power networks with distributed generators. This scheme uses fault directions identified using wavelet coefficients of current transients to determine the fault location. Further, this chapter includes the implementation of the software model of the relay algorithm to determine the fault directions, locate the fault and generate necessary trip signals to isolate the faulted segment.

The modified relay algorithm proposed to improve the reliability is presented in Chapter

5. This includes a fault transient classification scheme used to distinguish the fault transits from other non-fault transients such as capacitor switching and load switching and, power frequency phaser current based decision making technique during communication failures.

Chapter 6 includes simulations carried out to verify the applicability of proposed relay algorithms. Two test systems, a Medium Voltage (MV) distribution network and a High Voltage (HV) transmission network were simulated in PSCAD/EMTDC. The performance of the agent based relay algorithm was investigated for both radial and mesh network configurations using MV test distribution network. HV transmission network was used to investigate applicability of the proposed protection scheme in transmission systems. The investigations carried out to determine the effects of Current Transformer (CT) saturation and fault inception angle are also presented in this chapter.

Finally, in Chapter 7 conclusions and suggestions for further researches are given.

Appendix A includes implementation of wavelet transform using Mallat algorithm, wavelet filter coefficients and comparison of wavelet transformation results obtained using wavelet tool developed in PSCAD/EMTDC and wavelet toolbox in MATLAB.

The relay algorithms developed in MATLAB are presented in Appendix B.

Chapter 2

Protection of Networks with Distributed Generators

2.1 Introduction

The main purpose of a power system protection scheme is to ensure the safe operation of the system with guarantied public, worker and equipment safety. Protection is the most problematic issue related to distributed generation [1]. The coordination in existing protection system may be altered with the interconnection of DGs resulting in mal-operation of protection equipments in the system. Network topology can be radial, ring or mesh. Depending on the nature of the network topology, the required protection scheme may change. Radial systems are the simplest and the most common form of distribution network configuration. They are usually protected using a time graded over current protection scheme. The ring and mesh network protection is more complicated, and usually such systems are protected using directional overcurrent relays.

2.2 Protection Issues with Distributed Generators

Most distribution systems are initially designed as passive networks without DGs. Thus the protection system design based on the initial system criterions such as short circuit levels, power flow directions, nominal load currents etc will turn out to be unsuitable with the interconnection of DGs [11]. The main protection issues related to DG are briefly discussed below.

2.2.1 Change of Short Circuit Levels

The short circuit level is one of the main parameters used in protection design[1]. Specifically, the selection of the suitable current transformers (CTs) and coordination between overcurrent relays depend on this parameter. Short circuit level is characterized by the equivalent system impedance at the fault point and the performance of rotating machinery connected to the network. With the connection of DG, the equivalent network impedance can decrease due to parallel circuits, resulting in an increase in fault level. Thus in case of a fault, there could be unexpectedly high fault currents which may lead to mal-functioning of measuring and protection equipment, for example due to CT saturation. Furthermore, these high fault currents put system equipment such as transformers at a risk since they were not originally designed to operate under this circumstances.

2.2.2 Reverse Power Flow

Depending on the nature of the network configuration, power flows in distribution lines can be unidirectional or bidirectional.(ie. Power flows in radial network are unidirectional where as in mesh networks they are bidirectional). Protection schemes are initially designed based on these power flows. When a DG is connected, the power flows may be reversed[12]. This results in mal-operation of the protection equipment. Sometimes reverse power flow can affect the operation of phase shifting transformers in the system[13].

2.2.3 Lack of Sustained Fault Current

The DG can be an induction generator, small scale synchronous generator or power electronic interface. Induction generators cannot supply sustained fault currents to three phase faults and have limited contribution to asymmetrical faults. Small synchronous generators are usually not able to supply sustained fault currents significantly greater than the rated current. Power electronic interface devices cannot withstand significant overcurrent for sustained periods therefore power electronic control and protection are designed to limit the inverter overcurrent. This limited fault current makes it difficult for protection relays to detect fault currents and thereby compromising the ability of protecting the network from DG fault currents[2].

2.2.4 Islanding and Anti-islanding Protection

Islanding is the situation where a part of the utility network is disconnected from the main grid and operate as a independent system. Islanding results in abnormal variations in frequency and voltage in the power island. Operation of an auto reclosure during a fault in a network with DG may also lead to the formation of two independent systems operating at two different frequencies[1]. Reclosing of the auto reclosure switch would results in an out of phase fault situation[3]. Further, islanded operation may create an ungrounded system depending on the transformer connection. Also an unidentified island would be a hazard for repair crews. Due to the above reasons, islanding is recognized as a hazardous situation and immediate disconnection of the DG is recommended upon formation of an island[5].

There are several methods used to detect the islands. They are categorized into three groups; active methods, passive methods and telecommunication based methods. The passive detection method makes decisions based on measured quantities whereas in the active detection method disturbances are injected into the supply system and detect islanding conditions based on system responses[2]. The communication-based methods use telecommunication means to alert and trip DGs when islands are formed. Their performance is independent of the type of distributed generators involved.

Under/over voltage, under/over frequency, rate of change of frequency (ROCOF) and voltage vector surge (VVS) relays are the most widely used methods to detect the islands. Possibility of nuisance tripping for system disturbances is the main disadvantage of those methods. The transfer trip scheme, which is a telecommunication based method, is very reliable if the necessary infrastructure is available.

2.2.5 Grounding of Interface Transformers

This is a common issue encountered in interconnection of synchronous generating units[1] to any power system. If the interconnection transformer used is grounded delta-wye transformer, earth faults on the utility line can cause parallel ground currents (from the fault to the utility transformer and the generator transformer). Thus this should be considered in ground fault coordination when there is a DG connected to distribution network.

2.3 DG Interconnection Standards

In order to address the protection and safety issues, several DG interconnection standards/guidelines have been introduced. Some examples are IEEE Std. 1547-2003, "IEEE Standards for Interconnecting Distributed Recourses (DR) with Electric Power Systems 2003"[5] and Micro-Power Connect, "Interconnection Guideline for Inverter-controlled Micro-Distributed Resources Connected to 600 V or less distributed Systems 2003" [6]. Most major utilities have adopted IEEE Std. 1547-2003 in formulating guidelines/rules for interconnecting DG to their networks. A brief description of the salient features of IEEE Std. 1547-2003 is given below.

IEEE Std. 1547-2003 recommends disconnection of distributed generators when the voltage and/or frequency at the point of interconnection deviate from their base values due to faults and other disturbances (see Tables.2.1and 2.2).

Table 2.1: Interconnection system response to abnormal voltages

Voltage range	Clearing time(s)
$V < 0.5$	0.16
$0.5 \leq V < 0.88$	2.00
$1.1 \leq V < 1.2$	1.00
$V \geq 1.2$	0.16

Table 2.2: Interconnection system response to abnormal frequencies

DR size	Frequency range(Hz)	Clearing time(s)
≤30kW	>60.5	0.16
	<59.3	0.16
>30kW	>60.5	0.16
	<59.8-57.0(adjustable set point)	adjustable 0.16 to 300
	<57	0.16

Power quality is an another issue addressed in IEEE Std. 1547-2003. The dc injection is defined as one of the main factors that has an effect on poor power quality. Thus the DG and its interconnection system would not be allowed to inject a dc current greater than 0.5 percent of the full rated output current at the point of DG connection. When the DG is serving balanced linear loads, harmonic current injection into the area Electrical Power System (EPS) at the Point of Common Coupling (PCC) is not allowed to exceed the limits stated below in Table.2.3. The Area EPS is the electrical power system that serves the local power system which include DG. PCC is the point where local power system is connected to area EPS.The harmonic current injections will be exclusive of any harmonic currents due to harmonic voltage distortion present in the Area EPS without the DG connected.

Table 2.3: Maximum harmonic current distortion in percent of current $(I)^a$

harmonic order [b]	$h < 11$	$11 \leq h < 17$	$17 \leq h < 23$	$23 \leq h < 35$	$35 \leq h$	THD
Percent	4.0	2.0	1.5	0.6	0.3	5.0

[a] I = the greater of the Local EPS maximum load current integrated demand (15 or 30 minutes) without the DR unit, or the DR unit rated current capacity (transformed to the PCC when a transformer exists between the DR unit and the PCC).

[b] Even harmonics are limited to 25 percent of the odd harmonic limits above

For an unintentional island in which the DG energizes a portion of the Area EPS through the PCC, the DG interconnection system must detect the island and cease to energize the Area EPS within two seconds of the formation of an island. At distribution level, fluctuation in system voltages and frequencies are more common due to frequent load switching, capacitor switching and faults. Since DGs are connected at MV or LV level, satisfaction of above mentions criterion results in unavoidable, more frequent and unwanted disconnection of DGs. This will reduce the system reliability. Further frequent interruptions can be observed at load levels. This leads to poor power quality at load level and thereby reduces customer satisfaction.

2.4 Recent Research on Protection of Networks with DGs

Researchers have attempted to address the shortcomings in current DG interconnection practices and protection problems associated with distributed networks due to DGs. Several protection schemes have been proposed in literature. They are summarized below.

2.4.1 Microprocessor-Based Reclosing

A microprocessor-based reclosing scheme to coordinate fuses and reclosers in a system with high penetration of DG is proposed in [8]. This scheme adjusts recloser settings based on the fault level changers in the system due to interconnection of DG. This method uses a data base of worst condition fault level values determined at different locations of the network with and without DG. Based on the predetermined fault level values, a user can define the coordination curves that would coordinate in the presence of DG . However this scheme always needs to know whether the DG is connected to the system or not before adjusting the recloser settings, thus requires a telecommunication facilities. According to [8]this method is only feasible for radial network configuration. When there are many DGs connected to the network, fault level analysis and protection coordination will become complicated.

2.4.2 Adaptive Overcurrent Protection

Adaptive overcurrent protection for distribution feeders with inverter interconnected DGs is proposed in [7]. In this technique, minimum pickup of an overcurrent relay is updated based on a fault analysis of the system to compensate the reduction of the reach of the overcurrent relay due to interconnection of DG. Fault analysis is complicated for unbalanced networks with high penetration of DGs. This type of protection coordination is generally difficult to apply for mesh network configurations. Overcurrent relays need to know whether the DG is connected to the system or not in order to adjust the relay settings. Therefore it requires a telecommunication system in place to convey the DG connection status to relays.

2.4.3 Protection Using Synchronized Phasor Measurements

In this scheme, distribution system is divided into several zones by breakers capable of rapidly disconnecting the links between the zones[9]. The protection scheme relies on a centralized relay, which communicates with breakers and distributed generators. The central relay is capable of storing and handling a large amount of data and uses synchronized current vector measurements from the main source, distributed generators and breakers to identify the faulty section. This protection scheme uses a data base of results obtained from off line load flow analysis and short circuit analysis. The main drawback of this system is its heavy dependence on the centralized processing system and communication links. Use of synchronized current phasor measurements at all breaker and DG locations may be expensive. Further it requires to repeat the load flow and short circuit analysis at each time when there is a change in load or DG.

2.4.4 Decentralized Transient Based Protection Using Multi-Agents

This is an agent based protection scheme capable of locating faults and shedding loads in a system with DG [10]. These relay agents use spectral energies of post fault current and voltage measurements calculated using wavelet transformation to detect and locate the faults. The fault detection algorithm uses an artificial neural network based technique and is claimed to be capable of detecting even the high impedance faults. Fault location is achieved through fuzzy cluster analysis of spectral energies. This system uses distributed information processing and the relay agents make decisions cooperatively. Agent based protection systems consist of distributed equipment combined with a communication network to cooperate in the realization of adaptive protection functions. The agents can also be provided with the capability of acting autonomously when the communication channels fail.

2.5 Future Trend Towards Distribution Generation

Researchers have made different predictions about future distributed generation market. According to EPRI estimation, DG market could amount to 2.5 to 5 GW/year by 2010[14]. Research by Distributed Power Coalition of America (DPCA) has predicted that distributed power has the potential to capture up to 20 percent of all new generating capacity, or 35 GW, over the next two decades[15]. In Canada, NRCan targets 20 percent of all new generating capacity to be met with DG by 2025 [16]. The magazine " Smart Grids, European Technology Platform" published by European Commission has shown, how active management changes the current highly centralized power systems with low penetration of DG to an integrated secure network combining central generation and DG in future[17].

Widespread automation of distribution systems, which is known as Distribution Automation(DA), is a very favorable development with respect to DG. Infrastructure of DA systems can be used to implement DG protection and control. Features such as remote monitoring, supervisory control, decision support tools, etc. would facilitate to perform advanced control and protection functions in distribution networks with DGs. DA for systems with DGs can perform in four levels; DG level, substation level, feeder level and the customer level.

Digital Signal Processors (DSPs) are microprocessors specifically designed to handle Digital Signal Processing tasks. DSPs have seen tremendous growth in the last decade and widely used in many applications from cellular phones to advanced scientific instrument. [19]. DSP based digital relays play major role in power system protection. In the past, application of microprocessor based relays are limited to generator level and transmission level protection relays mainly due to high cost. However now, with the development of advanced technologies implementation of DSP based relays has become economical for distribution level applications. Thus the implementation of DSP based advanced protection algorithms for systems with DGs is very much feasible.

Furthermore use of communication enables the implementation of advanced protection applications that can overcome the difficulties identified in system with DGs. Communication methods typically used for transmission line applications such as power-line carrier, microwave and optical fiber are not always suitable for distribution applications. By nature, distribution lines are different from transmission lines: they are generally shorter and have more tapped loads. The cost of communication systems is a major concern. Some of the cost effective communication options available for distribution level applications include spread-spectrum radio, phone lines, fiber- optic cables, and copper pilot wires [20].

2.6 Chapter Summary

A literature survey was carried out to investigate the protection issues related to DGs and the following conclusions were made.

1. The issues related to distribution networks protection and the current DG interconnection practices have undermine some of the advantages of DG. Availability of a reliable and realizable protection solutions would eliminate most of these limitations.

2. The amount of research in this area is limited. There are few methods proposed in literature to address some of the protection related issues. But, there is a long way to go before these systems can be practically implemented. Thus there is a clear need for further research in this area.

3. Due to rapid increase in use of DGs for power generation, requirement of reliable protection schemes are more and more demanding. Development of powerful microprocessors and wider development of distribution automation systems, specially, the associated communication infrastructure, have enabled the capability of developing advanced protection algorithms.

Chapter 3

Analysis of Transients in Three Phase Networks

3.1 Introduction

The objective of this chapter is to provide a background for the techniques/methods that will be used later in this thesis.

Almost all power transmission and primary distribution systems are three-phase systems. In three-phase systems, faults of many different configurations involving only one phase, two phases and all three phases can occur. In order to handle all possible types of faults, currents (or voltages) of all three phases must be analyzed. However, the amount of processing can be reduced by transforming three phase quantities into Clarke components as will be shown in the next section.

High frequency content superimposed on power frequency signals can be detected using several different techniques. In this thesis, wavelet transform is used for this purpose. A brief introduction to wavelet transform and implementation of wavelet transform on a power system simulator is presented in Section 3.3.

3.2 Observation of Fault Transients in Clarke Components

The modal transformation resolves three-phase signals in a coupled network into three uncoupled modal components, namely the *ground mode*, *aerial mode-1* and *aerial mode-2* components. For non transposed multi-phase systems, an eigen vector based frequency dependent transformation matrix is required to convert the quantities from phase domain to modal domain. For balanced and ideally transposed lines, a frequency independent, real transformation matrix such as Clarke [24] matrix, Wedepohl matrix[25] or Karrenbauer[26] matrix can be used. Although the practical distribution systems do not satisfy the above conditions, a frequency independent real transformation matrix can be used to obtain somewhat decoupled signals, that can be advantageous in the transient based fault location.

For example, when the Clarke transformation is used, the relationship between the Clarke components and the phase components is given by:

$$\begin{pmatrix} I_0 \\ I_\alpha \\ I_\beta \end{pmatrix} = \frac{1}{3} \begin{pmatrix} 1 & 1 & 1 \\ 2 & -1 & -1 \\ 0 & \sqrt{3} & -\sqrt{3} \end{pmatrix} \begin{pmatrix} I_a \\ I_b \\ I_c \end{pmatrix} \tag{3.1}$$

where I_a, I_b and I_c are the phase currents and I_0, I_α and I_β are the respective Clarke components. Transients in the phase currents are well reflected in the Clarke components.

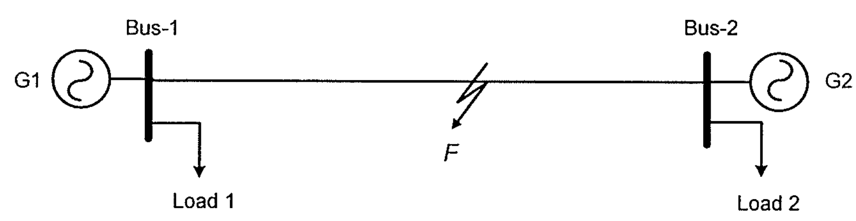

Figure 3.1: Test system

In order to understand the advantage of using Clarke components, consider the following examples, which uses Clarke transformation matrix to illustrate how the transients occurred in phase currents during faults are reflected in the Clarke components. The system shown

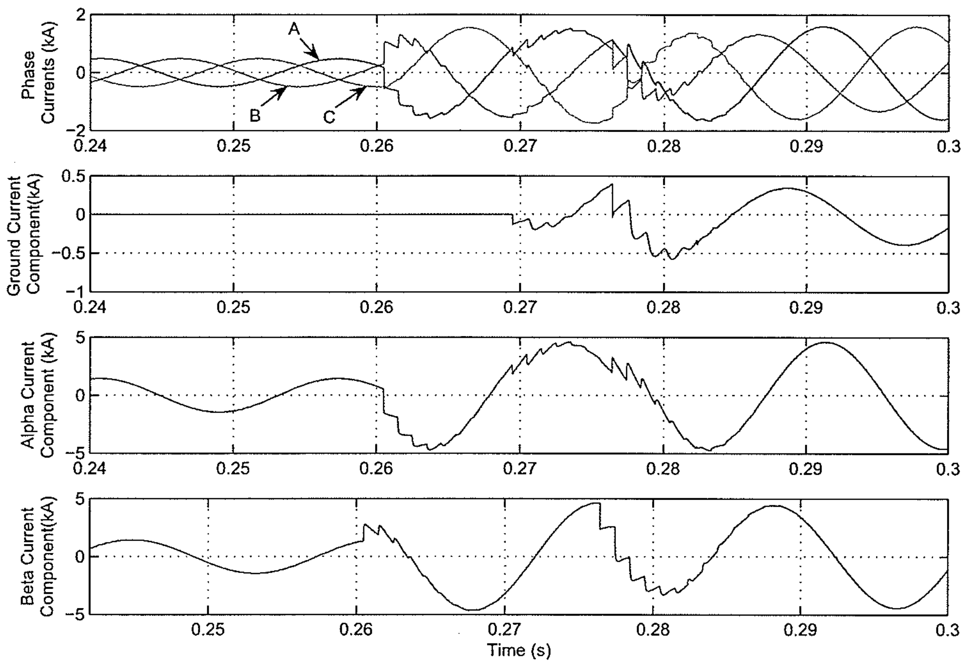

Figure 3.2: Three-phase current waveforms and corresponding Clarke components for ABC-G Fault

in Fig. 3.1 was simulated in PSCAD/EMTDC. Transients during different types of ground and ungrounded faults were recorded.

Figures 3.2 and 3.3 show the phase currents and the corresponding Clarke components obtained for a three-phase grounded fault and a three-phase ungrounded fault respectively. During these faults, all three phase currents are affected and those changes are reflected in both α and β components. In fact, the two α and β components obtained for both cases are almost identical. However, the ground component in three-phase grounded fault is significantly larger than those obtained for three phase ungrounded fault.

Figure 3.4 shows the phase and Clarke components for phase A to ground fault. Here only the phase A current is affected. The ground component and α component are significantly affected due to the fault. Figure 3.5 shows the situation for a line-to-line fault between phases A and B. Only the phase A and B currents are affected by the fault. For this fault both α and β components show significant changes. But when a similar fault

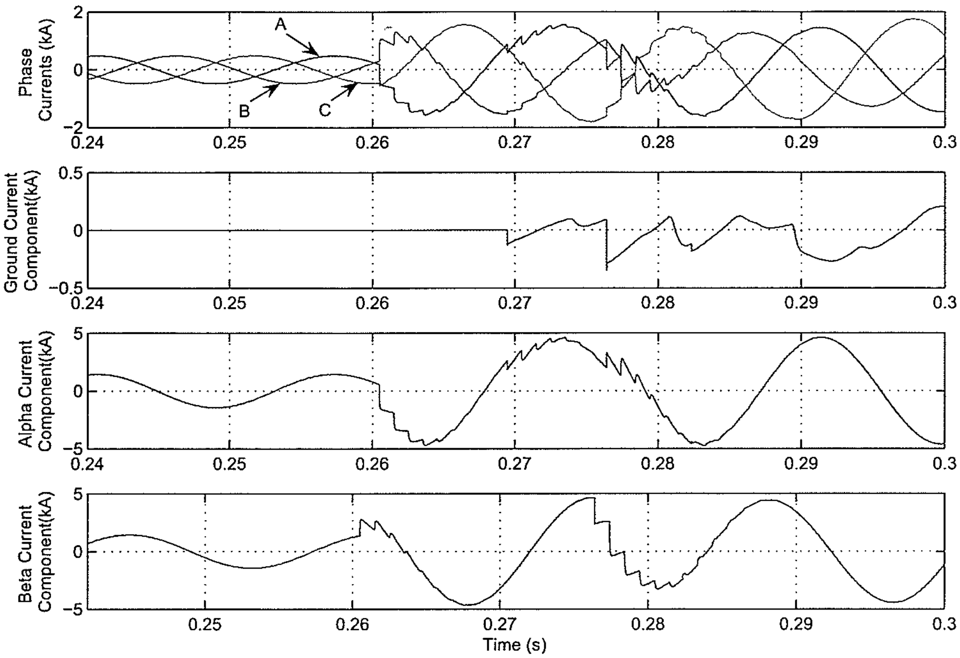

Figure 3.3: Three-phase current waveforms and corresponding Clarke components for ABC fault

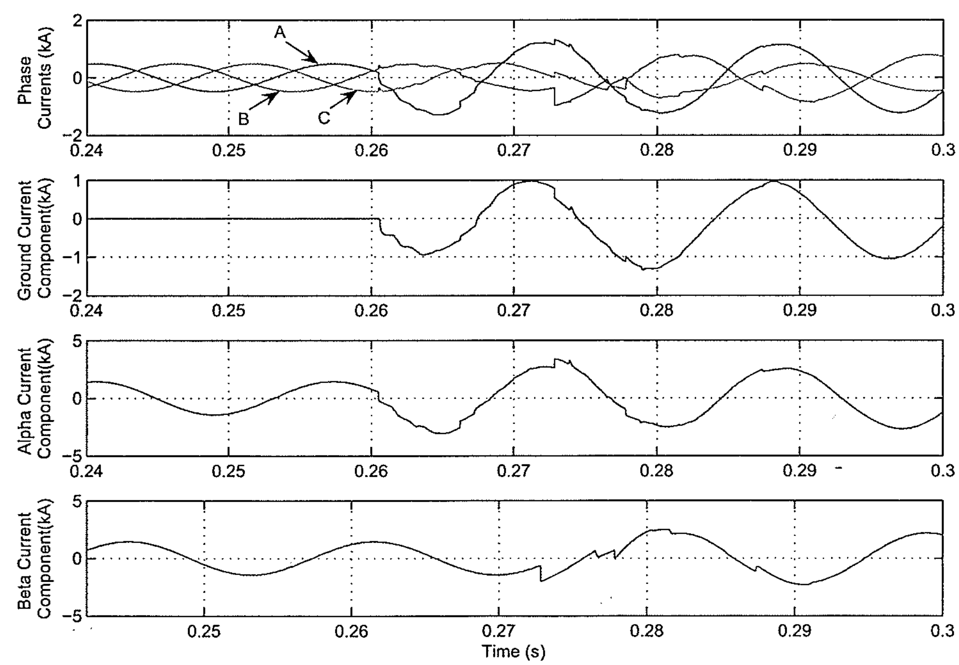

Figure 3.4: Three-phase current waveforms and corresponding Clarke components for phase A-G fault

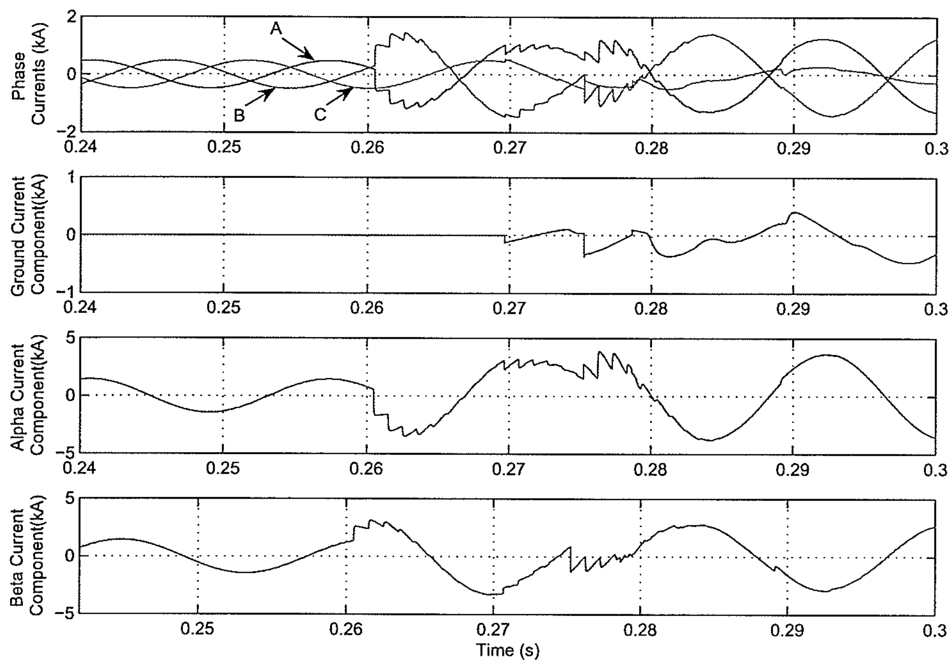

Figure 3.5: Three Phase Current Waveforms and corresponding Clarke components for phase A-B Fault

occurs between phases B and C as shown in Fig. 3.6, significant change is observed in β component.

Analysis of all possible types of faults in three-phase system (A-G, B-G, C-G, A-B, B-C, C-A, AB-G, BC-G, CA-G, ABC and ABC-G) yields following conclusions.

1. For all types of faults except for faults between phases B and C, the transient changes in phase currents are well reflected in α component.

2. For all types of faults, except for phase A-G fault, transient changes in the phase currents are well reflected in β component.

3. Ground component is significantly affected only by the faults that involve ground.

The above conclusions can also be arrived theoretically using the transformation matrix. Therefore, by analyzing α component, all types of faults, except phase B to phase C faults,

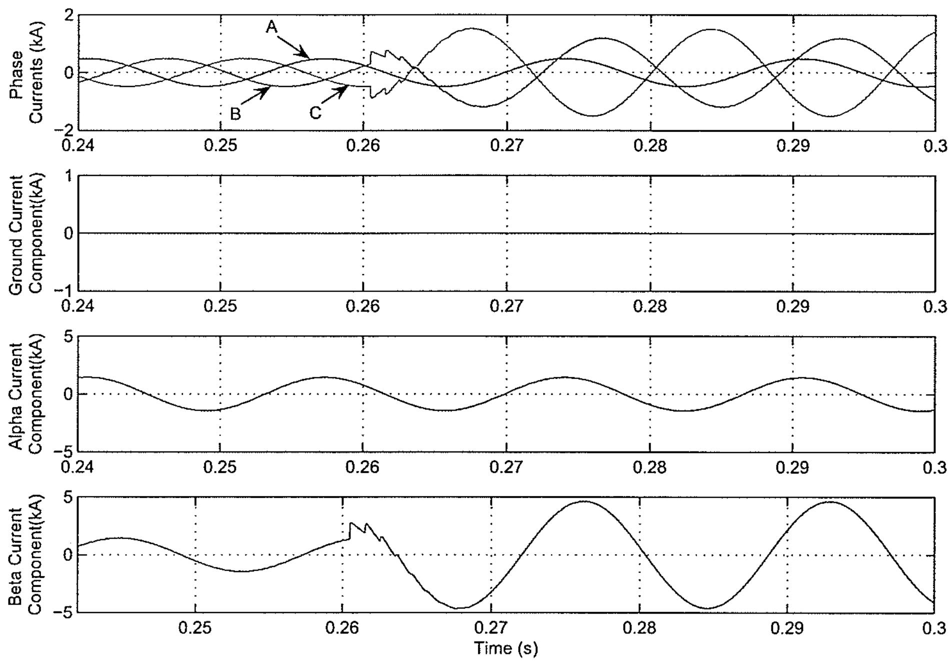

Figure 3.6: Three-phase current waveforms and corresponding Clarke components for phase B-C Fault

can be detected. This is more convenient than analyzing all three phase currents. In order to take the special case of phase B to phase C faults the β component can be used. In addition, if necessary, ground component can be used to distinguish ground faults from the others.

3.3 Transient Analysis Using Wavelets

The Fourier transform is a tool widely used in many engineering applications, but it is suited only to the study of stationary signals where all frequencies have an infinite coherence time. The Fourier analysis brings only global information which is not sufficient to detect compact patterns. On the other hand, the wavelet transform decomposes a signal into basis functions that are localized in scale as well as in time. Thus they are ideally suitable to analyze compact patterns in the time domain [21]. Fast electromagnetic transients which are typically non-periodic and contain both high frequency oscillations and localized impulses can be easily analyzed using wavelet transform. Thus it has become a powerful tool in power disturbances analysis, specially in power quality related applications and protection relaying[22]. Due to its favorable features, this thesis uses wavelet transform technique to analyze transient due to faults. As a background, a brief introduction to wavelet transformation is given below.

3.3.1 Wavelet Transform

The wavelet transformations can be Continuous Wavelet Transformation (CWT) or Discrete Wavelet Transformation (DWT). If *f(t)* is a signal with a finite energy, its CWT is defined as,

$$CWT_{\Psi} f(a,b) = \int_{-\infty}^{\infty} f(t)\Psi^{*}_{a,b}(t)dt \tag{3.2}$$

where

$$\Psi_{a,b}(t) = |a|^{-1/2}\Psi(\frac{t-b}{a}) \tag{3.3}$$

The function $\Psi(t)$ is the basis function or the mother wavelet, the asterisk denote a complex conjugate, and a ($\neq 0, \in R$) is the scale parameter and b ($\in R$) is the translation parameter. The mother wavelet function must satisfy several conditions: it should be short and oscillatory, i.e. it must have zero average and decay quickly at both ends. Several examples of wavelets are shown in Fig. 3.7. Some other popular mother wavelets include

Symlets, *Coeiflets*, etc.

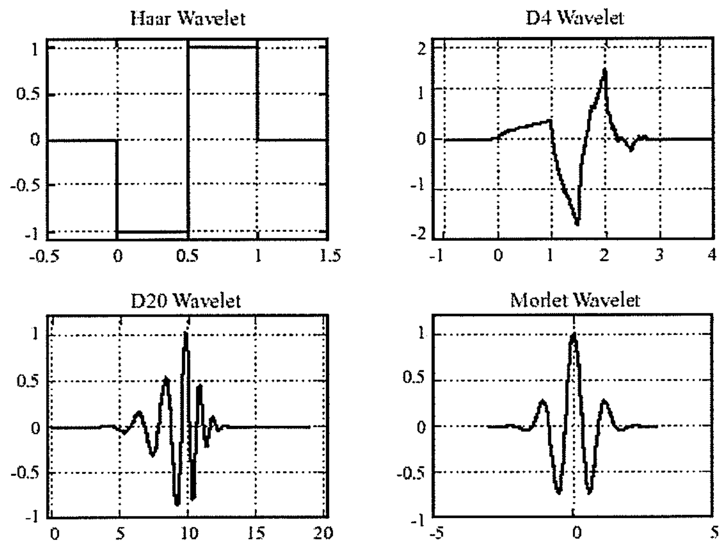

Figure 3.7: Examples of mother wavelets

In discrete wavelet transformation, the mother wavelet is dilated and translated discretely by selecting,

$$a = a_o^m ; b = nb_o a_o^m \tag{3.4}$$

where a_o (>1) and b_o (>0) are fixed real values and m and n are positive integers. Then the discretized mother wavelet becomes,

$$\Psi_{m,n}(t) = \frac{1}{\sqrt{a_o^m}} \Psi(\frac{t - b_o a_o^m}{a_o^m}) \tag{3.5}$$

The corresponding discrete wavelet transformation is given by,

$$DWT_{\Psi} f(m,n) = \sum_k f(k) \Psi_{m,n}^*(k) \tag{3.6}$$

DWT provides a decomposition of a signal into sub bands with a bandwidth that increases linearly with frequency. In the case of dyadic transform corresponding to $a_o = 2$ and $b_o = 1$, the result is geometric scaling, i.e. 1, $\frac{1}{a}$, $\frac{1}{a^2}$ ..... and translation by 0, n, $2n$,

..... This scaling gives the DWT logarithmic frequency coverage in contrast to the uniform frequency coverage of Windowed Fourier Transform (WFT) as illustrated in Fig. 3.8. Here, DWT uses long time intervals for low-frequency information, and short time intervals for high-frequency information whereas, WFT uses constant time intervals for all frequencies.

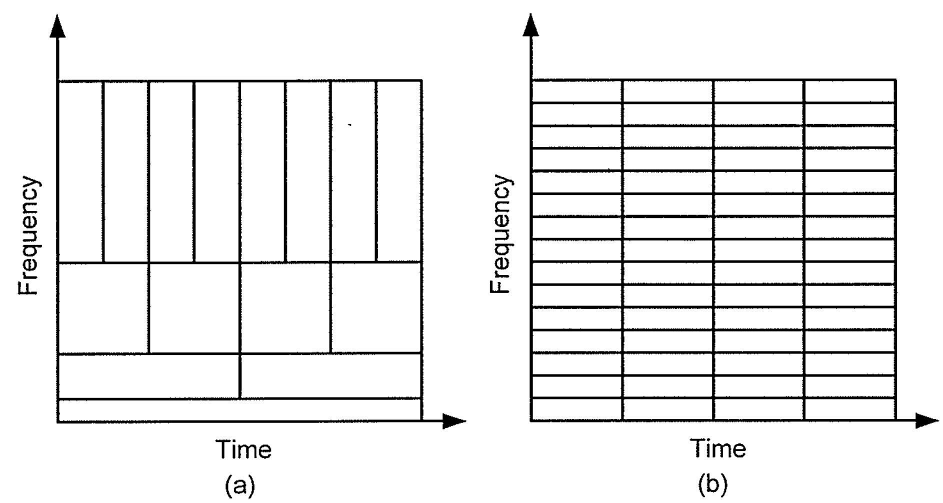

Figure 3.8: Frequency coverage of (a) Discrete Wavelet Transform (b) Windowed Fourier Transformation

DWT can be implemented efficiently as a filter bank as shown in Fig. 3.9. This implementation is commonly known as Mallat tree algorithm and consists of series of low-pass filters and their dual high pass filters. H(n) denotes a high pass filter and L(n) is its dual low pass filter. The filter coefficients are determined by the type of mother wavelet selected. The circle with downward arrow behind 2 denotes down sampling by a factor of 2. The outputs d1, d2, d3, etc. are called the detail coefficients while the output from the last low pass filter is referred to as the approximation coefficient.

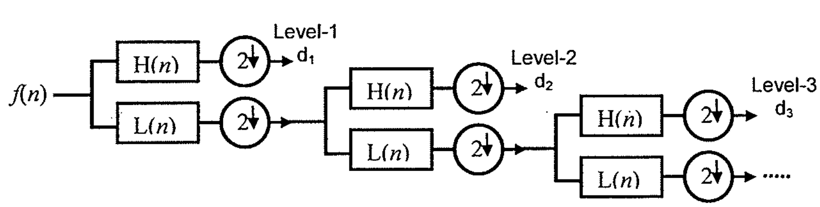

Figure 3.9: Mallat tree algorithm for decomposition.

It is possible to obtain the original signal *f(t)* through wavelet series reconstruction. The reconstruction can also be carried out efficiently using a tree algorithm as shown in Fig. 3.10. The filters H'(n) and L'(n) are the inverse filters of H(n) and L(n) respectively. In Fig. 3.10, the circles with upward arrow behind 2 denotes up sampling by a factor of 2.

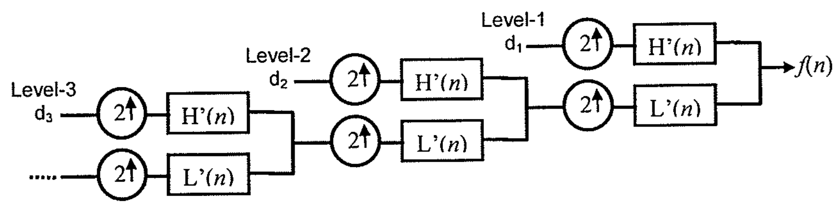

Figure 3.10: Mallat tree algorithm for reconstruction

Detailed description of the procedure used for computation of wavelet coefficients is given in Appendix A.

3.3.2 Wavelet Coefficients Reconstruction

The reconstruction algorithm can be used to provide the wavelet coefficients of different scales in a finer time resolution. Figure 3.11 illustrates how the decomposition and reconstruction filter banks can be combined to obtain so called reconstruction wavelet coefficients: the detail coefficients D1(n), D2(n), D3(n) and approximation coefficient A3(n). The original signal x(n) can now be easily reconstructed simply by adding the reconstruction wavelet coefficients. Note that all these coefficients now have the same sampling rate as the original signal.

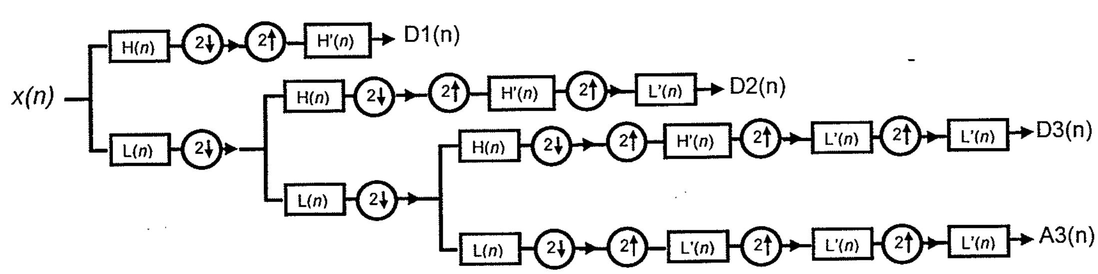

Figure 3.11: Algorithm for obtaining wavelet coefficients in finer resolution - example shows three levels.

3.3.3 Online Discrete Wavelet Transform

DWT can be performed off-line or on-line. Off-line DWT is the method used for studies carried out using stored signals such as power disturbances recorded in power quality recorders. But this is not suitable for applications such as protection relaying, which need to know what is happening in real time and take necessary measures based on that. Thus such applications need to perform DWT on-line. In on-line DWT, how frequently the calculations should be repeated depends on the number of levels of wavelet coefficients required. According to the Mallat algorithm previously explained, the calculation frequency holds the following relationship to the number of levels.

$$nB = 2^l \tag{3.7}$$

where nB is the number of samples after which the calculation is repeated and l is the number of levels.

Thus, calculations are repeated after every nB number of samples and yields the reconstruction wavelet coefficients with the same number of samples. However, in order to obtain this nB number of points , the algorithm needs a signal vector longer than nB (for some cases much longer that nB). The length of the signal vector (sample window) required for the calculation,nX, depends on the type of mother wavelet and the level of detail required. Therefore, a signal vector of sufficient length (which should be updated at each sampling step) needs to be kept in a buffer. Table 3.1 gives the minimum number of samples required for different types of mother wavelets at different levels considered.

The online calculations for Coeiflets-1 mother wavelet at level 1 can be illustrated as shown in Fig. 3.12. Length of the signal vector(nX) required can be determined from Table 3.1 as 10 samples. According to Eq.3.7 calculations are repeated (nB) after each 2 samples.

Table 3.1: Window length (nX) required for different mother wavelets at different levels

Level	Haar	Db2/sym2	Db4/sym4	Db8/sym8	Coif1	Coif2
1	2	6	14	30	10	22
2	4	14	34	74	24	54
3	8	30	74	162	52	118
4	16	62	154	338	108	246
5	32	126	314	690	220	502
6	64	254	634	1394	444	1114

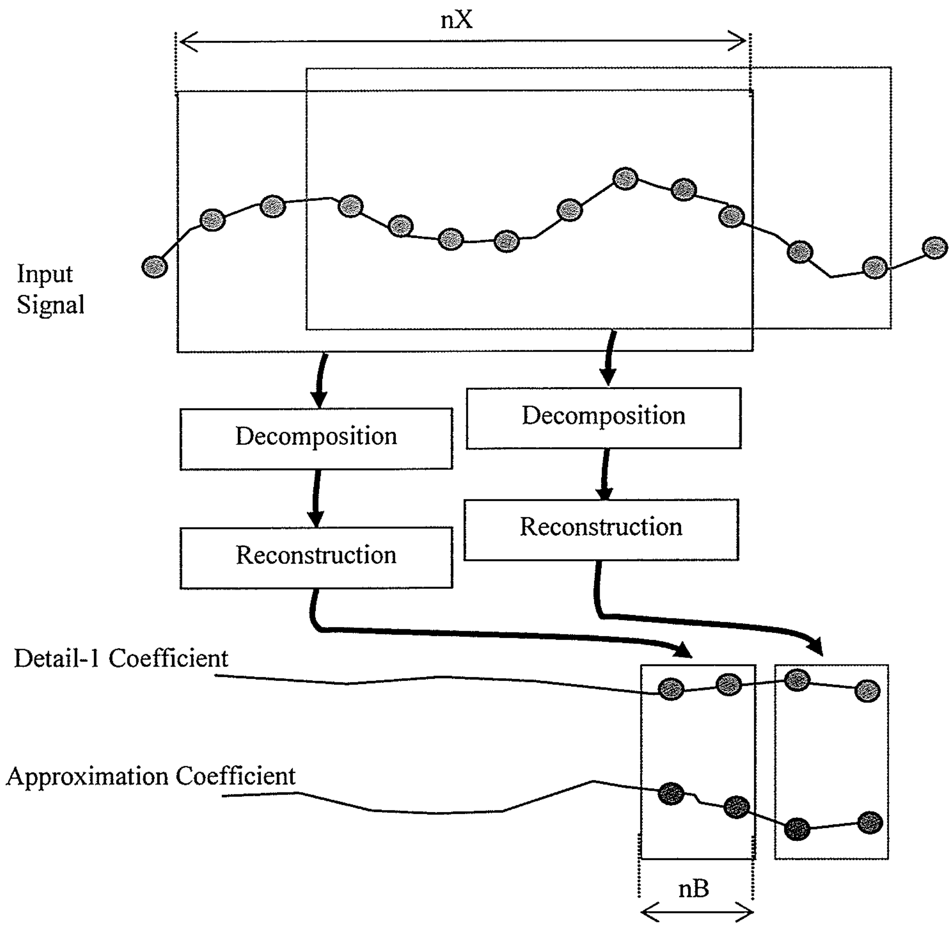

Figure 3.12: Online wavelet transform

3.4 Development of Online DWT in PSCAD/EMTDC Environment

As mentioned in Chapter 1, protection algorithm developed in this thesis will be tested using time domain simulations carried out in PSCAD/EMTDC. In order to simulate algorithms that use wavelet transformation, it is necessary to have a mean for performing wavelet transformation on the signals being generated from the simulation. Since PSCAD/EMTDC software package does not have wavelet transformation as a standard feature, it was necessary to implement online wavelet transformation tool in the PSCAD/EMTDC simulation environment. Although computer programs such as MATLAB has wavelet tool, and can be linked with PSCAD, that is not convenient as it significantly slows down the simulation speed. Therefore it was decided to implement new wavelet transform tool for PSCAD/EMTDC.

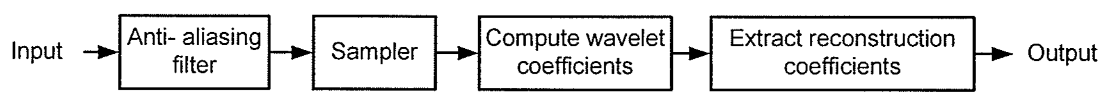

Figure 3.13: Discrete wavelet transformation

Figure 3.13 shows the basic block diagram for DWT tool implemented in PSCAD/EMTDC environment. The input signal is passed through an anti-aliasing filter before sampling. Sampled signals and corresponding reconstruction coefficients are computed using Mallat tree algorithm.

3.4.1 User Interface

Figure 3.14 DWT component developed in PSCAD/ EMTDC environment. The outputs are the reconstruction wavelet coefficients. The output A is the approximation, which is the low frequency content of the input signal component and the multi dimensional output D gives the details or the high frequency components of the input signal at various levels (up to level 6). This component can perform the wavelet transformation for different types of mother wavelets. Fig. 3.15 shows the user interface of the wavelet transform component.

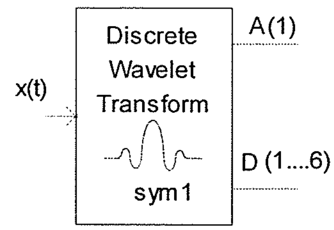

Figure 3.14: Discrete wavelet transform

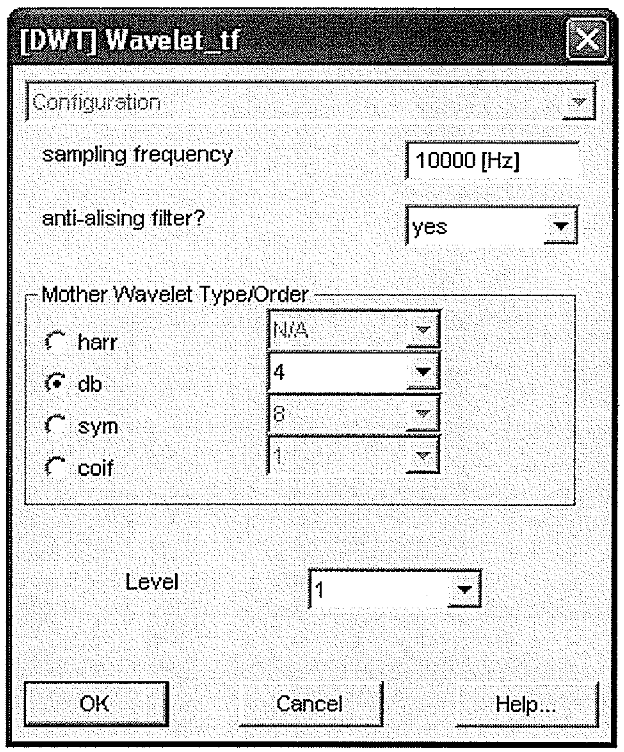

Figure 3.15: Discrete wavelet transform interface

User can specify the sampling frequency as required by the application. An anti-aliasing filter is available to filter out high frequency noise. The anti-aliasing filter can be enabled or disabled. This tool includes most popular families of mother wavelets: Harr, Daubechies(db), Symlets (sym),Coeiflets(coif). The user can chose the type of the mother wavelet interested. Further, the number of detail levels can also be set according to the requirement.

3.4.2 Validation

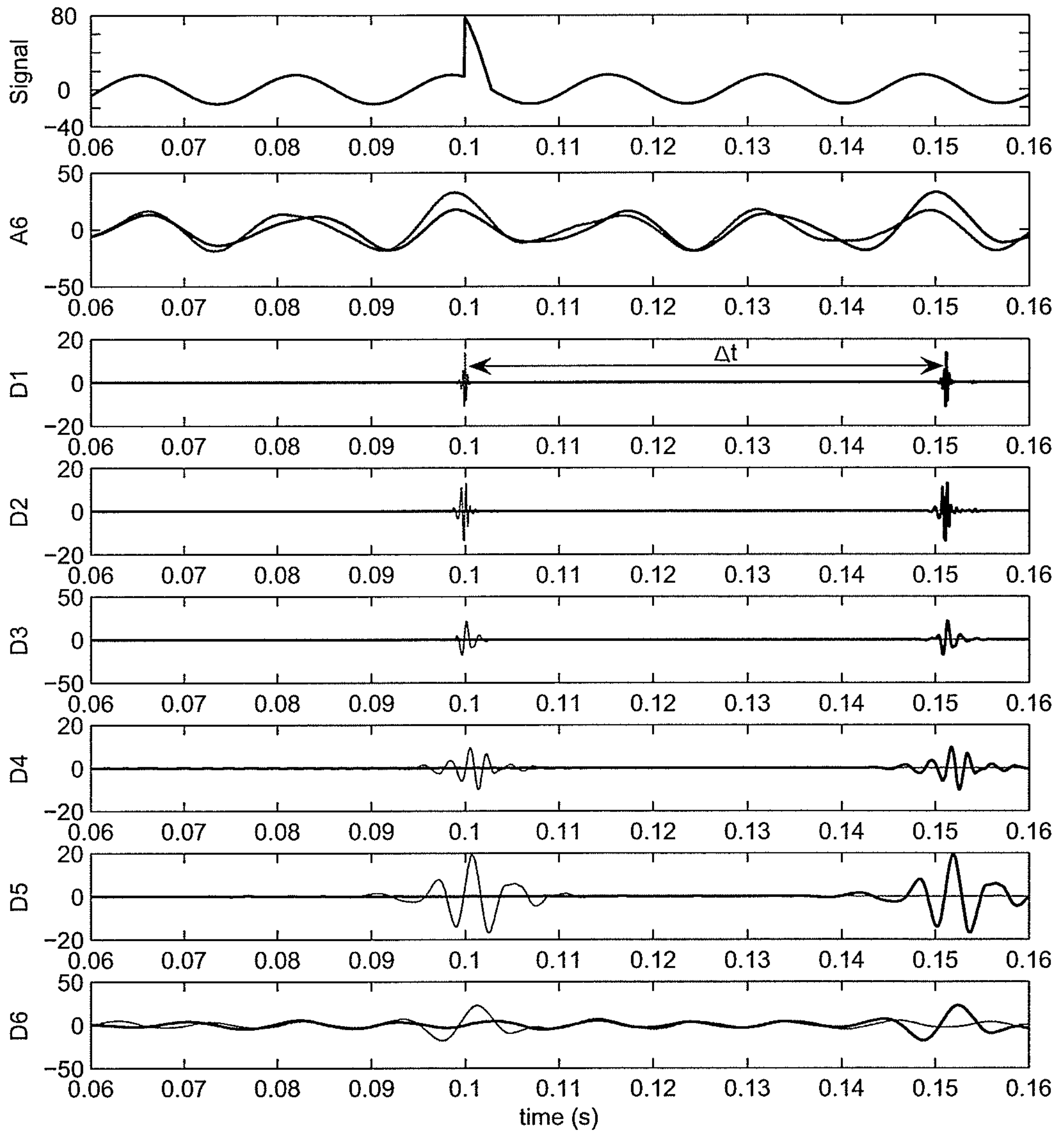

Figure 3.16: Transient signal and its *sym8* wavelet coefficients at level 6 using Online DWT in PSCAD (thick lines) and DWT in MATLAB (thin lines)

In order to validate the accuracy of the computations, MATLAB wavelet toolbox was used. Figure 3.16 shows the wavelet coefficients obtained for a transient signal using wavelet tool developed in PSCAD/EMTDC and wavelet toolbox in MATLAB.

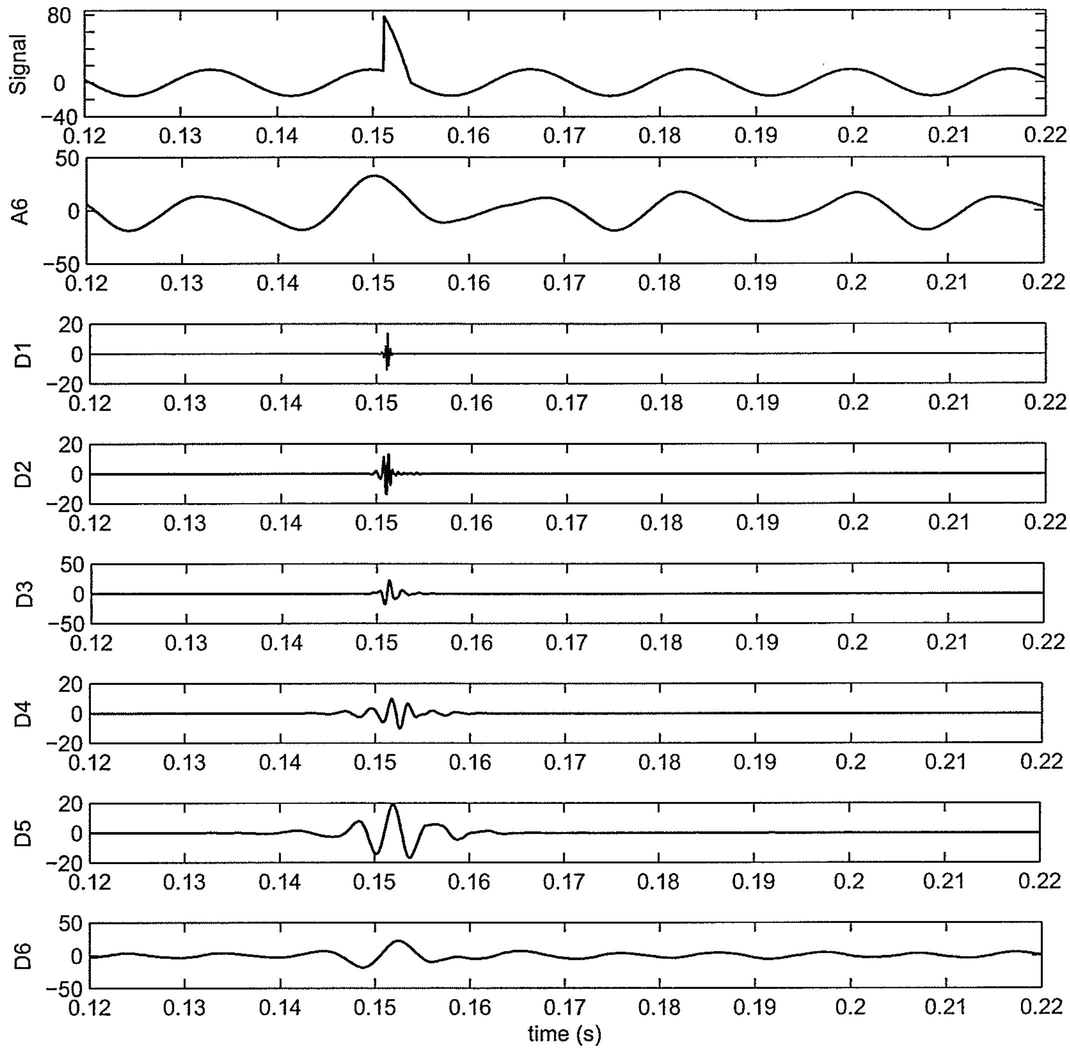

Figure 3.17: Transient signal and its *sym8* wavelet coefficients at level 6 using Online DWT in PSCAD and DWT in MATLAB with out the time delay

In Fig. 3.16 wavelet coefficients obtained with *sym8* mother wavelet are shown. The solid lines show the results obtained using PSCAD/EMTDC whereas, the thin lines show the results obtained using MATLAB. Except for the time delays, both sets of wavelet coefficients looks the same. Note that the MATLAB toolbox used the recorded waveforms after the simulation, whereas the PSCAD/EMTDC generated the wavelet coefficients as the waveform was being generated form the simulation; hence causing a time delay, $\triangle$t as shown. For further verification, both results were plotted by omitting the time delays as shown in Fig. 3.17. Now Fig. 3.17 clearly shows perfect matching between the results obtained using the wavelet tool developed for PSCAD/EMTDC and MATLAB toolbox.

The wavelet coefficients obtained for the same transient using different types of mother wavelets are shown in Appendix A in Figs.A.1-A.3. Based on these results, it can be concluded that the developed wavelet tool gives accurate results.

3.5 Chapter Summary

This chapter studied the possibility of using modal transformation of three-phase currents to reduce the number of signals required to be analyzed in fault location. The wavelet transformation and its use for analyzing the transients in power system signals was discussed. Finally, a tool for performing wavelet transformation in a power system simulator was developed and its accuracy was verified against an established wavelet transform software.

Chapter 4

Fault Isolation Using Current Transients

4.1 Introduction

This chapter presents the development of a technique for fault direction identification using transients in the network currents following a fault. This technique uses wavelet coefficients of the Clarke components of the fault currents to determine the fault directions. Fault current directions determined at several places are used to locate the faulted section in the network. Use of transients for fault direction estimation has certain advantages over phasor based techniques. It is fast, and less affected by the errors in voltage and current phaser measurements due to power system frequency swings that happen during the faults.Transient based fault locating technique will be particularly helpful in networks with DG, since these techniques will not be affected by the lack of sustained fault currents.

4.2 Previous Work on Transient Based Fault Location

Several transient based fault locating methods can be found in literature. Most of these use traveling waves and their successive reflections created by the fault to determine the location of a fault in a transmission line. However, such methods are difficult to apply in distribution systems due to *(i)* short lengths of line segments and *(ii)* presence of branches/loads along the distribution lines.

Other methods attempt to determine the fault direction using the transients. In [23] a wavelet based faulty segment identification technique has been proposed. In this technique, three phase voltages measured at various locations on the network are transformed into modal quantities. Next, the magnitudes of the wavelet coefficients of modal signals are compared to determine the faulty segment. According to [23], wavelet coefficients calculated at the terminal of a faulted line are comparatively larger than those of the non-faulted lines.

An algorithm for fault direction identification using current transient has been proposed in [27]. In this study, three phase current signals are transformed into modal domain signals and passed through a band pass filter to remove the highest frequencies and the lowest frequencies from the signal. The filtered signal is used to identify the fault directions. This method which uses only current measurements to determine fault direction is economically attractive for protecting DG systems as the installation of voltage transformers at many locations is expensive.

4.3 Fault Categorization and Direction Identification

In this thesis, the current transient based fault direction identification method proposed in [27] is improved by using Wavelet Coefficients ($WTCs$) in place of the band pass filtered waveforms of the current transients. The main shortcoming in the band pass filter approach, according to the author's experience, is the selection of cutoff frequencies to accommodate all types of faults and line configurations. This difficulty is largely overcome in the proposed method.

In order to explain the technique, consider the simple power system shown in Fig. 4.1. A relay R is installed at busbar-2 where three lines are interconnected. Three sets of Current Transformers (CTs) are installed on each of the branches at X, Y, and Z to measure the currents leaving the node. A fault in the region between the CTs , such as fault F_1, is considered an *internal fault* whereas a fault outside the CTs, such as fault F_2 or F_3, is considered an *external fault* for relay *R*.

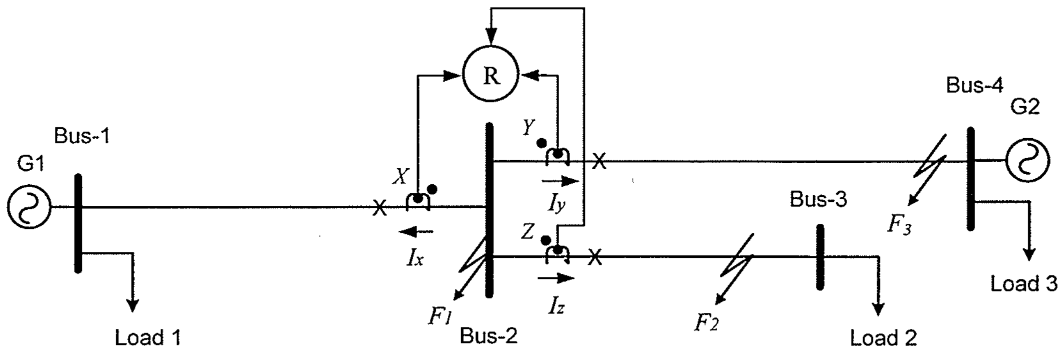

Figure 4.1: Internal and external faults for relay agent R

For an internal fault such as F_1 in Fig. 4.1, the high frequency transients that are observed by the relay agent originate within the boundary of measurement points (X, Y and Z) and travel outwards. According to the chosen CT arrangement all measurements should show the same sign. For example, consider Fig. 4.2 which shows the three phase current measurements at X, Y and Z, for a three-phase ground (ABC-G) fault and their α components. The corresponding WTCs are also shown. In this example, Level-1 WTCs obtained with *db4* mother wavelet are used; therefore the WTCs in Fig. 4.2 reflect the shape of *db4* mother wavelet. As expected, WTCs observed at X,Y and Z shows the same sign. Figure 4.3, where all three WTCs are drawn on the same axis, clearly shows that they are of the same sign. Thus any fault inside the region of CTs can be determined as internal based on this criterion.

For an external fault, CTs on the faulted branch will measure the incident current surges (plus the reflections) while the CTs on the other branches measure the transmitted components. As per the chosen CT connection, transients measured on the non faulted branches should be opposite in sign compared to those measured on the faulted branch. Figure 4.4 shows three-phase current measurements at X, Y and Z for a three-phase (ABC) fault on line segment Z. Figure 4.4 also shows their α components and corresponding WTCs.

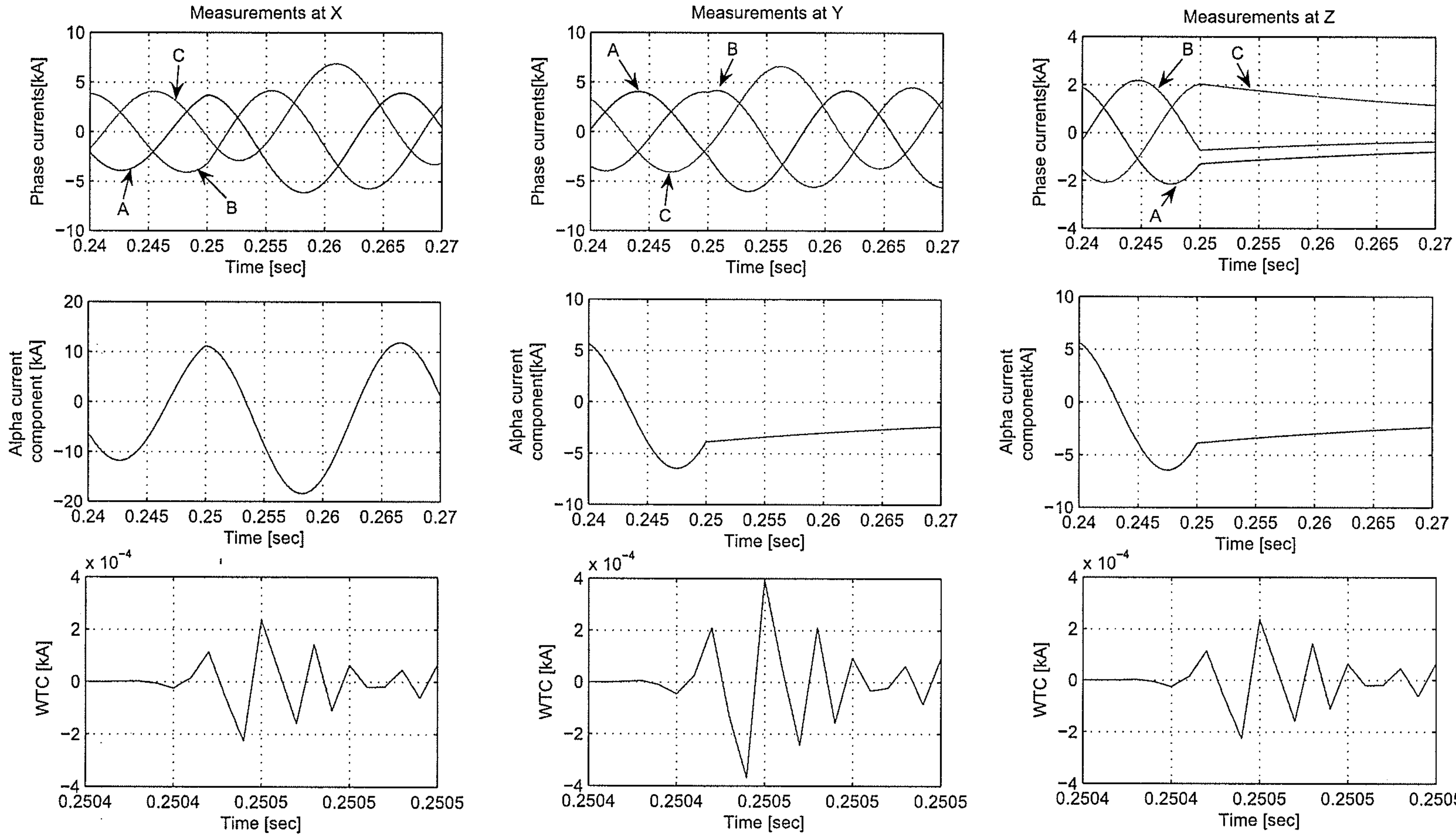

Figure 4.2: Phase currents, corresponding Clarke components and their WTCs following an internal ABC-G fault.

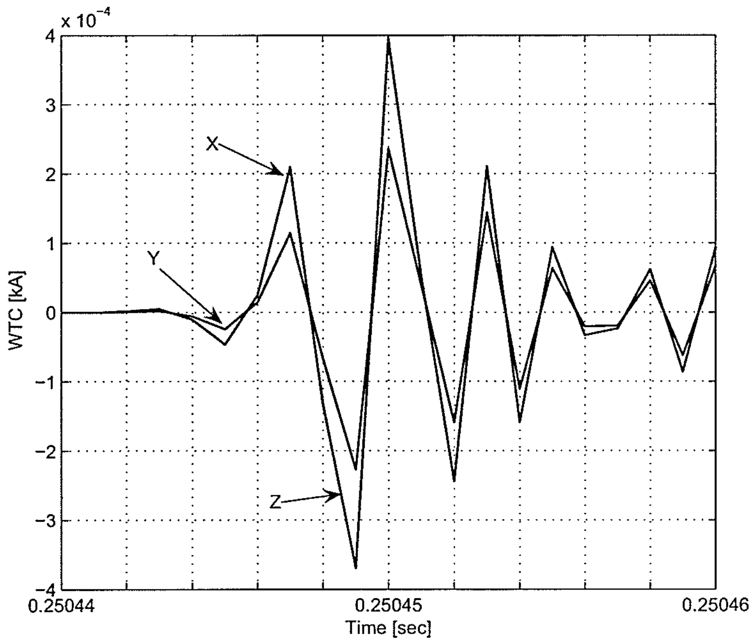

Figure 4.3: WTCs for fault F1

Figure 4.5 shows these WTCs on the same axis. The sign difference can now be clearly observed. The sign of WTC for the currents measured at Z is opposite to those measured at X and Y. Further it can be observed that the magnitude of the WTC determined at faulted branch (ie. segment Z) is comparatively greater than the WTCs determined at non faulted branches(ie. X and Y).

WTCs of β components determined for a phase B-C fault, F_3, are shown in Fig. 4.6. Figure 4.7 shows these WTCs on the same axis. Using the sign difference observed between WTCs, fault F_3 can be categorized as an external fault. Since this fault is on the line segment Y, the WTC for the current measured at Y shows opposite sign to those at X and Z . The WTC of the faulted segment has a larger magnitude than the WTCs of the non-faulted segments.

Any fault outside the region of the CTs can be recognized as external, if the WTCs are not of the same sign. Further, the fault direction can be determined as the WTC which is having an opposite sign to the others or the highest magnitude.

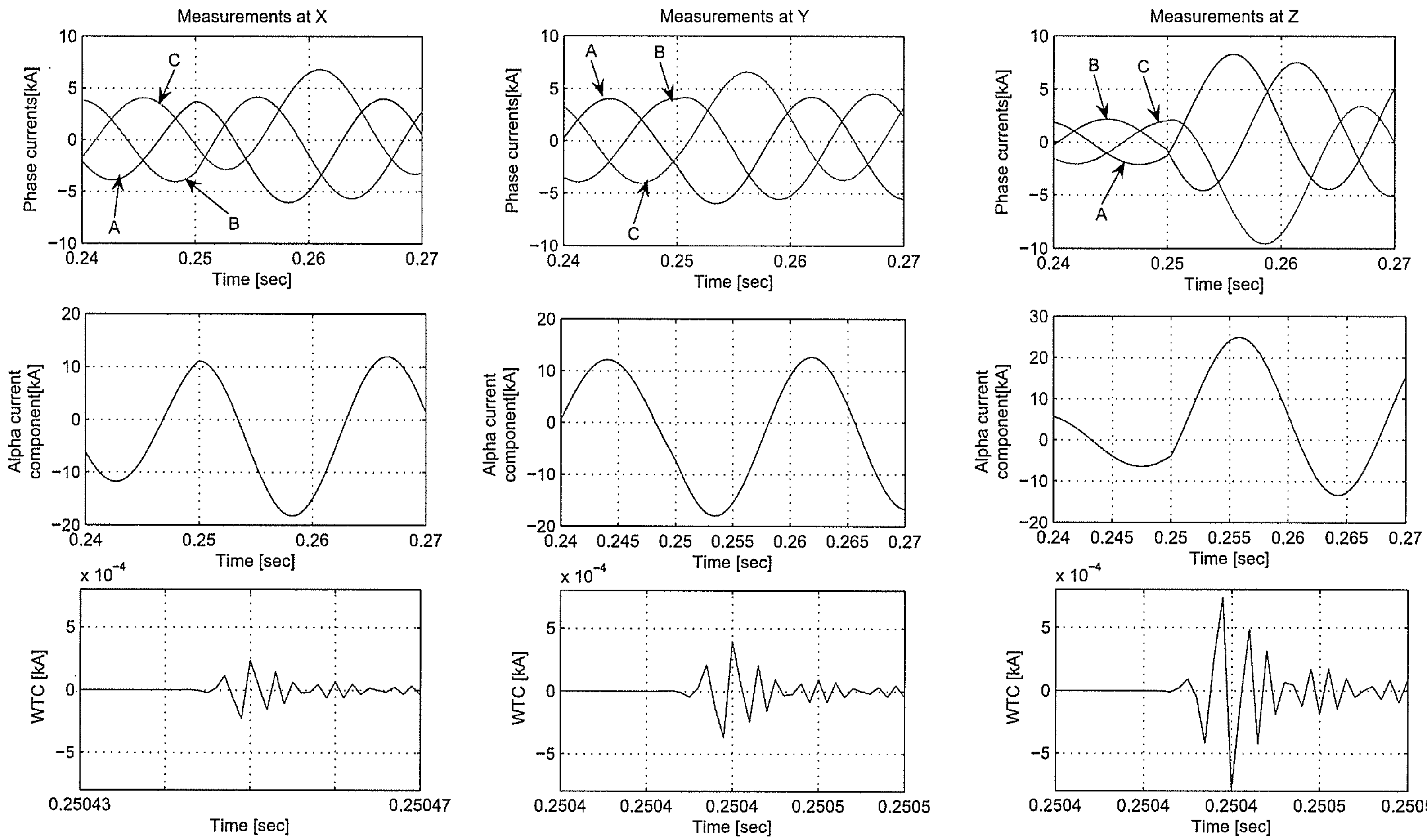

Figure 4.4: Phase currents, corresponding Clarke components and their WTCs following an external ABC fault

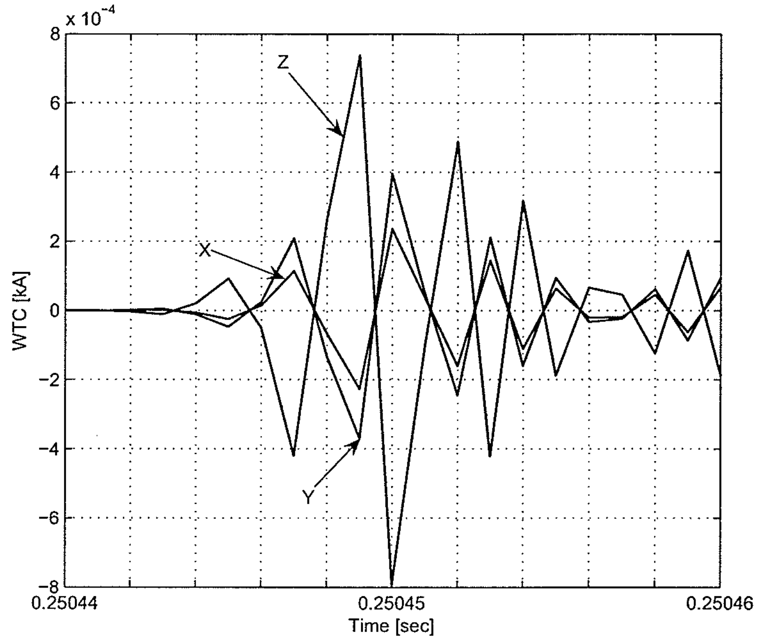

Figure 4.5: WTCs for fault F2

Thus based on the above observations in signs and magnitudes of WTCs , it can be concluded that,

1. If WTCs corresponding to all the branches connected to a node have the same sign, the fault is an internal fault with respective to that node.

2. If WTCs corresponding to all the branches connected to a node are not of the same sign, the fault is an external fault with respective to that node.

3. In the case of an external fault, the fault direction can be determined as the branch that is having a WTC with opposite sign to the rest of the WTCs or the branch with the highest WTC magnitude.

For an unknown fault, WTC of both α and β components need to be computed. Then, α or β component which gives the highest WTC is used for fault categorization and direction identification. Although fault direction can be determined either by using the sign of WTCs or the magnitude of WTCs, a combination of both sign and magnitude can be used to get more reliable results.

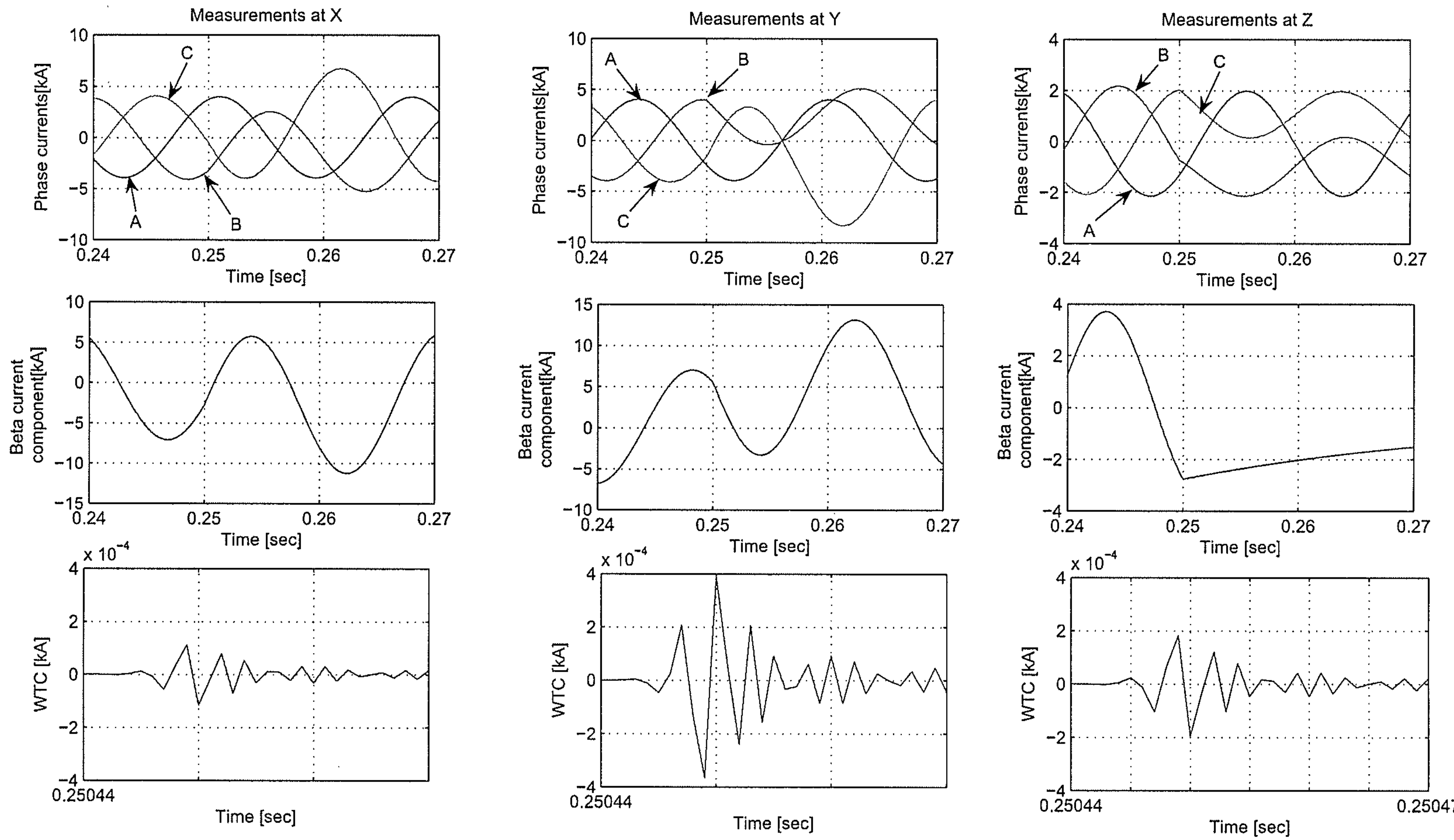

Figure 4.6: Phase currents, corresponding Clarke components and their WTCs following an external BC fault.

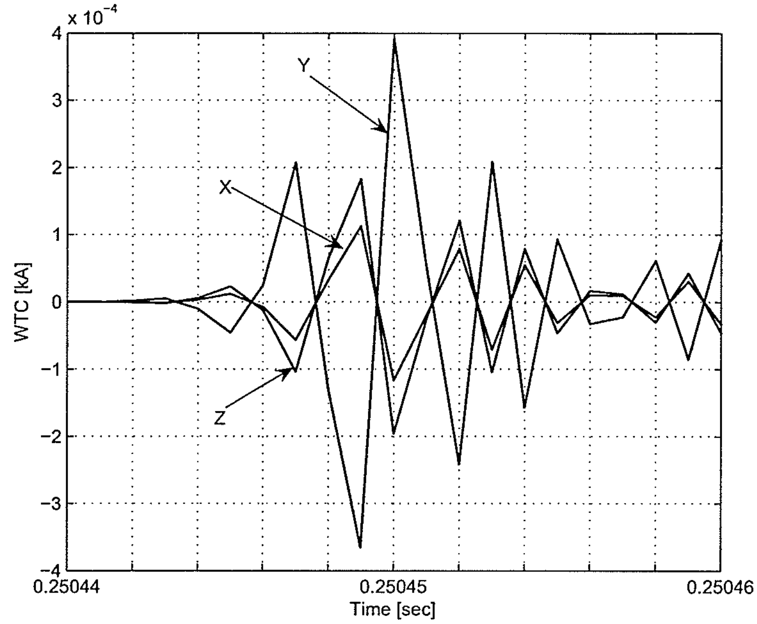

Figure 4.7: WTCs for fault F3

4.4 Implementation of Fault Categorization and Direction Identification Algorithm

As described in section 4.3, WTCs of the currents measured on different branches connected to a node can be used to determine the direction of fault. Implementation of the method requires determination of whether the WTCs are of the same sign or not. Cross correlation is a standard method of estimating the degree to which two signals are correlated. Thus cross correlation between wavelet coefficients can be used to determine whether two WTCs are of the same sign or not.

Consider two sampled signals $x(i)$ and $y(i)$ where i =0,1,2...N-1. The cross correlation r between the two signals at delay d is defined as,

$$r(d) = \frac{\sum_i [(x(i) - \bar{x}) * (y(i-d) - \bar{y})]}{\sqrt{\sum_i (x(i) - \bar{x})^2} \sqrt{\sum_i (y(i-d) - \bar{y})^2}} \tag{4.1}$$

where $\bar{x}$ and $\bar{y}$ are the means of the corresponding series. The denominator in the expression above serves to normalize the correlation coefficients such that -1 $\leq r(d) \leq$ 1, the bounds indicating maximum correlation and 0 indicating no correlation. A high negative correlation indicates a high correlation but of the inverse of one of the series[40].

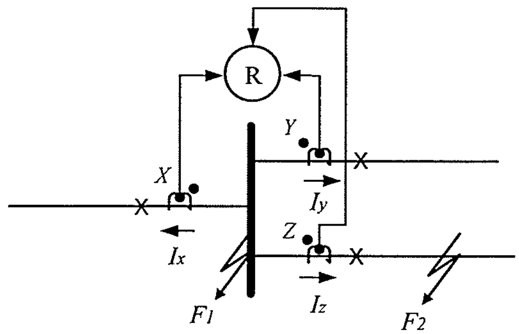

Figure 4.8: Internal fault and external fault for relay agent R

Consider a relay agent R installed at a busbar connecting three line segments as shown in Fig. 4.8, where $F1$ is an internal fault and $F2$ is an external fault. For the internal fault

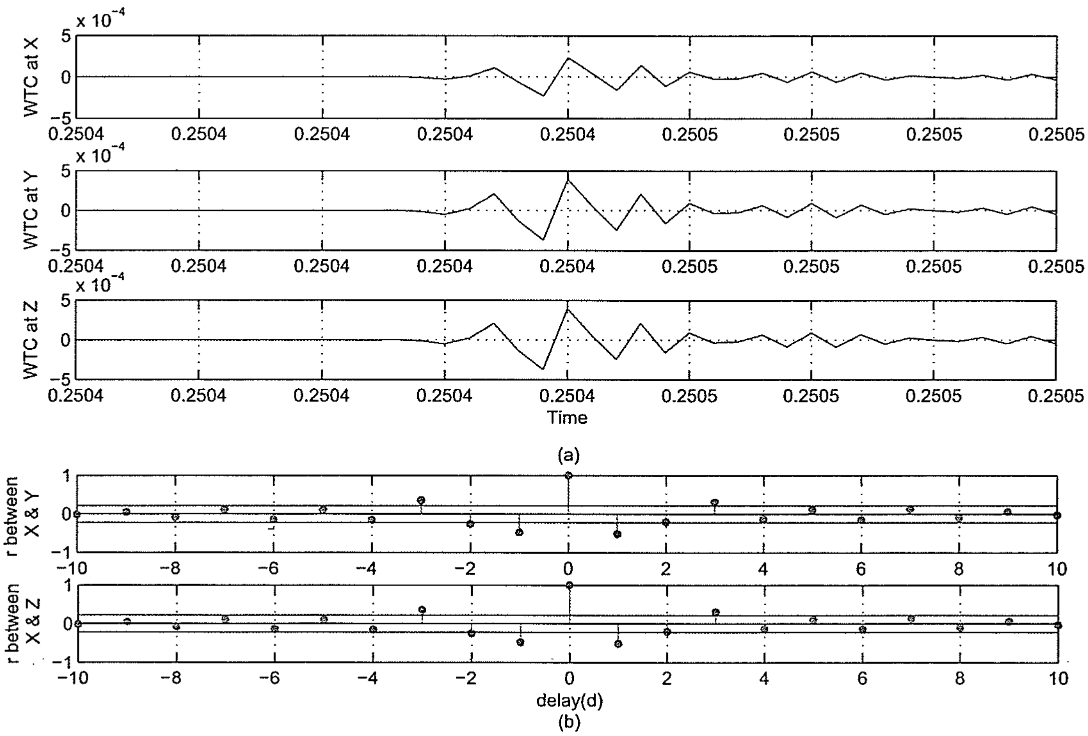

Figure 4.9: (a) WTCs and (b) Correlation Coefficients for internal fault, F1

$F1$ (Fig. 4.8) the variation of WTCs of α components of the current signals and the cross correlation of coefficients calculated between X-Y and X-Z for different sample delays are shown in Fig. 4.9. Since the fault is internal, all three WTCs have the same sign. Thus the highest cross correlation coefficients between X-Y and X-Z are close to +1.

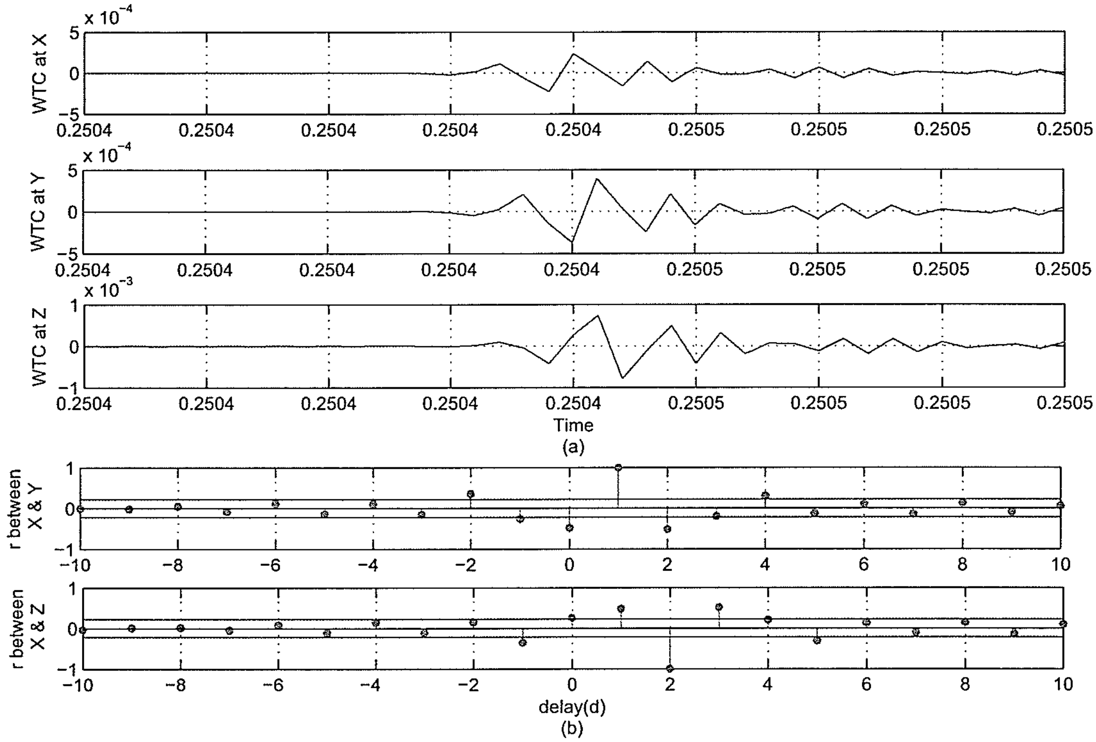

Figure 4.10: (a) WTCs and (b) Correlation Coefficients for external fault, F2

Figure 4.10 shows the variation of WTCs of α components of the current signals and cross correlation between WTCs for X-Y and X-Z respectively for different sample delays, for the external fault $F2$. Since fault $F2$ is in segment Z, WTCs determined at segment Z is having negative sign to those of X and Y. This can be clearly determined using cross correlation coefficients. The highest cross correlation coefficients calculated between X-Y and X-Z are approximately equal to +1 and -1 respectively.

The flow chart of the fault type categorization and direction identification algorithm developed based on cross correlation of coefficients is shown in Fig. 4.11. When there is

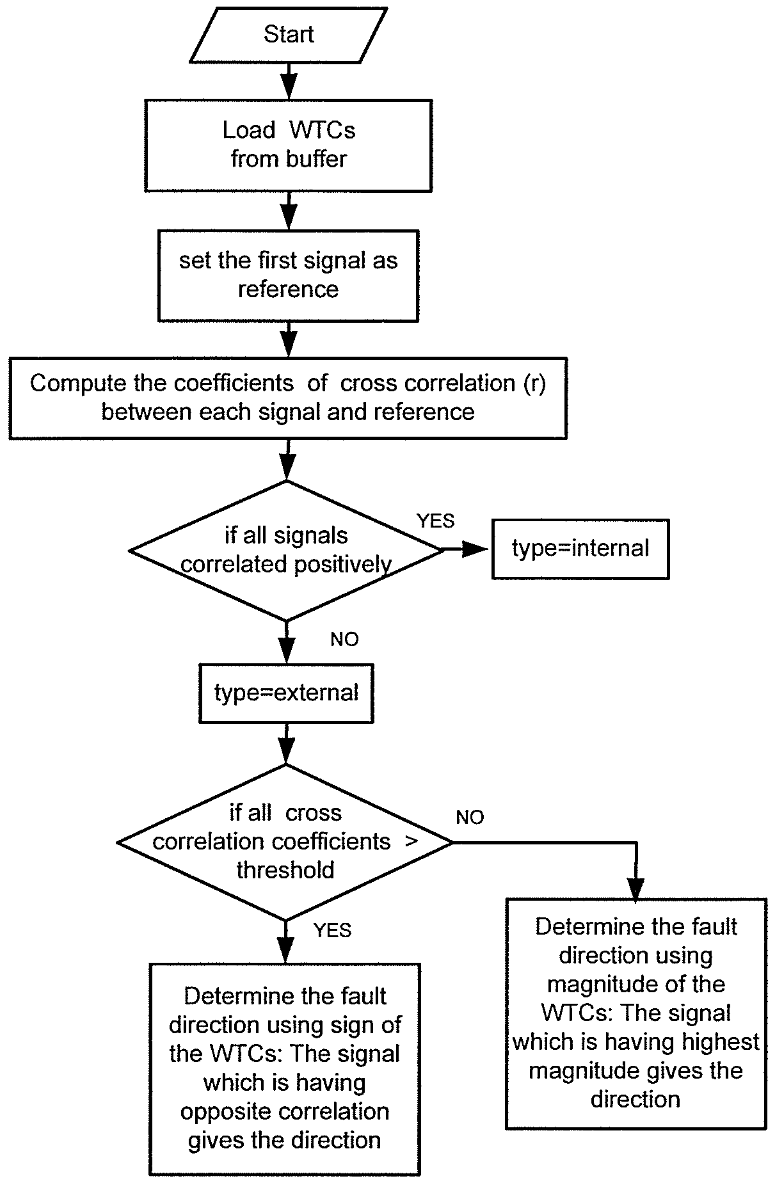

Figure 4.11: Algorithm for fault categorization and direction identification

a fault, the WTCs of the α and β components of the current signals are loaded into the program. One signal is taken as the reference and coefficients of cross correlation between the reference signal and other signals for different time delays are calculated. If all of them are correlated positively above a threshold level, the fault is categorized as an internal fault, and otherwise it is categorized as an external fault.

When the fault category is external, the relay agent needs to take further actions to determine the fault direction. This algorithm uses coefficients of cross correlation between WTCs as well as the magnitudes of the WTCs to determine the fault direction. If the coefficients of cross correlation between the reference WTC and other WTCs match up to an acceptable threshold limit positively or negatively, fault direction is determined based on the cross correlation coefficients. Otherwise the program uses magnitude of the WTCs to determine the fault direction. Here the signal which gives highest WTC magnitude is determined as the fault direction. The block diagram of fault categorization and direction identification algorithm is given in Fig. B.1 in Appendix B .

When the number of segments connected to a relay is two, this algorithm can be used for fault categorization only. Further, during external fault situations when there are two parallel fault current paths are available this algorithm can fail in fault direction identification.

4.5 Faulty Segment Location Using Fault Direction Information

As found out in section 4.4, the direction of a fault in relation to a node can be determined from the current transients observed at the node. Although the direction of the fault can be determined relative to the node, the exact faulty segment can not be determined by a single point observation. For example consider the simple system shown in Fig. 4.12.

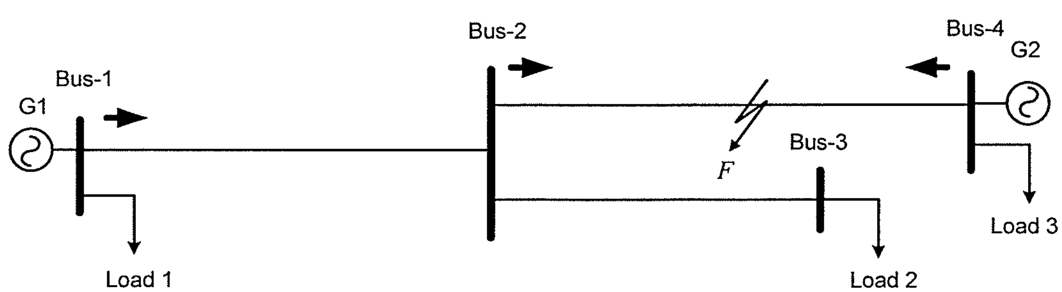

Figure 4.12: Faulty segment location using fault directions

For Fault F, observations at bus-1 and bus-2 would indicate fault direction as shown by the arrows. But a relay at bus-1 can not decide whether the fault is between bus-1 and 2 or bus-2 and 4 or on generator G2 or in the load branch at bus-4. Relay at bus 2 cannot decide whether the fault is between bus-2 and 4 or on the generator G2 or in the load branch at bus-4. Similarly the relay on bus-4 cannot decide whether the fault is between bus 4 and 2 or bus-2 and 1 or on the generator G1 or in the load branch at bus-1 or between bus 2 and 3 or in the load branch at bus-3. However if the direction information observed at different points is combined, the faulty segment can be determined. For example, combining the fault direction information at bus-1 and 2, we can very easily conclude that the fault is not in between bus-1 and 2. On the other hand, by considering fault direction information found at bus-2 and 3 it is straightforward to say that the fault is between bus-2 and 3. Therefore if some form of communication between the relays can be introduced, a technique to locate the faults can be developed.

4.6 Agent Based System for Faulty Segment Location

As pointed out in the previous section, the observations made at one point do not allow the determination of fault locations. By sharing the information, faulted branches can be located. In order to achieve this, a protection system comprising of cooperative relay agents is proposed. The concept of a cooperative protection system with an agent model (relay agent) and its advantages are described in[18]. As proposed in[18], such a system would consist of distributed equipment combined with a wide area communication network. The equipment need to be capable of performing local protection functions and cooperate with each other to perform adaptive protection functions. The protection system should have a substitution ability for equipment with problems, so that it will be able secure high reliability with less redundant hardware.The protection system should also be able to reorganize itself according to the topological changes in power system or trouble with the communication line. This will allow the protection system to separate itself into some subsystems, where the minimum subsystem consists of only one piece of equipment. Each subsystem can then

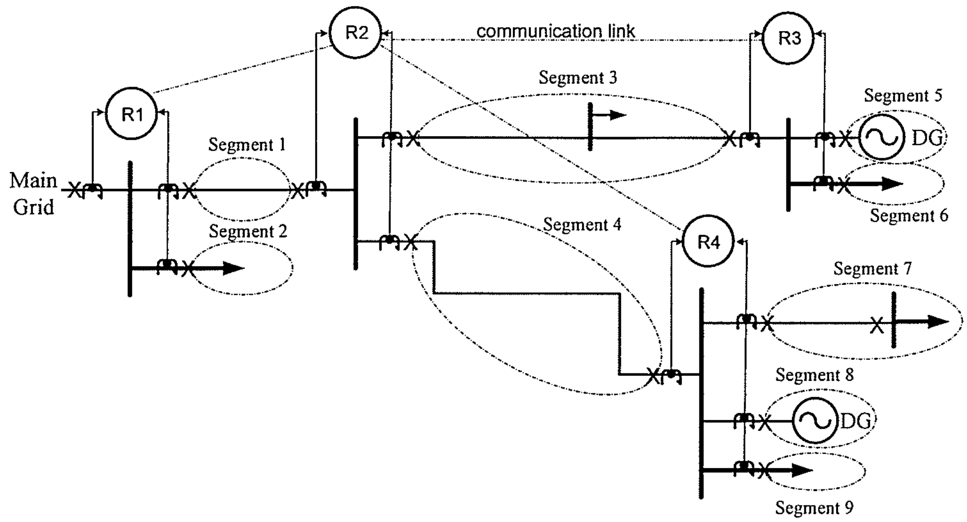

Figure 4.13: Structure of the proposed protection scheme

adjust its functions so that they are workable within the collectible information. Such a system is an ideal platform to implement the proposed protection scheme.

4.6.1 Faulty Segment Location Procedure

The distribution network is divided into a number of network segments as shown in Fig. 4.13 for fault isolation purposes. Circuit Breakers (CBs) are installed at interconnecting points to facilitate the isolation of a network segment from rest of the system for a fault inside it. Relay agents are installed at the busbars interconnecting different network segments. Current Transformers (CTs) installed on the interconnected branches feed the relay agents. These CTs are connected to measure the currents leaving a node. A telecommunication network facilitates data exchange between the neighboring relay agents.

If the fault category determined by a relay agent is internal, it will immediately generate the trip signals to isolate all the segments connected to it and send the information "NO" for all the relay agents connected to it. If the fault category determined by the relay agent is external, relay agent will send the information "YES" to the relay agent in the direction of identified fault and information "NO" to all other neighboring relay agents. If a relay agent receive information "YES" from the identified fault direction(i.e. both information send to a relay and received from that relay are "YES") relay will generate trip signal to isolate the segment in the identified direction. When the fault is on a terminal segment, corresponding relay agent can immediately isolate the fault without depending on the information coming from the neighboring relay agents.

The following example cases illustrates faulty segment location procedure for different scenarios such as internal fault, external fault on a segment in between two relay agents and external fault on a terminal segment.

Case-1 : Internal Fault

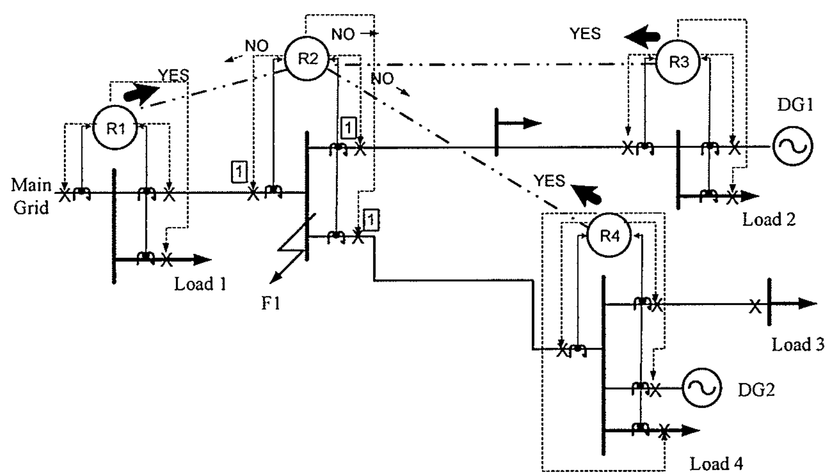

Figure 4.14: Fault isolation for an internal fault

Figure 4.14 shows a distribution network which consists of four relay agents. Consider a fault on the busbar where the relay agent R2 is installed. This is an internal fault for relay agent R2 and external fault for other relay agents (R1,R3 and R4). R2 can identify the internal fault situation and issue trip signals to isolate the fault. The fault directions identified by R1,R3 and R4 are shown using solid arrows along the telecommunication link. Information send by relay agents are also shown (YES/NO) close to each relay agent. The resultant trip signals generated by relay agents are shown near the CBs (1 denotes the CB open).

Case-2: External Fault on a Segment Between Two Relay Agents

Figure 4.15 shows an external fault occurred on a line segment between relay agents R2 and R3. The identified fault directions and information sent and received by the relay agents are also shown. The information sent and received each other by the relay agents R2 and R3 is "YES". Thus based on the information interchanged they can locate the fault as in between R2 and R3, and send the required trip signals to isolate the faulty segment.

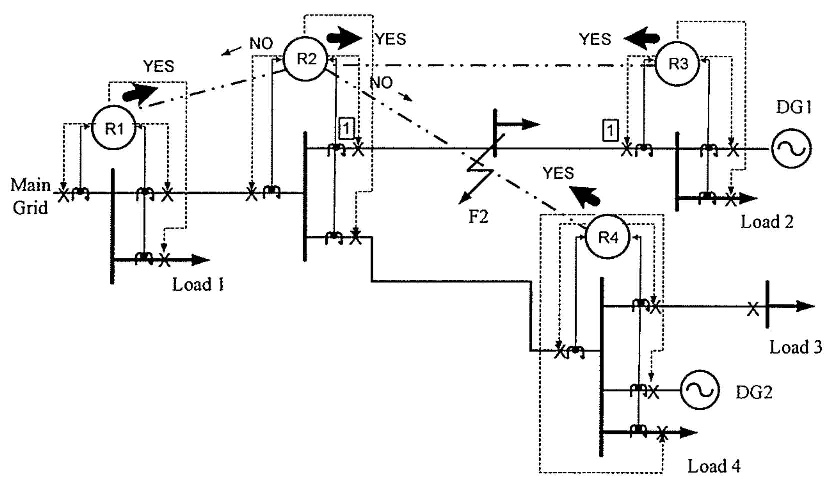

Figure 4.15: Fault isolation for an external fault

Case-3: External Fault on a Terminal Segment

An external fault occurred on a terminal line segment connected to relay agent R4 is shown in Fig. 4.16. Since there is no relay agent connected in the direction of the identified fault, relay agent R4 can locate the fault only using local information and send the trip signal to isolate the fault. The identified fault directions and information sent and received by the relay agents are also shown.

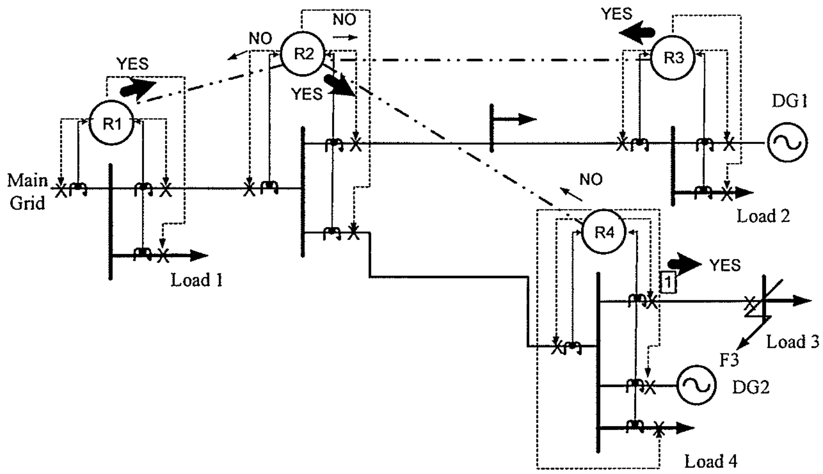

Figure 4.16: Fault isolation when the fault is on terminal segment

As described above, the proposed protection algorithm can locate and isolate the faulty segments using the fault category and direction information determined from the WTCs of the Clarke components of the current signals.

4.6.2 Faulty Segment Locating Algorithm

The flow chart for the proposed agent based faulty segment locating algorithm is shown in Fig. 4.17. When a fault is detected by a relay agent, the fault is first categorized as either an internal fault or an external fault, depending on its location. Any relay agent can identify an internal fault very fast without information from the other locations. It can isolate the faulted busbar by giving trip signals to the relevant circuit breakers. Although this decision is taken independent of the other relay agents, the information that an internal fault occurred on its bus_bar is communicated to the nearest relay agents. Then the other relay agents can take appropriate actions. In an external fault situation, the transients will be detected by the relay agents located close to the fault point. These relay agents then identify the fault direction and communicate this information to the adjacent relay agents. With the fault direction information received from the neighboring agents, relay agents located on the boundary of the faulted segment can establish the presence of a fault

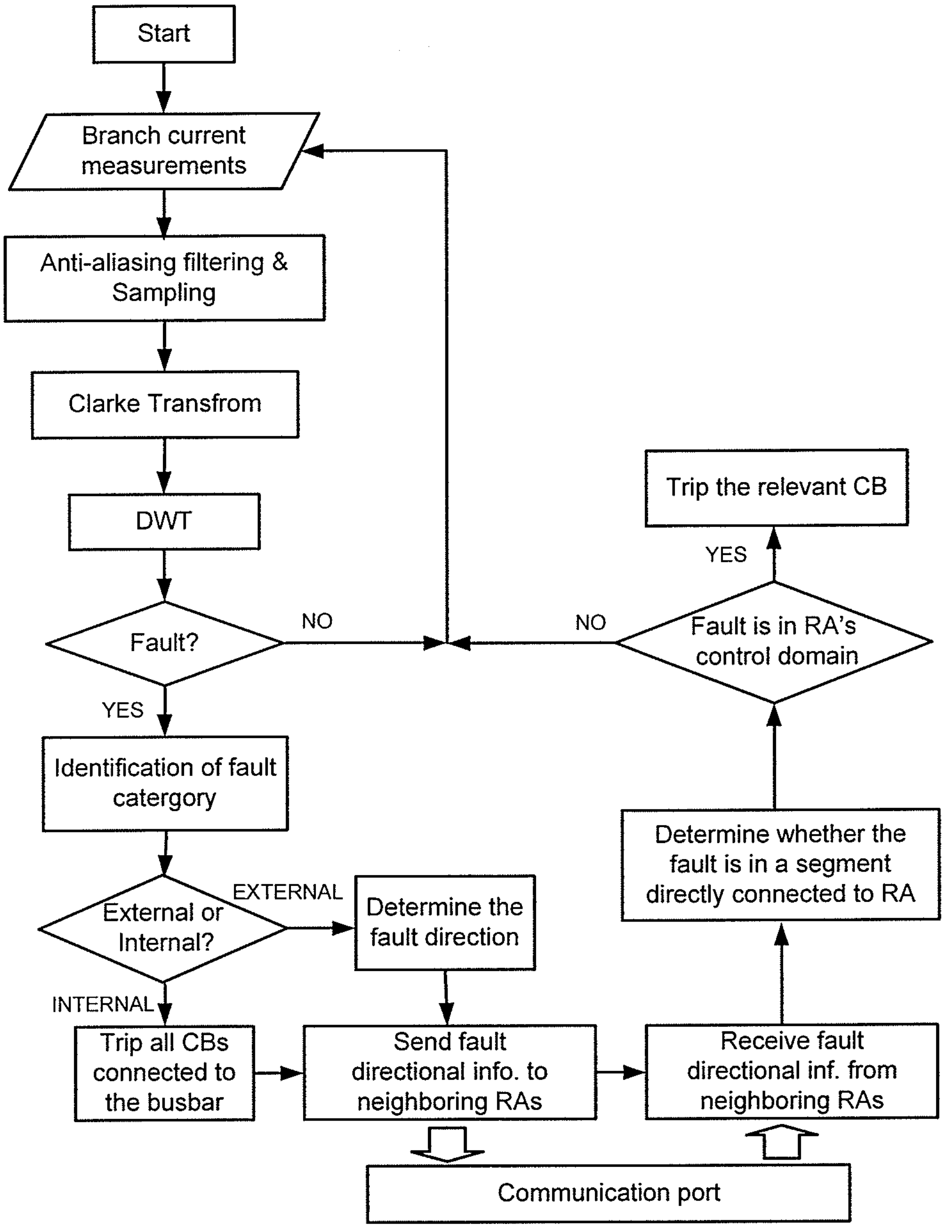

Figure 4.17: Algorithm for faulty segment location

within the network segment encircled by them (from the fact that all relay agents on the network segment boundary indicate a fault in the direction of the segment). Once the faulted segment is established, the necessary circuit breakers will be tripped. The detailed block diagram of fault locating algorithm is given in Fig. B.2 in Appendix B.

4.7 Chapter Summary

This chapter developed a method for identification of the direction of fault currents using the transients generated in the currents due to a fault. It was shown that the fault directions determined at several locations in a network can be used to locate the faulted segment. An agent based protection scheme based on the above principle was proposed, and algorithms required to implement the relay agents was presented.

Chapter 5

Modified Relay Algorithm to Improve Reliability

5.1 Reliability of the Fault Location and Isolation System

A protection system needs to be

(i) dependable, i.e. operate for every fault

(ii) secure, i.e. does not operate unnecessarily during normal operation.

There are several situations where the proposed method for faulty segment location may not work as intended. One possible scenario is the failure of the proposed relay algorithm to identify the faulted branch when there is a communication failure. In such a situation, a relay agent can combine the data coming through the available communication links together with the power frequency current magnitude estimations to make a decision. Also, when the node at the relay agent involves only two branches, it is difficult to determine the fault direction for an external fault using the proposed fault direction identification technique. In such situations, which can occasionally arise in practice due to temporary outages of lines, loads, etc., a fault on a segment connected to that relay agent location can be determined only by the relay agents which are further away from the faulted segment. This will result in the removal of two or more segments depending on the network configuration.

There are numerous transients occurring during the normal operation of a power system due to load switching, load changers, capacitor switching, etc. Transient based protection systems may operate due to such transients. Thus, a mean is required to prevent this. This thesis proposes to integrate a transient classifier system into the relay in order to distinguish fault related transients from others.

5.2 Transient Classification

Recently, many automated systems for power disturbance classification have been designed. Implementation of a numerical relay which is capable of classifying fault transients from non-fault transients is very useful in power system protection. There are several classification methods proposed in literature. They are based on Artificial Neural Networks (ANNs)[33], Dynamic Time Warping (DTW)[34], rule-based systems[35], and Decision Trees(DTs) [38]-[39].

ANNs can approximate any well-behaved function with an arbitrary accuracy and can deal with hard problems such as, significantly overlapping patterns, high background noise, dynamically changing environments, etc. Therefore ANNs are particularly suitable for identification of dynamic events. The main disadvantages of ANN based classifiers are the large training time and the retraining requirement due to the addition of new phenomenon[28][29]. DTW measures similarity between two sequences which may vary in time or speed. In power disturbance analysis the DTW approach can be applied to recognize the time alignments between the test signals and the stored power disturbance templates[30]. The main disadvantage of this method is that it requires too much computation time. On the other hand, building a rule-based classifier is complicated for power disturbance classification since there is a large number of disturbance classes.

5.2.1 Decision Tree Classifier

The Decision Tree Classifier (DTC) is capable of breaking down a complex decision-making process into a collection of simple decisions. Thus DTC provides simple solutions for complicated problems. DTC are widely used in many diverse areas such as radar signal classification, character recognition, remote sensing, medical diagnosis, expert systems, and speech recognition. Decision tree is a predictive model in machine learning, which maps observations about an item to conclusions about the item's target value. Altogether decision trees have several advantages over the other data mining methods. They can be summarized as follows[32] [37].

a) They are simple to understand and interpret

b) The required data preparation is minimum

c) They are capable to handle both nominal and categorical data

d) They use a white box model

e) They make it possible to validate a model using statistical tests

f) They are robust and perform well with large amount of data in a short time

DT can be described mathematically, where the data comes in records of the form;

$$(x, y) = (x_1, x_2, x_3, ..., x_k, y) \tag{5.1}$$

The dependent variable, y, is the variable that needs to understand, classify or generalize. The other variables x_1, x_2, x_3, etc. are the features that help on this process.

The structure of a general DT is shown in Fig. 5.1. An interior node corresponds to a feature whereas, an arc to a child represents a possible value of that feature. A leaf represents the predicted value of target feature given the values of the features represented by the path from the root. A decision tree can be learned by splitting the source feature set into subsets based on an attribute value test. This process is repeated on each derived subset in a recursive manner. The recursion is completed when splitting is either non-feasible, or a singular classification can be applied to each element of the derived subset. The depth of a node is the length of the path from the root to the node. Decision trees are also a descriptive means for calculating conditional probabilities [38]-[39].

The main objectives of DTCs are to classify correctly as much of the training sample as

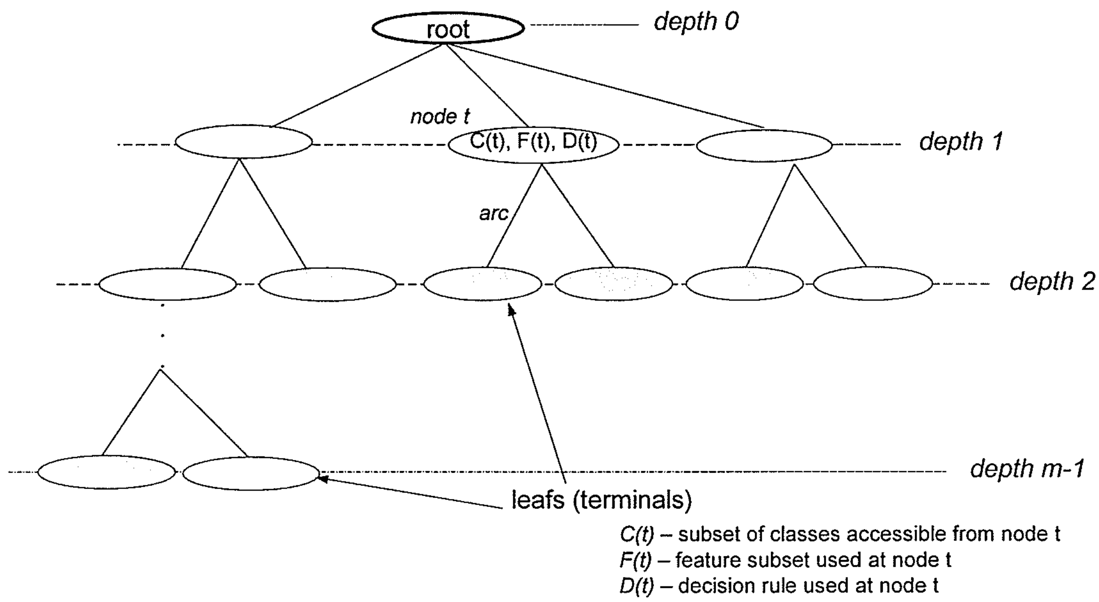

Figure 5.1: DT structure

possible, generalize beyond the training sample so that unseen samples could be classified with as high of an accuracy as possible, be easy to update as more training sample becomes available and have as simple a structure as possible. Thus the design of a DTC can be decomposed into following tasks.

a) The appropriate choice of the tree structure

b) The choice of feature subsets to be used at each internal node

c) The choice of the decision rule or strategy to be used at each internal node

The optimal DT design can be defined as an optimization problem:

$$Minimize_{T,F,D} = p_e(T, F, D) \tag{5.2}$$

where p_e is the overall probability of error, T is a specific choice of the tree structure, F and D are the feature subsets and decision rules to be used at nodes, respectively.

The construction of DTC can be carried out in various heuristic methods namely bottom-up approach, top-down approach, hybrid approach and growing-pruning approach. In bottom-up approach a binary tree is constructed using the training set whereas, in top-down approach sets of classes are successively decomposed into smaller subsets of classes to design the tree. Hybrid approach uses a bottom-up procedure to direct and assist a top-down procedure. The growing-pruning approach is essentially a top-down algorithm, which avoids difficulties in choosing a stopping rule and grows the tree to its maximum size where the terminal nodes are pure or almost pure. This has been incorporated into a computer program known as CART. The name CART is an acronym from the words Classification And Regression Trees[36].

In CART approach, there are six general kinds of questions arise during the training:

i) Number of splits at a node

ii) Which property should be tested at a node?

iii) When should a node be declared a leaf?

iv) If the tree becomes too large, how can it made smaller and simpler that is pruned?

v) If leaf node is impure, how should the category label be assigned?

vi) How missing data should be handled?

The number of splits at a node is closely related to the property, which we are going to test at a node. Normally the number of splits is set by the designer and can be varied throughout the tree. However any tree can also be represented with two splits at each node, which is known as binary decision trees. Due to the fast training and classification capability they have become more popular[37].

A full description of DTC training algorithm is beyond the scope of this thesis, and interested readers can refer to [36] for details.

5.2.2 Decision Tree Based Fault Classifier

Decision Tree (DT) based methodology for High Impedance Fault(HIF) detection has been proposed in [38]. This method could successfully distinguish the HIFs from most normal operations including switching loads, switching shunt capacitors, and load transformer inrush currents. In this thesis, a method similar to that used in [38] with some changes to feature extraction is proposed to distinguish the fault transients from non faulty transients. In[38], feature vector required for the classification purpose has been generated using Fast Fourier Transform(FFT) of the current signals. This thesis propose to use DWT instead of FFT, which is already available and well suited for transient analysis. The complete DT algorithm and DT based classifiers can be found in[36].

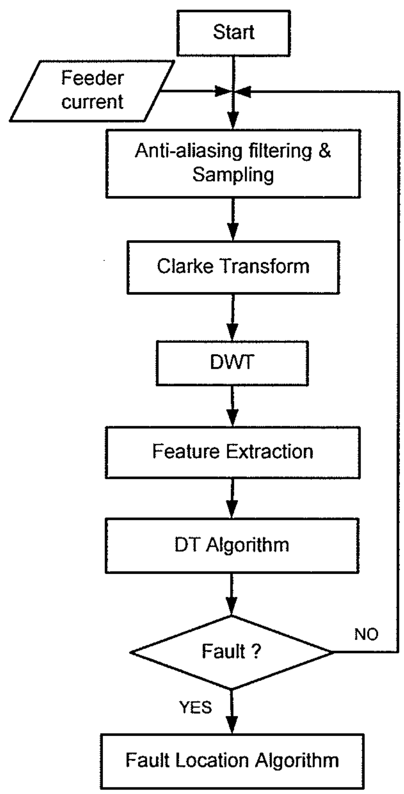

Figure 5.2: Flowchart of the proposed DT based classifier

Figure 5.2 shows the flowchart of the proposed DT based fault classifier. This is an extended version of the method proposed in[38]. The current signals coming from feeders are low-pass filtered before sampling is done. Next the sampled phase current signals are transformed into Clarke components. The approximate and detail WTCs of the Clarke components are used to determine the feature vectors. Finally the trained DT algorithm is used to recognize the fault situation. DT algorithm must train off-line using a sample of training data before using. The main difference between the method proposed in [38] and this method is that, this method use WTCs of the Clarke components instead of fundamental phase currents and their harmonics.

Even though the main scope of this thesis is to develop a fault location algorithm for distribution networks with DGs, investigations are carried to demonstrate the applicability of the DT based classifier using a set of simulation data.

5.2.3 Data Generation

The training set of the disturbance classes were generated using PSCAD/EMTDC power system simulation software. In order to provide a variety of transients data, the medium voltage test distribution system shown in Fig. 5.3 which is derived from proposed CIGRE MV benchmark system was used. The current signals during different types of fault scenarios, capacitor switching and load switching occurrences were recorded at different locations of the system. These recorded signals were used to generate required feature vectors to train and test the DTC. Feature vector generation is described below.

5.2.4 Generation of Feature Vectors

To efficiently recognize the types of disturbances detected, appropriate information must be extracted from the detected disturbance waveforms. The wavelet based feature vector extraction procedure is described as follows.

1. Obtain sampled three phase disturbance signal with one cycle. The length of disturbance signal must be appropriately selected. It should not be either too short or too long. If it is too short some characteristics of a disturbance cannot be clearly seen and if it is too long it requires long computation time for classification.

2. Transform the signal into Clarke components. In three phase systems, disturbances can be present in all the three phases, in any of the two phases or in any phase.

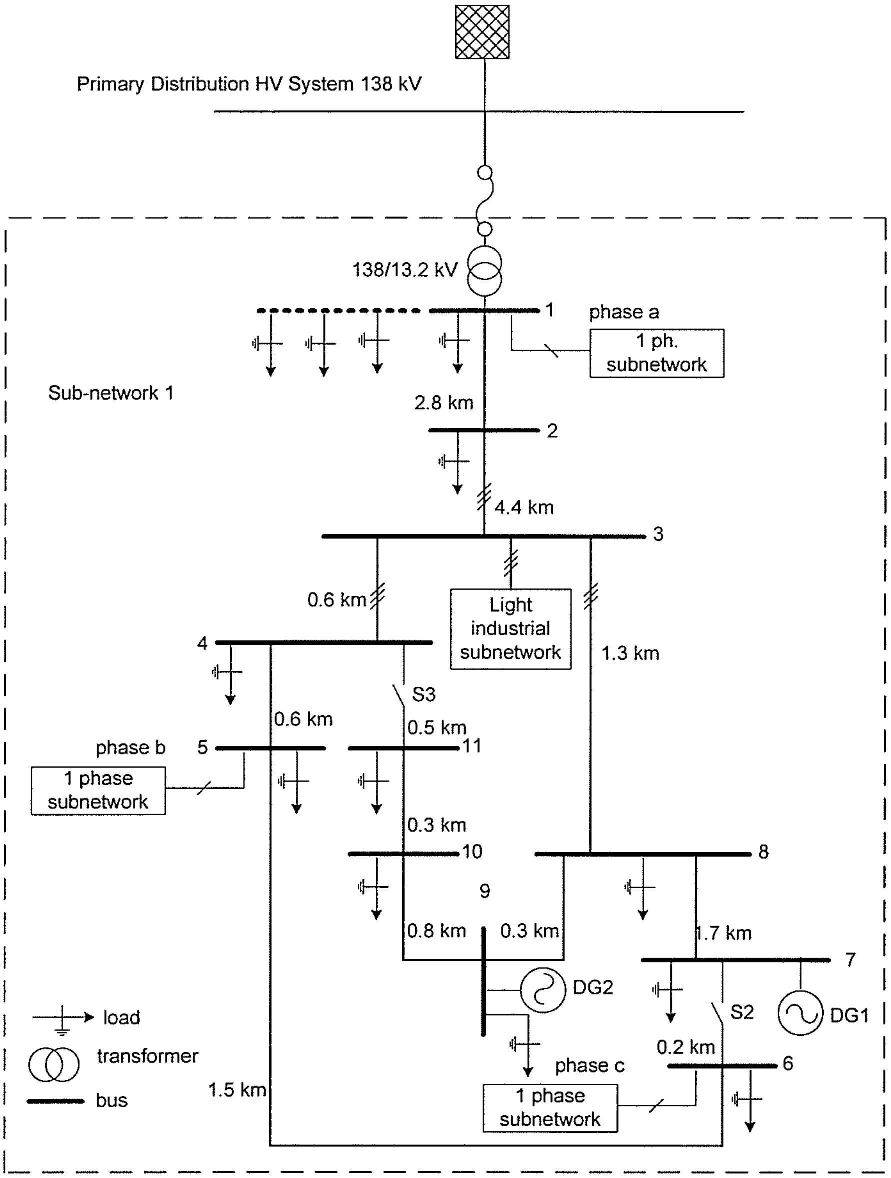

Figure 5.3: MV test distribution system

Analysis of the signal using Clarke components enables the using of a single waveform which represents the disturbances in all phases instead of signals from all three phases.

3. Transform the Clarke components using DWT. In order to obtain complete characteristics included in both low frequency and high frequency signal content, associated

energies are obtained using the approximate and detail components of the wavelet coefficients. The energies associated with wavelet coefficients are computed as shown in Eq.5.3 and Eq.5.4 .

$$EA_l = \sum_{j=1}^{N} |A_{l,j}|^2 \tag{5.3}$$

$$ED_i = \sum_{j=1}^{N} |D_{i,j}|^2, i = 1...l \tag{5.4}$$

Where, i is the wavelet decomposition level from level *1* to *l*. N is the number of the coefficients of detail or approximate at each decomposition level. $A_{l,j}$ is the j^{th} approximation coefficient at level l and $D_{i,j}$ is the j^{th} detail coefficient at level i(A detailed description of approximation and detail wavelet coefficients are given in Chapter 3, Section 3.3). ED_i is the energy of the detail at decomposition level i. EA_l is the energy of the approximation at decomposition level l.

5.2.5 Training and Testing

CART is a DT based software program which can handle large, complex data bases searching and isolating significant patterns and relationships[44]. It was selected for use in this study as in[38]. A set of feature vectors was generated using simulated data. Thirty fault events consisting of 690 cases and 60 non-fault switching events consisting of 1380 cases were used to train and test the classifier. These non-fault transients include transients occurred during load switching as well as capacitor switching. Investigations were carried out using two mother wavelets types; Daub4 (*db4*), and Daub8 (*db8*) which are considered as well suited for power disturbance analysis. Wavelet transformation was performed up to 5 levels. The normalized energy values corresponding to detailed levels were used as features. These feature vectors are used to train and test the DTC as described below.

The relative misclassification cost, the parameter which specifies the consequence of misclassification, was used to adjust the frequency of the misclassification of a fault event to a non-fault event versus a non-fault event to a fault event. Non-operation of the relay due to misclassification of a fault event as a non-fault event may result in a grave consequences. On the other hand, misclassification of a non-fault event as a fault event results in nuisance tripping which is troublesome but not dangerous. Thus the misclassification cost for fault event to non-fault event was set to be ten times larger than the cost for non-fault event to fault event to make it much less likely for a fault event to be classified as a non-fault event.

Total of 1735 cases, consists of 608 fault disturbances and 1127 capacitor and load switching disturbances were used as the training data set. The rest of the faulty and non-faulty disturbances were used as the test data set in order to find out the classification performances. The fault data set included different types of faults (ABC-G, ABC, AB, AG, AC, etc.) and were created with different fault impendence values and different fault interception angles.

5.2.6 Classification Results

The classification results obtained for both mother wavelet types are summarized in Tables 5.1 and 5.2.

Table 5.1: Classification results obtained using '*db8*' mother wavelet

Actual class	Total cases	Fault	Non fault	Percentage correct
Fault	82	82	0	100
Non fault	253	7	246	97.23

Table 5.2: Classification results obtained using '*db4*' mother wavelet

Actual class	Total cases	Fault	Non fault	Percentage correct
Fault	82	77	5	93.9
Non fault	253	2	251	99.21

According to the classification results obtained using '*db8*' wavelet, all the fault disturbances were classified correctly as faults whereas, only 2.77 percent of the non faulty disturbances were misclassified as faults. According to the results obtained using '*db4*' wavelet, 93.9 percent of the faults were classified correctly as faults whereas, only 0.79 percent of the non faulty disturbances were misclassified as faults. Out of the two mother wavelets '*db8*' gave much better results over '*db4*' for simulated transients. These results shows that the proposed DTC can be used to differentiate the fault disturbances form non fault disturbances. However, present study was limited to simulated data obtained with only one test system. Further investigations must be carried out using experimental set of data since a perfect dependable system is required in protection applications. Nevertheless, the limited results presented conformed the possibility of developing such a system.

As pointed out in Sections 5.1 and 5.2 in this chapter, by introducing a DTC to distinguish fault disturbances from non fault disturbances, and an alternative decision making scheme based on power frequency current measurements during communication failures, reliability of the fault locating algorithm can be improved. Next section explains the modified relay algorithm with these features.

5.3 Modified Relay Algorithm

The flow chart for the modified relay algorithm is shown in Fig. 5.4. In this algorithm, once a transient is observed, WTCs of the Clarke current components are sent to the DTC to recognize the situation. If the transients are classified as originating from a fault the relevant WTCs are used for faulty segment location purpose. Fault categorization, fault direction identification and directional information exchange is very much similar to the original relay algorithm. The only difference is when there is failure in a communication, power frequency current measurements are used to make decisions. If the information from other relay agents are not forthcoming within some pre-specified time and the measured power frequency current remains above a certain threshold, a trip signal is issued after a time delay to the breaker in the direction of fault(which has been identified from the transient signals). Such measure is required only when there is a communication failure during an external fault in the direction of identified fault.

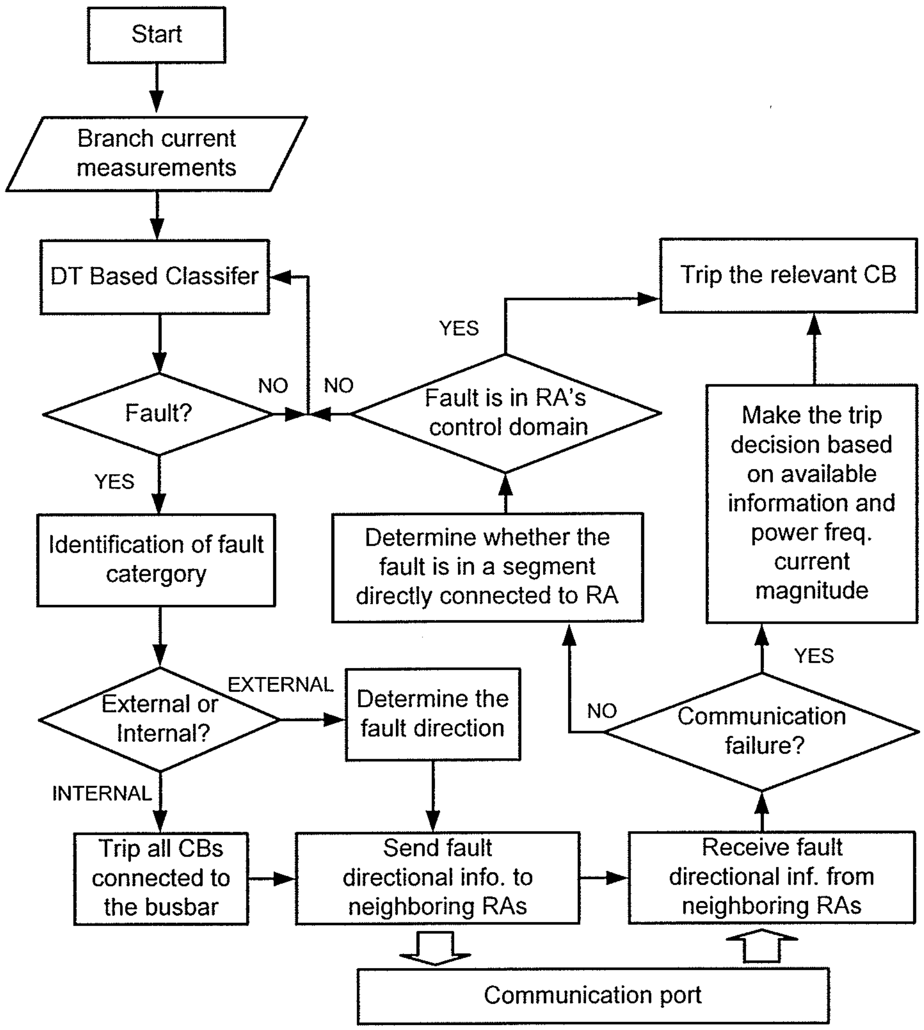

Figure 5.4: Modified relay algorithm for faulty segment location

5.4 Chapter Summary

In this chapter, few modifications to the relay algorithm proposed in Chapter 4 was proposed to ensure acceptable operation under communication failures and to avoid the operation of relay due to transients generated during normal operation. The possibility of developing a transient classification scheme to distinguish fault transients from the other transients was explored. An investigation using simulated transients showed very encouraging results.

Chapter 6

Simulations and Results

6.1 Introduction

This chapter presents the results of investigations carried out to test the performance of the proposed protection algorithm. Two test power systems simulated in PSCAD/EMTDC electromagnetic transient simulation program were used for the investigations. Proposed CIGRE medium voltage test distribution system with distributed generators [42] and IEEE, 12-bus high voltage test system[43] were used for simulation studies. A relay logic algorithm was implemented in MATLAB.

6.2 Medium Voltage Test System

The distribution network shown in Fig. 6.1 was simulated in PSCAD/EMTDC. This system has been derived from CIGRE Medium Voltage Benchmark test distribution system. The system used in study has two distributed generators. Distributed Generator-1 is a 1500 kVA three phase induction generator running from a wind turbine and Distributed Generator-2 is a 200 kVA small size three phase synchronous generator running from a hydro turbine. Distribution lines were modeled using transmission line π model. The current transformers were also modeled in the simulation so that the effects of CT on the protection performance is accommodated. CT ratios were determined according to the nominal cur-

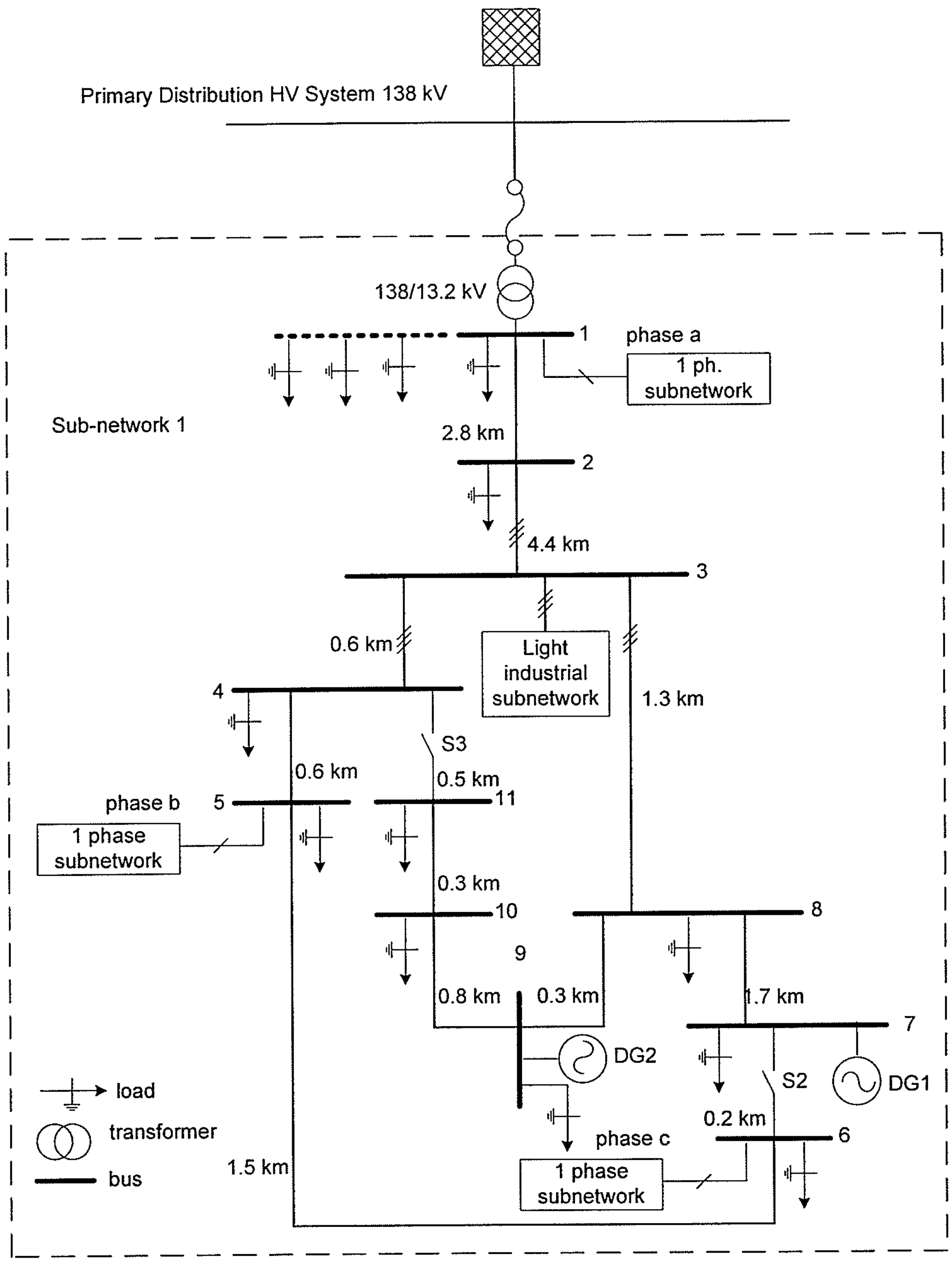

Figure 6.1: MV test distribution system

rents and fault levels at each point. Each relay agent takes the measurements from all the branches connected to the corresponding bus bar located near the relay agent. Loads were modeled as constant impendence loads. The subnetwork connected to bus-1 was modeled as three individual loads. Similarly single phase subnetworks were also replaced by equivalent concentrated loads.

6.2.1 Locating Relay Agents

Locations of the relay agents were determined based on the network configuration, interconnection to the grid and locations of the DGs. Figure 6.2 shows how relay agents were placed in the system. As described in Chapter-3, system is divided into different segments and relay agents are located at their boundaries. Relay agent R1 is placed at the substation on the boundary between the MV network and HV network. Relay agents R2, R3 and R4 are installed at the junction bus bars. Relay agents R5 and R6 are placed at the points where distributed generators are interconnected to the network. Communication links between relays are indicated by dotted lines. These communication links are considered two way channels facilitating information exchange. Communication channels were not modeled, but assumed perfect in the simulation.

To investigate the performance of the proposed protection scheme, different types of faults (internal and external) were created at different locations of the network. Simulations were carried out for both radial and meshed network configurations. Operation of the protection scheme was investigated under various scenarios It was assumed that the relay samples current signals at a frequency of 10 kHz.The network was simulated with a simulation time step of 20 μs which is sufficient to generate the transients considered in the study on short distribution lines.

6.2.2 Radial Network

Most of the distribution networks are radial in nature. In the proposed CIGRE MV benchmark network, switches S2 and S3 were kept open to obtain a radial network. Thus the communication links between R3 and R6, and R3 and R4 were disabled during the simulations of radial network.

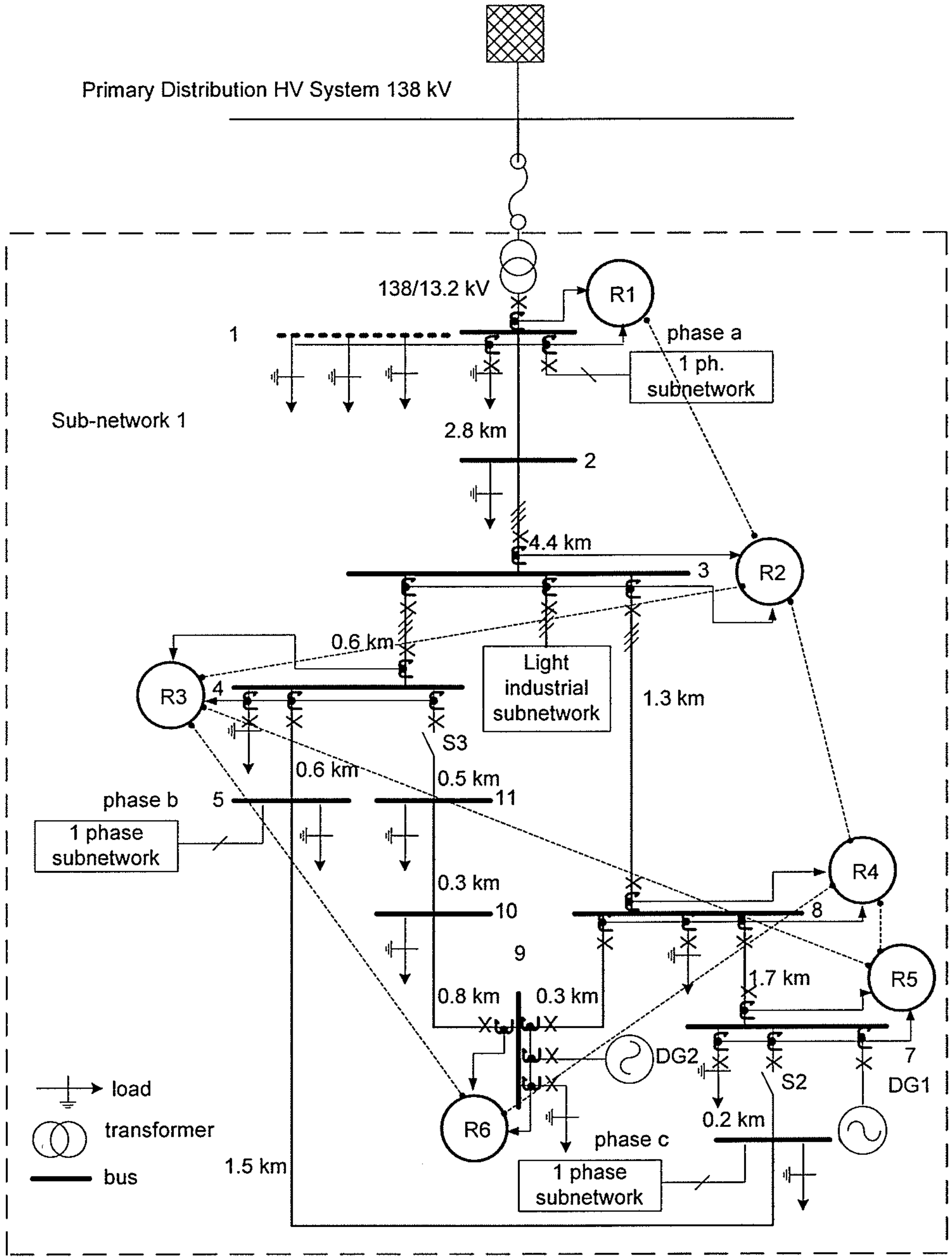

Figure 6.2: MV test distribution system with RAs

Internal Fault Location

Fault F1 at bus-1 shown in Fig. 6.3 is a solid three phase to ground fault. Relay agent R1 is located at bus-1,thus F1 is an internal fault for relay agent R1, while it is an external fault for all the other relay agents. Wavelet Transform Coefficients (WTCs) extracted from the

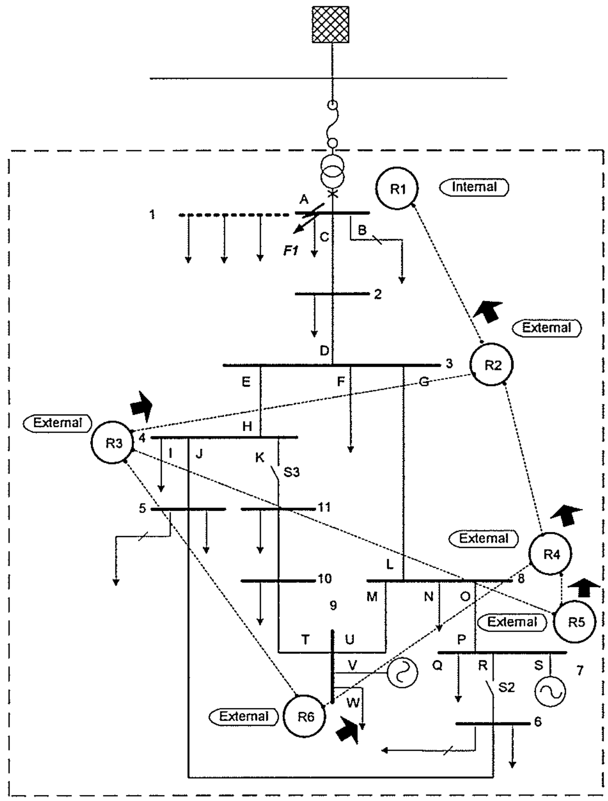

Figure 6.3: Fault categories and directions identified by Relay Agents for fault, F1

α component current signals after the fault F1 for all relay agents are shown in Fig. 6.4. The WTCs observed by R1 are having an identical sign. Feeding this WTCs to the faulty segment location algorithm described in Chapter-4 resulted in fault F1 being categorized as an internal fault. Figure 6.5 shows the correlation of coefficients calculated by relay R1 during the decision making process.

The other relay agents, R2-R6 see WTCs with different signs. The faulty segment location algorithm classified fault F1 as an external fault, and identified fault directions. Fault category and fault direction identified by each relay agent for fault F1 are shown in Fig. 6.3.

The category of the fault is indicated close to the relay agent as internal or external and the direction of the faults are marked using solid arrows along the communication link. For

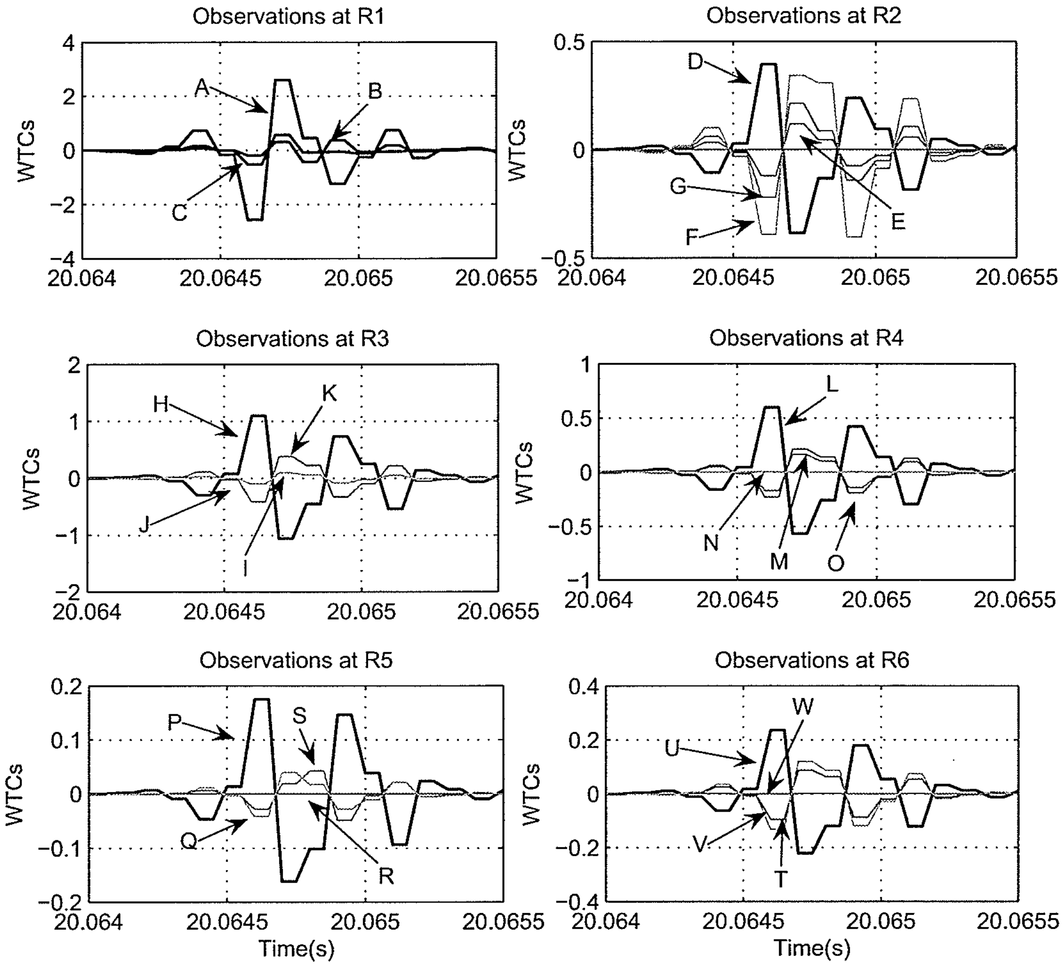

Figure 6.4: WTCs observed by Relay Agents for fault F1

the above case, all relay agents identified the fault category and direction correctly.

In order to verify the correct operation for internal faults, many internal faults were simulated at different buses, as indicated in Fig. 6.6.

Table 6.1 summarizes the type of the fault, fault impendence and the categories and directions identified by the proposed relay algorithm for different internal faults simulated. In Table 6.1 R_f is the fault impendence in ohms, while "IN" and "EX" denotes the internal and external faults respectively. Fault directions identified by the relay agents are shown within brackets. For example, for fault F5, the entry corresponding to relay agent R1 is

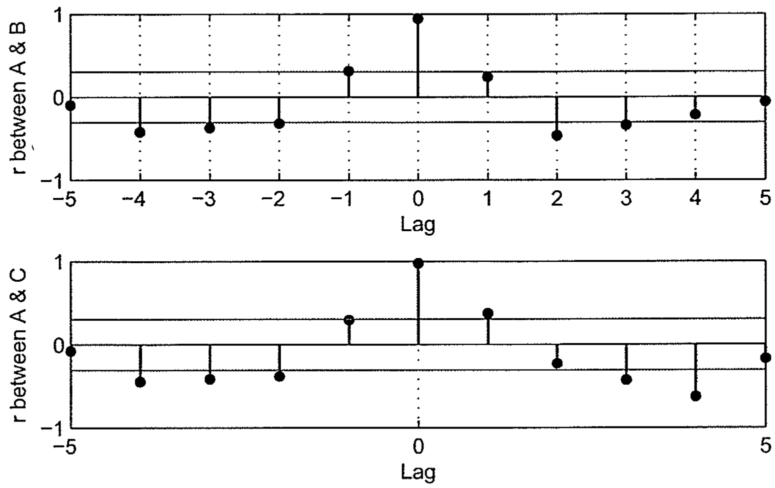

Figure 6.5: Correlation Coefficients (r) determined by Relay Agent R1 for fault F1

"Ex(R2)". This means that R1 categorized the fault as an "external fault" in the direction of R2. The same fault is identified by R2 as an internal fault. In this case direction is not relevant.

All the relay agents detected the fault category and direction correctly, even for high impendence faults such as F12.

Table 6.1: Fault Categories and Directions identified for internal faults in MV radial network

Fault	Type	$R_f(\Omega)$	R1	R2	R3	R4	R5	R6
$F5$	AB-G	100	EX(R2)	IN	EX(R2)	EX(R2)	EX(R4)	EX(R4)
$F9$	ABC	10	EX(R2)	EX(R3)	IN	EX(R2)	EX(R4)	EX(R4)
$F7$	A-G	200	EX(R2)	EX(R4)	EX(R2)	IN	EX(R4)	EX(R4)
$F20$	BC	50	EX(R2)	EX(R4)	EX(R2)	EX(R5)	IN	EX(R4)
$F12$	AC-G	250	EX(R2)	EX(R4)	EX(R2)	EX(R6)	EX(R4)	IN

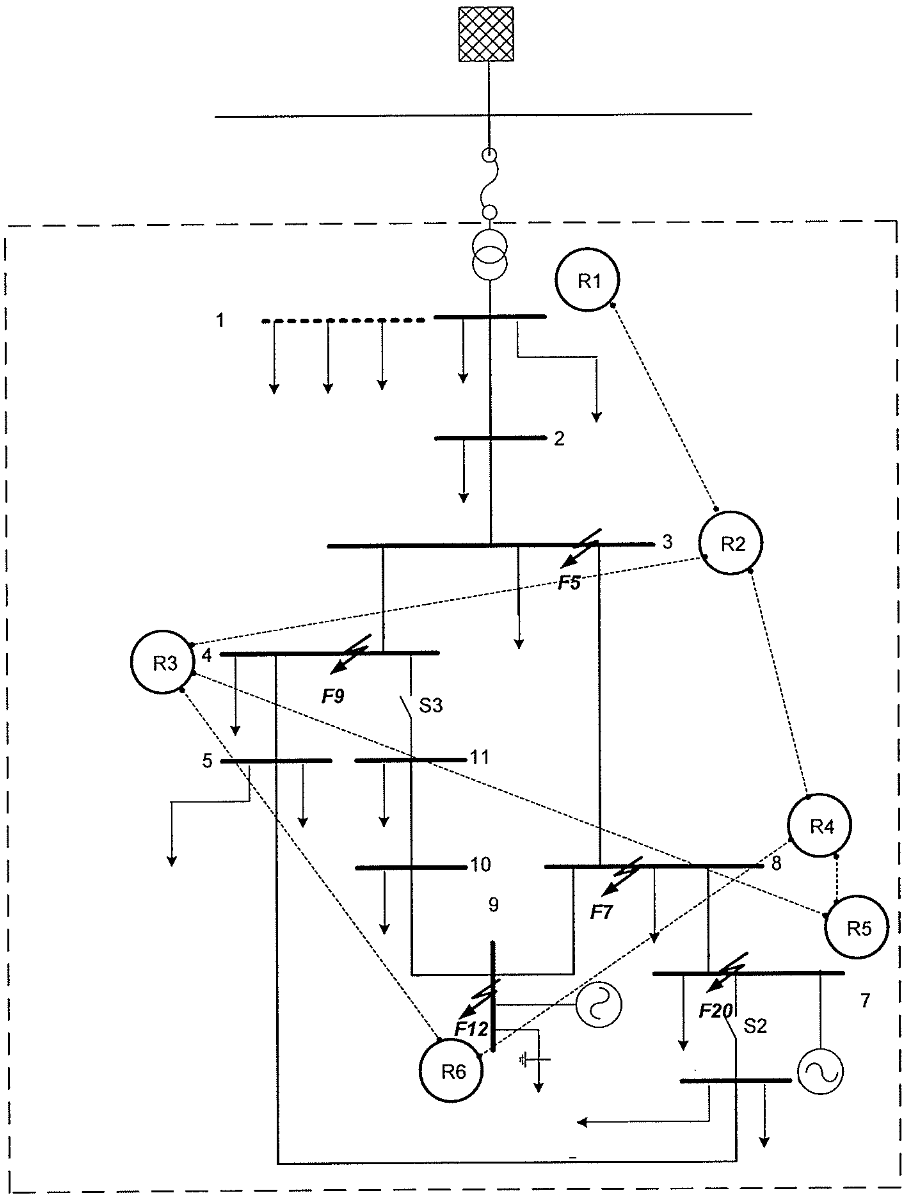

Figure 6.6: Locations of the internal faults simulated in the MV radial network

External Fault Location

Fault F2 is a three-phase to ground fault on bus-2 with 100 Ω fault impendence. Bus-2 is located between the relay agents R1 and R2. The WTCs of the α components of the current signals as observed by different relay agents are shown in Fig. 6.7.

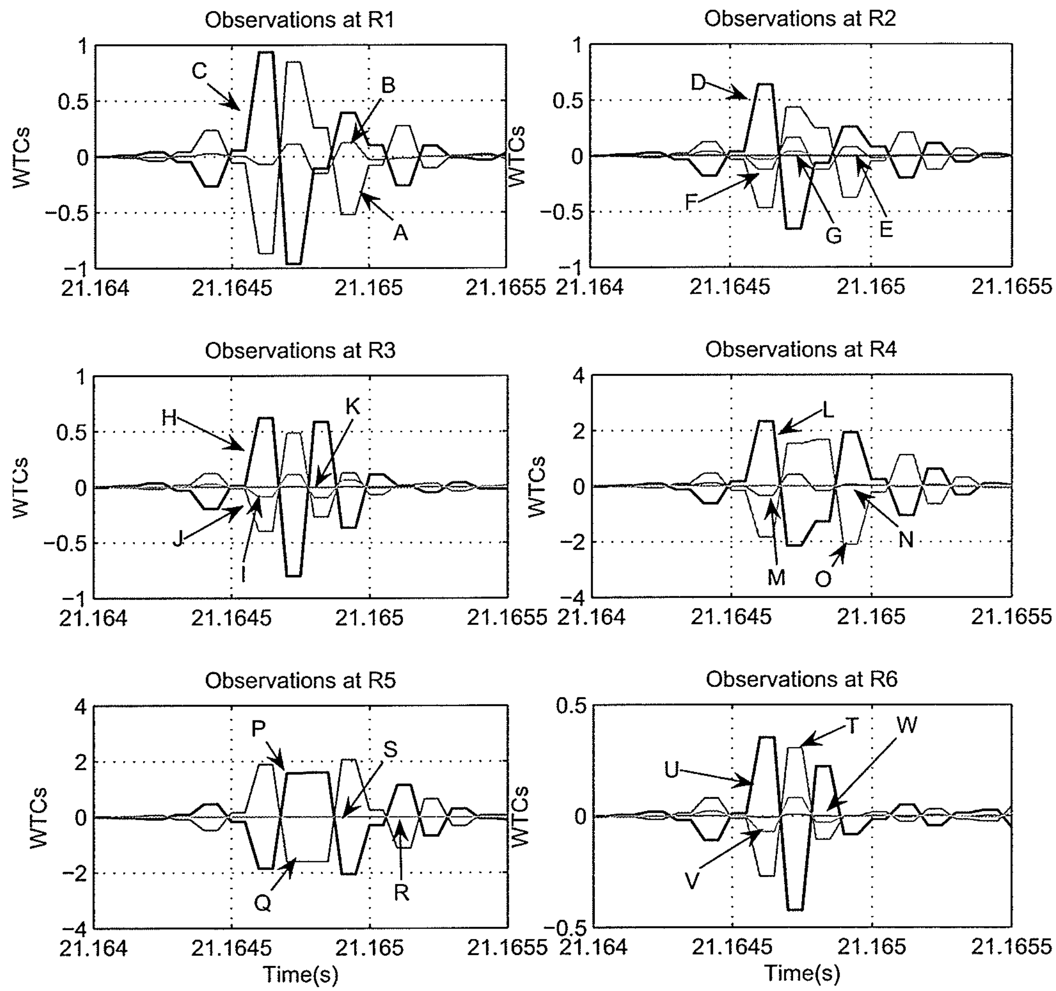

Figure 6.7: WTCs observed by Relay Agents for fault F2

The fault categories and directions identified by the relay agents are shown in Fig. 6.8. Based on this information, protection scheme correctly located the faulted segment and determined the trip signals necessary to isolate it.

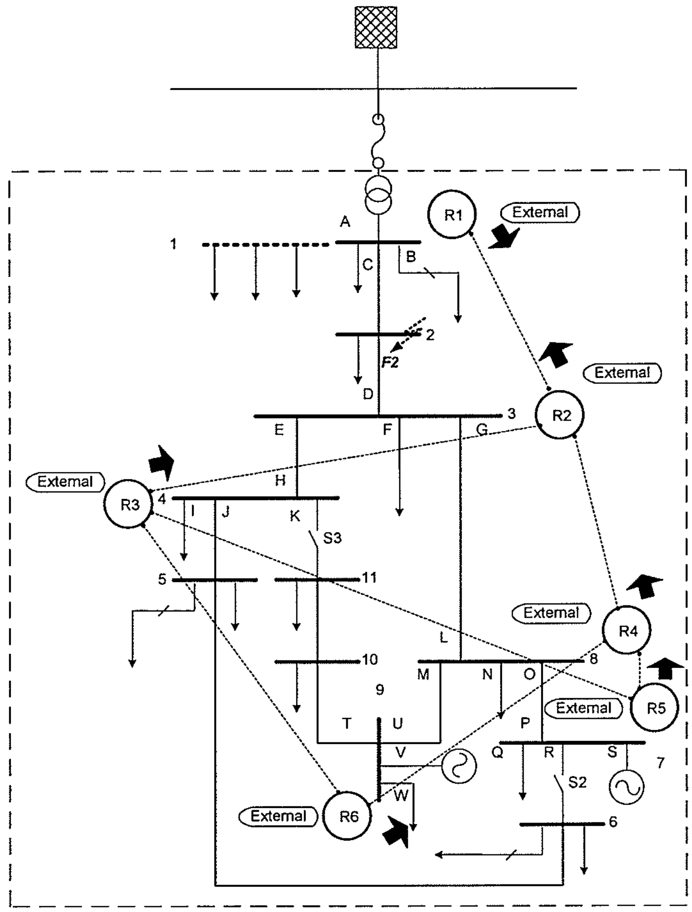

Figure 6.8: Fault categories and directions identified for Fault, F2

As in the case of internal faults, a number of different external faults were simulated to investigate the performance. The locations of the faults are shown in Fig. 6.9.

Table 6.2 summarizes the type of the fault, fault impendence and fault category and direction identified by each relay agent. Faults F3, F6 and F18 were simulated on terminal loads whereas, faults F11 and F19 were simulated on the line segments connecting DGs to the grid. All the others faults are on the distribution lines. For all these cases, the proposed protection algorithm correctly recognized the faulty segment and determined the trip signals to isolate them.

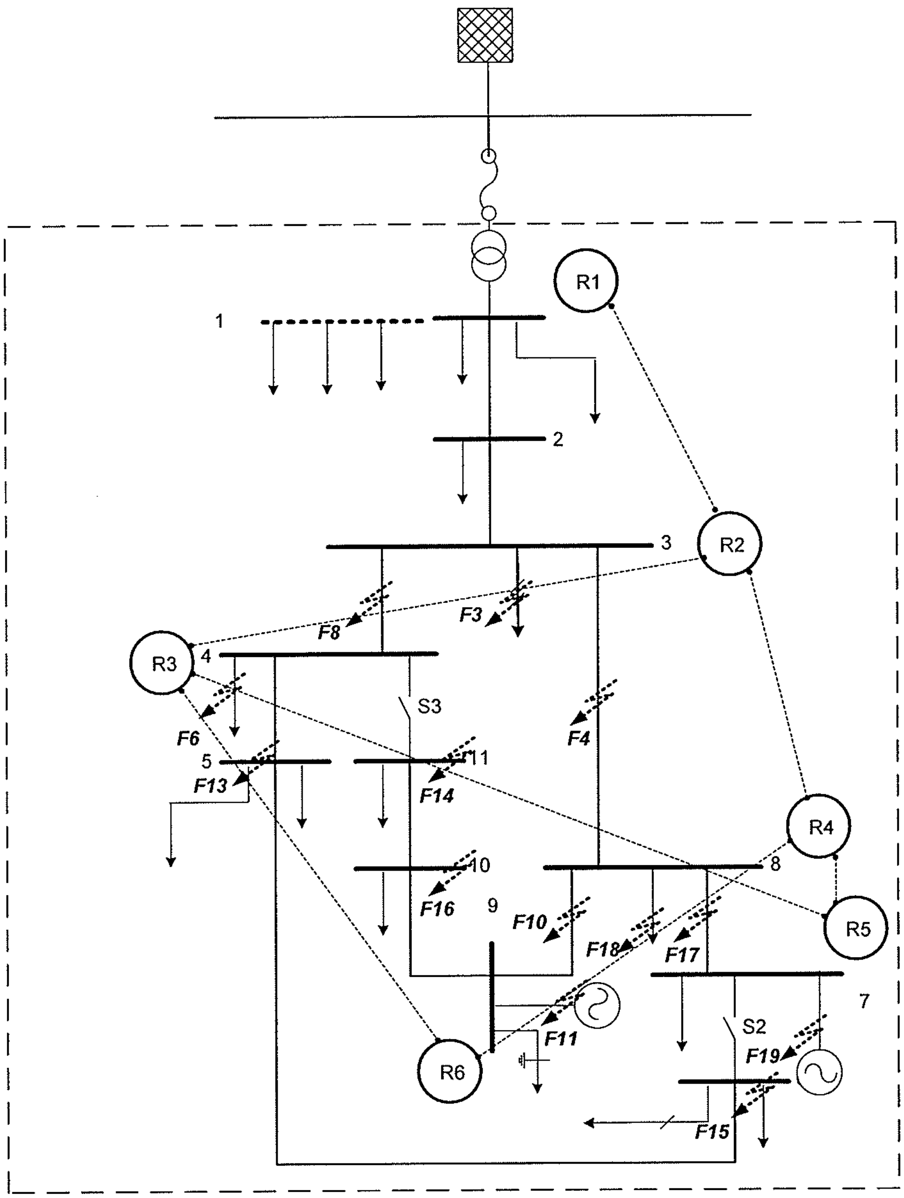

Figure 6.9: Locations of the external faults simulated in the MV radial network

Table 6.2: Fault Categories and Directions identified for External faults in MV radial network

Fault	Type	$R_f(\Omega)$	R1	R2	R3	R4	R5	R6
$F3$	AC	10	EX(R2)	EX(L)	EX(R2)	EX(R2)	EX(R4)	EX(R4)
$F4$	ABC	100	EX(R2)	EX(R4)	EX(R2)	EX(R2)	EX(R4)	EX(R4)
$F6$	AB	200	EX(R2)	EX(R3)	EX(L)	EX(R2)	EX(R4)	EX(R4)
$F8$	AB-G	250	EX(R2)	EX(R3)	EX(R2)	EX(R2)	EX(R4)	EX(R4)
$F10$	BC	100	EX(R2)	EX(R4)	EX(R2)	EX(R6)	EX(R4)	EX(R4)
$F11$	ABC-G	150	EX(R2)	EX(R4)	EX(R2)	EX(R6)	EX(R4)	EX(G2)
$F13$	A-G	0	EX(R2)	EX(R3)	EX(B5)	EX(R2)	EX(R4)	EX(R4)
$F14$	ABC-G	100	EX(R2)	EX(R4)	EX(R2)	EX(R6)	EX(R4)	EX(B10)
$F15$	AC-G	200	EX(R2)	EX(R3)	EX(B5)	EX(R2)	EX(R4)	EX(R4)
$F16$	AB	250	EX(R2)	EX(R4)	EX(R2)	EX(R6)	EX(R4)	EX(B10)
$F17$	C-G	100	EX(R2)	EX(R4)	EX(B2)	EX(R5)	EX(R4)	EX(R4)
$F18$	ABC-G	50	EX(R2)	EX(R4)	EX(R2)	EX(L)	EX(R4)	EX(4)
$F19$	BC	10	EX(R2)	EX(R4)	EX(R2)	EX(R5)	EX(G1)	EX(R4)

L- Load segments
B5 and B10- Bus numbers
G1 and G2 - DGs

Based on the above results, it can be concluded that the proposed faulty segment location technique can correctly locate and isolate the faulted segments with a minimum interruption to the network in radial distribution networks.

6.2.3 Meshed Network

Distribution networks are sometime operated as meshed networks, to improve the reliability and voltage profile. In order to investigate the performance of the proposed protection scheme in mesh networks, S2 and S3 switches in CIGRE bench mark MV network shown in Fig. 6.1 were closed.

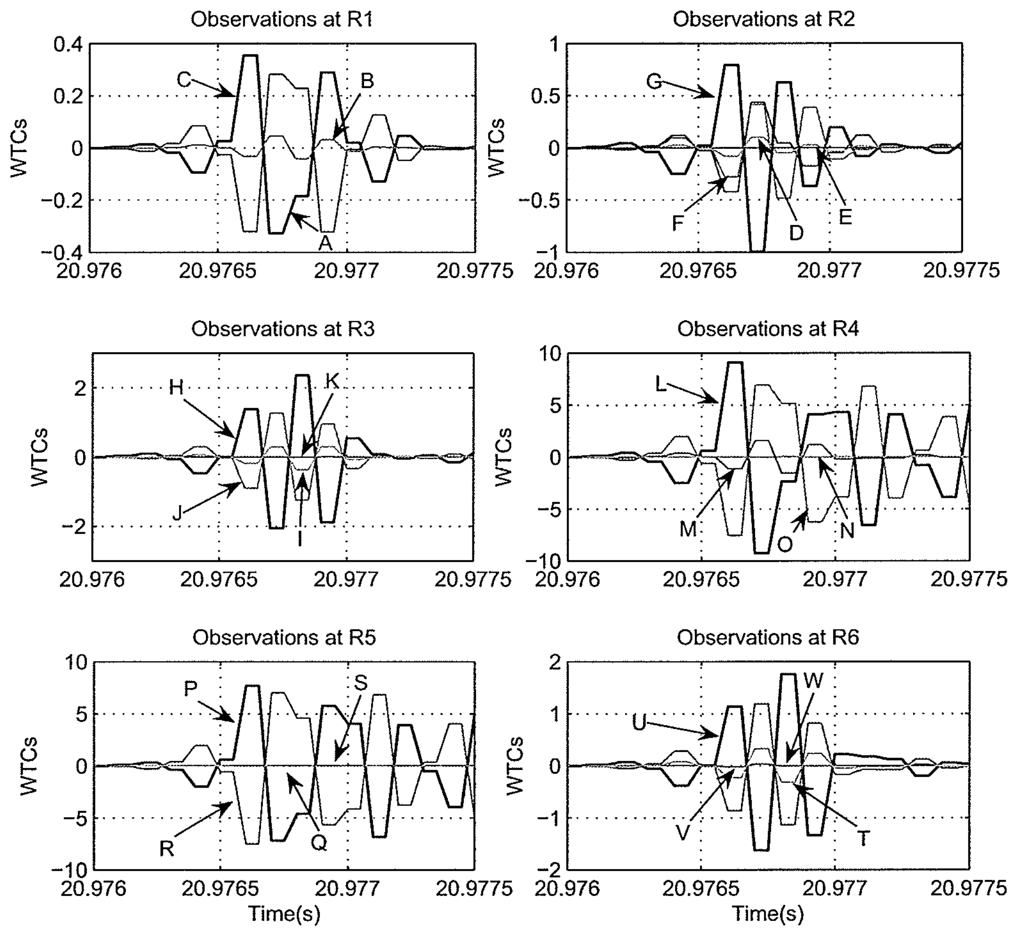

Figure 6.10: WTCs observed by Relay Agents for fault F4

Figure 6.10 shows the WTCs of the the α components of the current signals for the external fault F4 (Phase A-B, fault impendence of 100 Ω) simulated on the segment connecting bus-3 and bus-8. Since this is an external fault for all the relay agents, the sets of

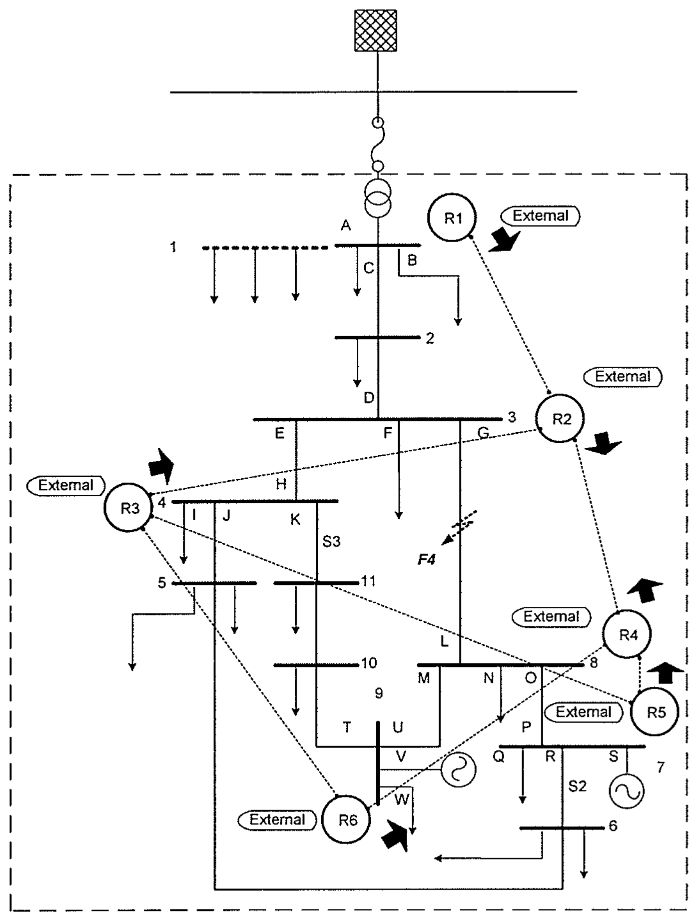

Figure 6.11: Fault categories and directions identified for fault, F4

WCTs determined at each point shows different signs. After feeding these WTCs to the faulty segment location algorithm, the fault categories and directions identified by all relay agents are also shown in Fig. 6.11.

In order to investigate the performance of the proposed protection scheme in meshed networks, the faults simulated in the radial network (shown in Tables 6.1 and6.2) were applied for the meshed network as shown in Fig. 6.12. Here the internal faults are drawn using solid lines whereas, the external faults are drawn in dotted lines. Table 6.3 summarizes the fault types, fault impendence, fault categories and fault directions identified by the relay agents.

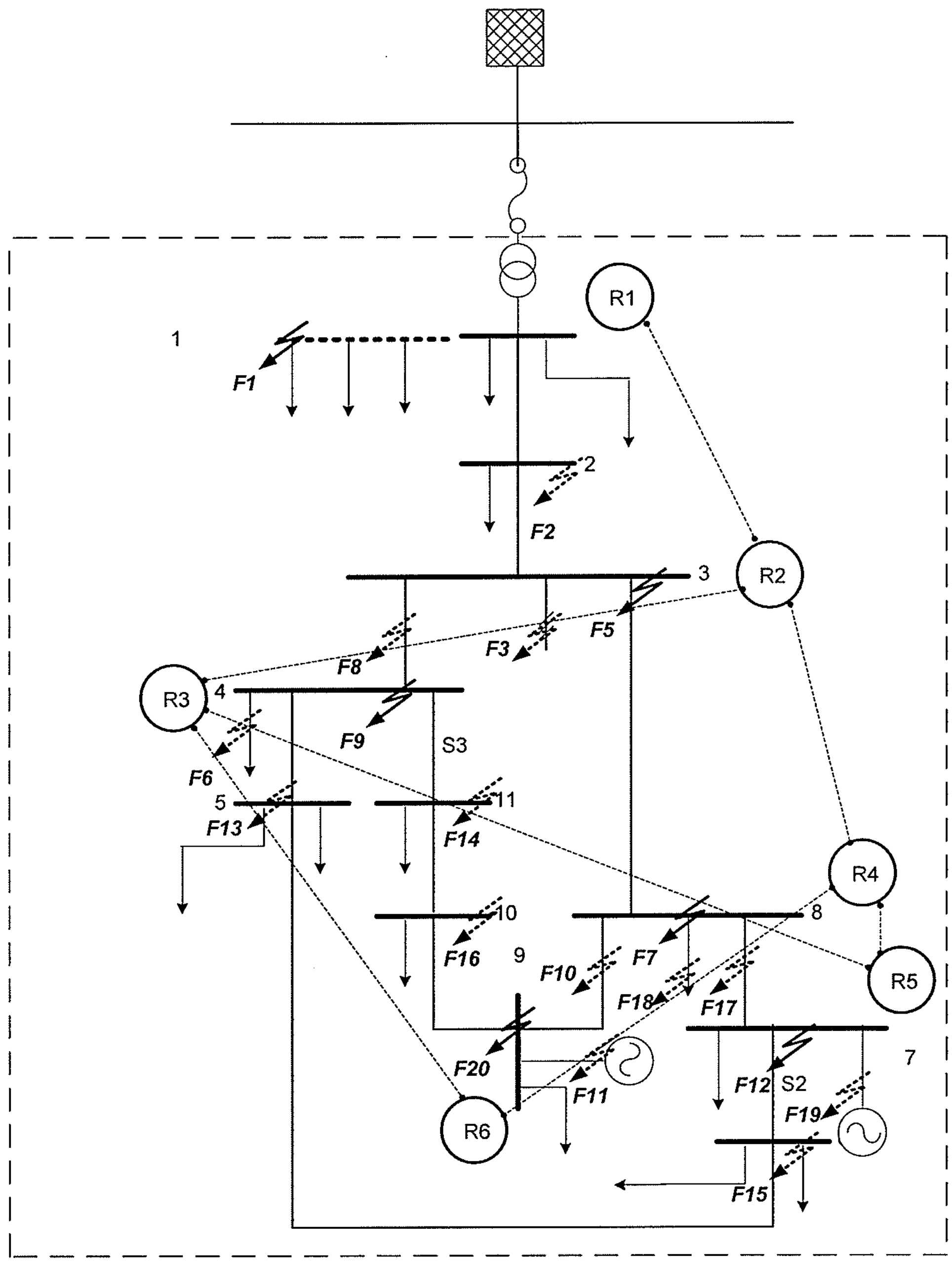

Figure 6.12: Locations of the faults simulated in the MV meshed network

According to the simulation results, the proposed fault location algorithm shows correct fault direction and faulty segment identification and faulty segment isolation for the faults F1-F10, F13 and F18. During the other faults, all the relay agents except R2 showed correct direction identification. The failures in direction identification at R2 is due to the fact that, the fault currents are flowing through two branches at relay R2 during these faults, thus the sampling frequency is not sufficient to capture the initial transient current which gives the fault direction. In such circumstances, the relay algorithm in its current form does not take any action against the fault. This situation usually happens for a fault that occurs far from the relay agent. Such a fault is likely to be isolated by the other relay agents that are located close to the fault. For example, the simulation results in Table 6.3 showed correct faulty segment identification and isolation for all the cases, despite the failure of relay agent R2.

Table 6.3: Fault categories and directions identified for faults in MV meshed network

Fault	Type	$R_f(\Omega)$	R1	R2	R3	R4	R5	R6
$F1$	ABC-G	0	IN	EX(R1)	EX(R2)	EX(R2)	EX(R4)	EX(R4)
$F2$	ABC	10	EX(R2)	EX(R1)	EX(R2)	EX(R2)	EX(R4)	EX(R4)
$F3$	AB-G	50	EX(R2)	EX(L)	EX(R2)	EX(R2)	EX(R4)	EX(R4)
$F5$	BC	150	EX(R2)	IN	EX(R2)	EX(R2)	EX(R4)	EX(R4)
$F6$	A-G	200	EX(R2)	EX(R3)	EX(L)	EX(R2)	EX(R3)	EX(R3)
$F7$	BC-G	100	EX(R2)	EX(R4)	EX(R2)	IN	EX(R4)	EX(R4)
$F8$	AC-G	250	EX(R2)	EX(R3)	EX(R2)	EX(R2)	EX(R4)	EX(R4)
$F9$	C-G	10	EX(R2)	EX(R3)	IN	EX(R2)	EX(R3)	EX(R3)
$F10$	AB-G	20	EX(R2)	EX(R4)	EX(R6)	EX(R6)	EX(R4)	EX(R4)
$F11$	ABC-G	100	EX(R2)	EX(-)	EX(R6)	EX(R6)	EX(R4)	EX(G2)
$F12$	AC-G	0	EX(R2)	EX(-)	EX(R6)	EX(R6)	EX(R4)	IN
$F13$	ABC	10	EX(R2)	EX(R3)	EX(R5)	EX(R5)	EX(R3)	EX(R4)
$F14$	BC-G	200	EX(R2)	EX(-)	EX(R6)	EX(R6)	EX(R4)	EX(R3)
$F15$	AB	250	EX(R2)	EX(-)	EX(R5)	EX(R5)	EX(R3)	EX(R4)
$F16$	BC	300	EX(R2)	EX(-)	EX(R6)	EX(R6)	EX(R4)	EX(R3)
$F17$	B-G	150	EX(R2)	EX(-)	EX(R5)	EX(R6)	EX(R4)	EX(R4)
$F18$	AC-G	50	EX(R2)	EX(R4)	EX(R2)	EX(L)	EX(R4)	EX(R4)
$F19$	AC	10	EX(R2)	EX(-)	EX(R5)	EX(R5)	EX(G1)	EX(R4)
$F20$	ABC-G	100	EX(R2)	EX(-)	EX(R5)	EX(R5)	IN	EX(R4)

Note: - denotes failure in direction identification

Even though, an accurate fault direction identification has been shown by the relay agent R2 for all the external faults occurred in its control area (faults F2,F3, F4 and F8), the possibility of the proposed faulty segment location algorithm failing due to parallel fault currents at the relay cannot be ruled out. Therefore, an investigation was carried out to determine the possibility of improving the fault direction identification capability by increasing the sampling rate.

Sampling frequency was increased to 50 kHz. Table 6.4 summarizes the fault types, fault impedance, and fault category and direction determined by each relay agent. Now, for all the faults except F11, relay agent R2 determined the fault directions correctly. This is because, at 50 kHz sampling frequency, the relay could recognize the difference in the arrival times of the high frequency transients from the two paths. Powerful processors are required to handle higher sampling frequencies. However use of higher sampling rate does not affect the communication bandwidth requirements.

Table 6.4: Fault categories and directions identified for faults in MV meshed network at f_s=50kHz

Fault	Type	$R_f(\Omega)$	R1	R2	R3	R4	R5	R6
$F11$	ABC-G	100	EX(R2)	EX(-)	EX(R6)	EX(R6)	EX(R4)	EX(G2)
$F12$	AC-G	0	EX(R2)	EX(R4)	EX(R6)	EX(R6)	EX(R4)	IN
$F14$	BC-G	200	EX(R2)	EX(R3)	EX(R6)	EX(R6)	EX(R4)	EX(R3)
$F15$	AB	250	EX(R2)	EX(R4)	EX(R5)	EX(R5)	EX(R3)	EX(R4)
$F16$	BC	300	EX(R2)	EX(R3)	EX(R6)	EX(R6)	EX(R4)	EX(R3)
$F17$	B-G	150	EX(R2)	EX(R4)	EX(R5)	EX(R6)	EX(R4)	EX(R4)
$F19$	AC	10	EX(R2)	EX(R3)	EX(R5)	EX(R5)	EX(G1)	EX(R4)
$F20$	ABC-G	100	EX(R2)	EX(R4)	EX(R5)	EX(R5)	IN	EX(R4)

Thus simulation results can be summarized as, the proposed protection algorithm may fail to determine the fault directions accurately when there are more than one fault current paths available through the relay location. The situation can be improved by using a higher sampling frequency(50kHz). However, simulation results obtained at lower sampling rate (10kHz) showed that the proposed faulty segment location scheme could locate all the faulty segments correctly, even if some of the relays failed to identify the fault directions.

6.3 High Voltage Test System

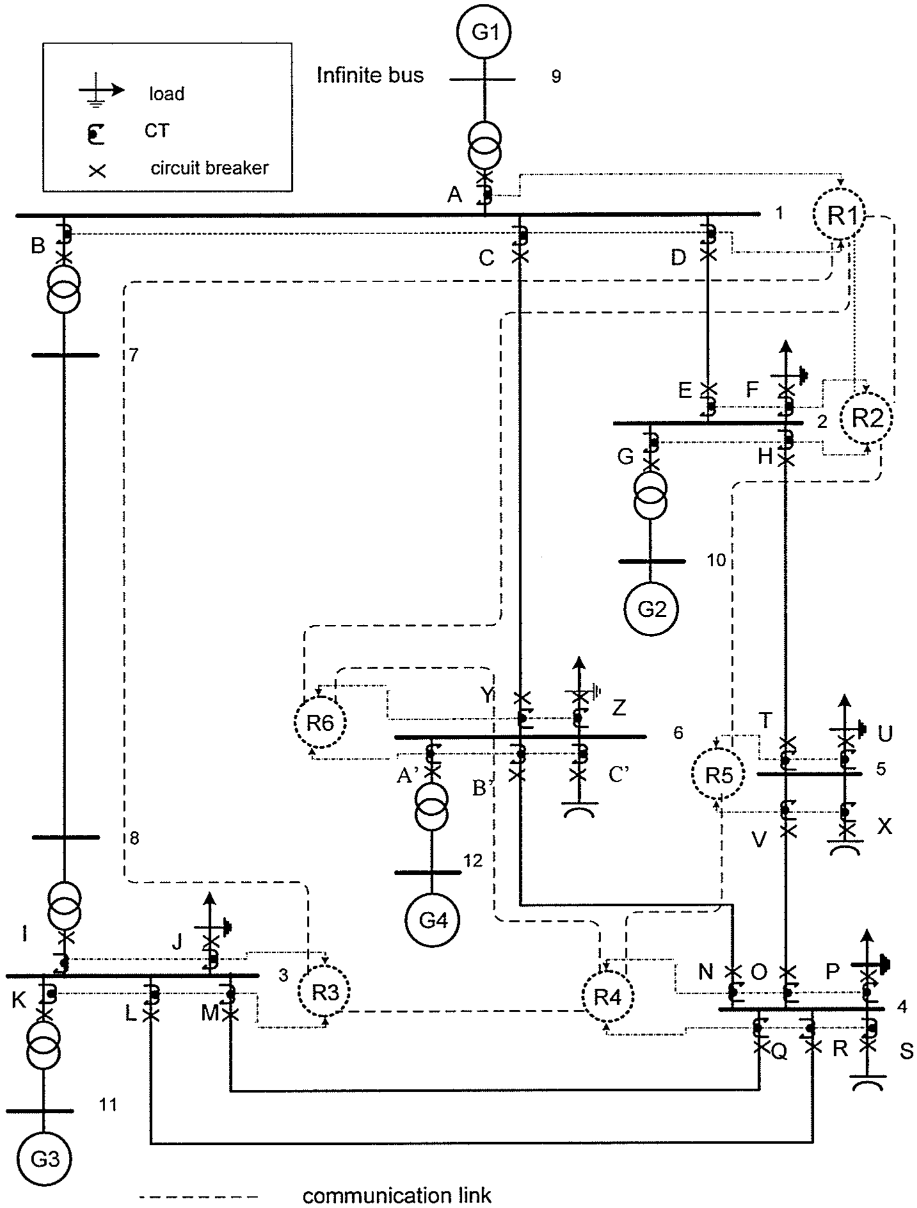

Figure 6.13: 230kV 12 Bus Test System

Although the proposed protection scheme was developed for addressing the protection needs of distribution systems, this scheme can be applied for the protection of high voltage transmission systems. The rapid fault isolation capability of the proposed protection scheme may be a useful feature in HV transmission system applications. For example,

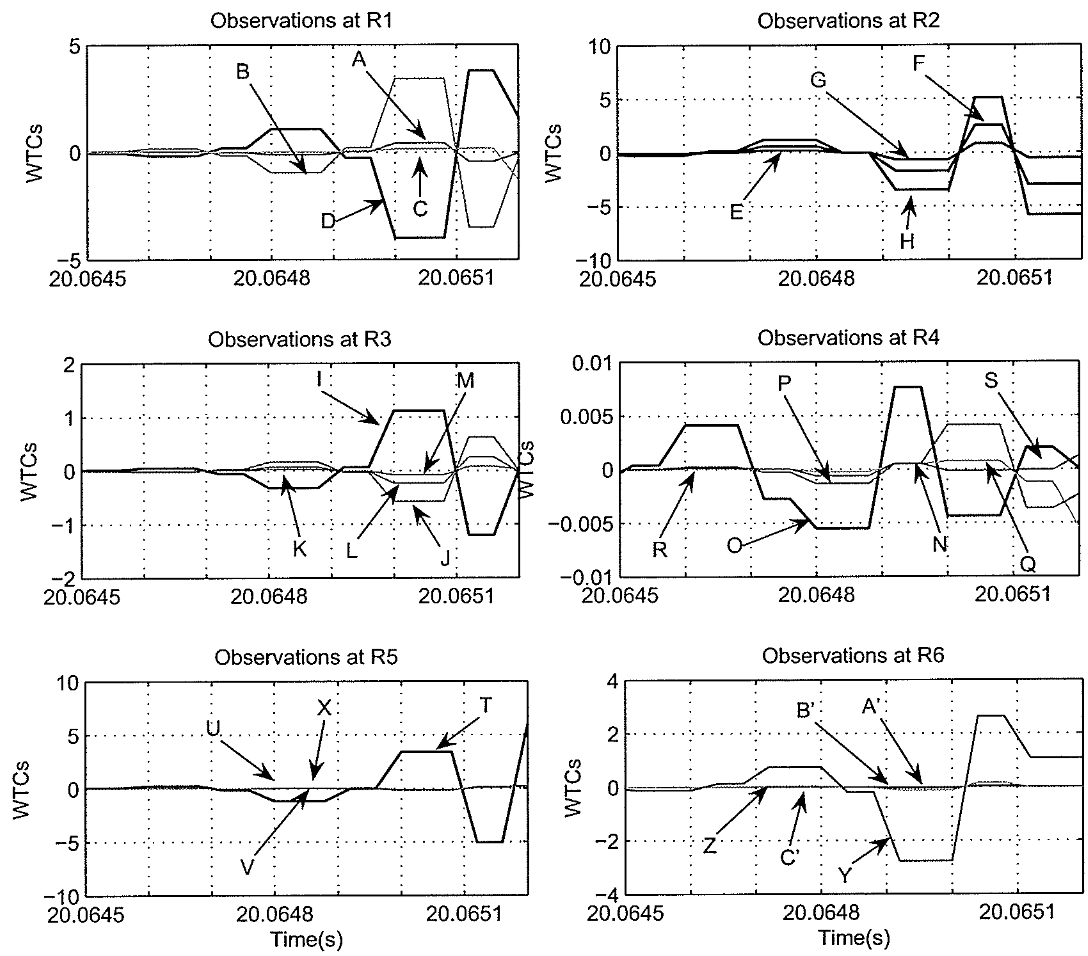

Figure 6.14: WTCs observed by Relay Agents for fault F2

Figs. 4.2, 4.4 and 4.6 show that information required to determine the faulted segment can be collected in less than a quarter cycle after the fault. The actual detection time is determined by the processing and communication speed. In order to demonstrate the applicability of the proposed protection scheme for high voltage transmission systems, the 230kV, 12-bus transmission system [43] shown in Fig. 6.13 was used. The system was simulated in PSCAD/EMTDC. Six locations were selected to install relay agents considering the network configuration and locations of the generators. Different types of faults (balanced and unbalanced) with different fault impendences were simulated at 20 different locations of the network. First consider Fault F2, which is a phase B-G fault with 100 Ω fault impendence at bus-2. Again the sampling rate of the relays were set to 10 kHz. The

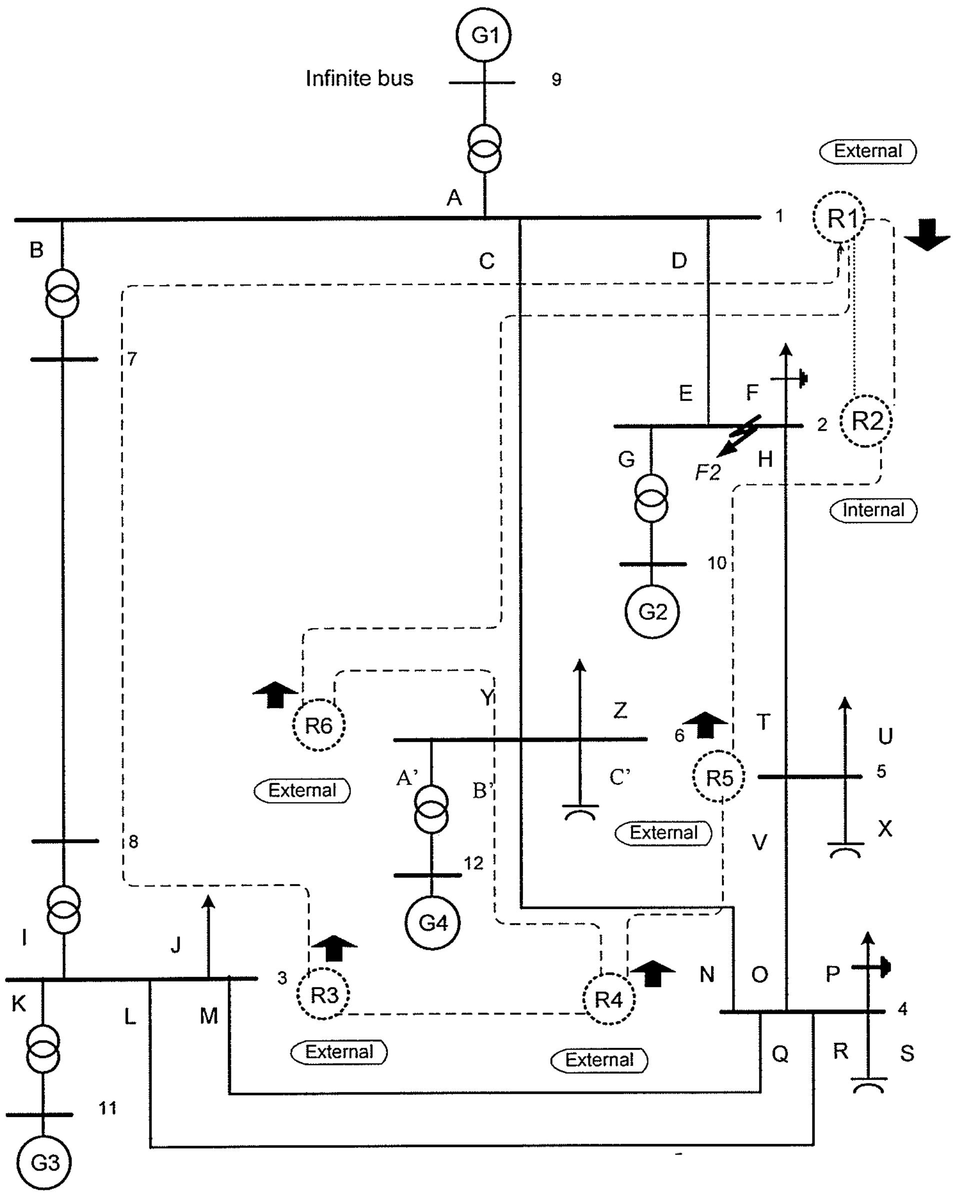

Figure 6.15: Fault types and directions identified for fault F2

WTCs observed by relay agents for fault F2 are shown in Fig. 6.14. The WTCs observed by R2 which correspond to branches connected to bus-2 have identical sign. This caused R2

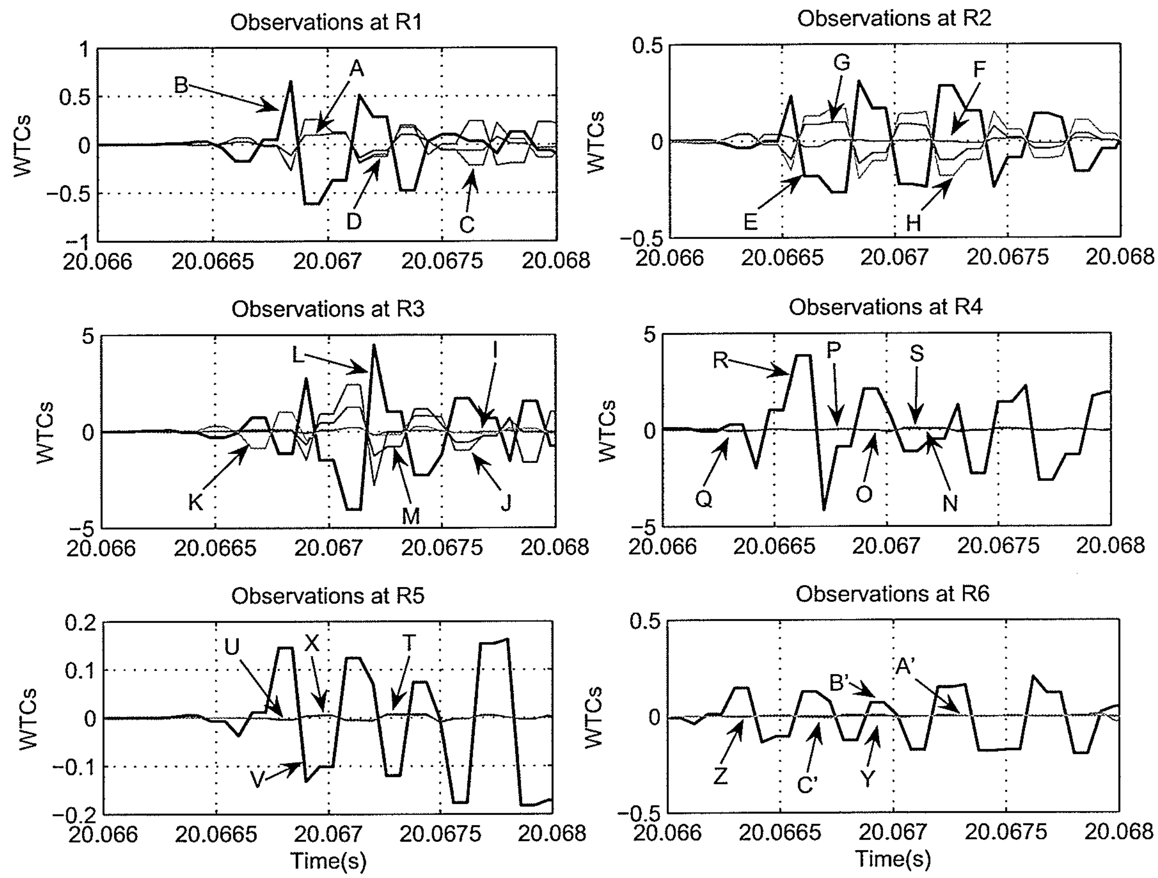

Figure 6.16: WTCs observed by Relay Agents for fault F12

to determine F2 as an internal fault at bus-2. The WTCs observed at other relay locations indicate that F2 is an external fault to them.The fault types and fault directions identified by the six relay agents are also shown in Fig. 6.15

Next consider the fault F12 on one of the parallel lines connecting buses 3 and 4. It is a three phase fault with 10 Ω fault resistance. This is a special case, since the fault is on a parallel line, a situation that rarely occur in distribution systems.

Figure 6.16 shows the WTCs observed for fault F12. Each of the relay agents see a WTC that has an opposite sign to the other WTCs observed by it. WTCs which are having opposite sign to those of others are shown in thick black lines. These observation results in F12 being categorized as an external fault by relay agents. Fault types and directions identified using WTCs by the the relay agents are also shown in Fig. 6.17.

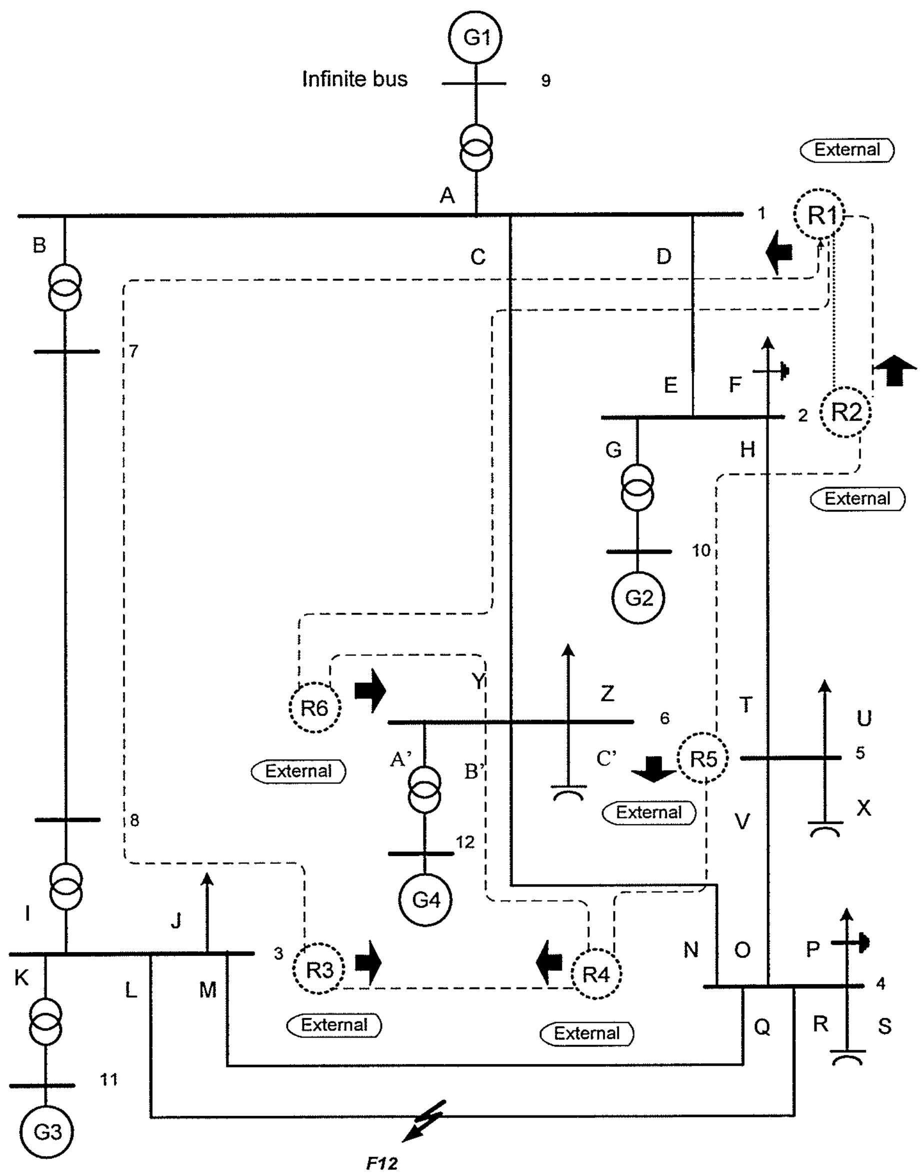

Figure 6.17: Fault types and directions identified for fault F12

When there are two parallel lines between two buses and only one communication link is available between them, the fault location algorithm need to exchange two sets of 'YES', 'NO' information between each other. Thus one relay agent can treat the other relay agent as two individual relay agents. In this case using the above mentioned approach, the fault location algorithm correctly determined the faulty segment out of the two parallel lines.

Table 6.5 summarizes the fault categories and directions identified by the relay agents for the other faults simulated in HV network. The simulation results showed accurate fault direction identification at all relay locations except at relay R3. R3 was unable to determine the fault direction for two cases. This could be overcome by using high sampling rate. However, the faulty segment identification results were accurate for all 20 cases, even with R3 being unable to determine the fault direction.

Table 6.5: Fault categories and directions identified for faults in HV network

Fault	Type	$R_f(\Omega)$	R1	R2	R3	R4	R5	R6
$F1$	ABC-G	0	IN	EX(R1)	EX(R1)	EX(R3)	EX(R2)	EX(R1)
$F2$	ABC	10	EX(R2)	IN	EX(R1)	EX(R4)	EX(R2)	EX(R1)
$F3$	AB-G	100	EX(R3)	EX(R1)	IN	EX(R3)	EX(R4)	EX(R4)
$F4$	AB-G	200	EX(R3)	EX(R1)	EX(-)	IN	EX(R4)	EX(R4)
$F5$	A-G	50	EX(R2)	EX(R5)	EX(R4)	EX(R5)	IN	EX(R1)
$F6$	ABC-G	100	EX(R6)	EX(R1)	EX(R4)	EX(R6)	EX(R2)	IN
$F7$	BC-G	150	EX(R2)	EX(R1)	EX(R1)	EX(R3)	EX(R2)	EX(R1)
$F8$	BC	200	EX(R3)	EX(R5)	EX(R4)	EX(R5)	EX(R2)	EX(R1)
$F9$	ABC	0	EX(R6)	EX(R1)	EX(R1)	EX(R3)	EX(R2)	EX(R1)
$F10$	C-G	50	EX(R2)	EX(R5)	EX(R4)	EX(R5)	EX(R4)	EX(R4)
$F11$	AC-G	250	EX(R6)	EX(R1)	EX(R4)	EX(R6)	EX(R4)	EX(R4)
$F13$	BC-G	50	EX(R3)	EX(R1)	EX(R4)	EX(R3)	EX(R4)	EX(R4)
$F14$	ABC-G	0	EX(R3)	EX(R1)	EX(R1)	EX(R3)	EX(R2)	EX(R1)
$F15$	AB-G	250	EX(R2)	EX(G2)	EX(R1)	EX(R3)	EX(R2)	EX(R1)
$F16$	AC	300	EX(R3)	EX(R1)	EX(R1)	EX(R3)	EX(R4)	EX(R4)
$F17$	ABC-G	250	EX(R3)	EX(R1)	EX(G3)	EX(R3)	EX(R4)	EX(R1)
$F18$	ABC	100	EX(R3)	EX(R1)	EX(R4)	EX(L)	EX(R4)	EX(R4)
$F19$	BC	10	EX(R2)	EX(R5)	EX(-)	EX(R5)	EX(L)	EX(R1)
$F20$	ABC	100	EX(R6)	EX(R1)	EX(R4)	EX(R6)	EX(R2)	EX(L)

Based on the simulation studies carried out using HV transmission system, it can be concluded that the proposed protection scheme gives accurate faulty segment identification and isolation with minimum interruption to the network. Further, the simulation results showed that the proposed protection scheme is capable of handling the networks with parallel lines.

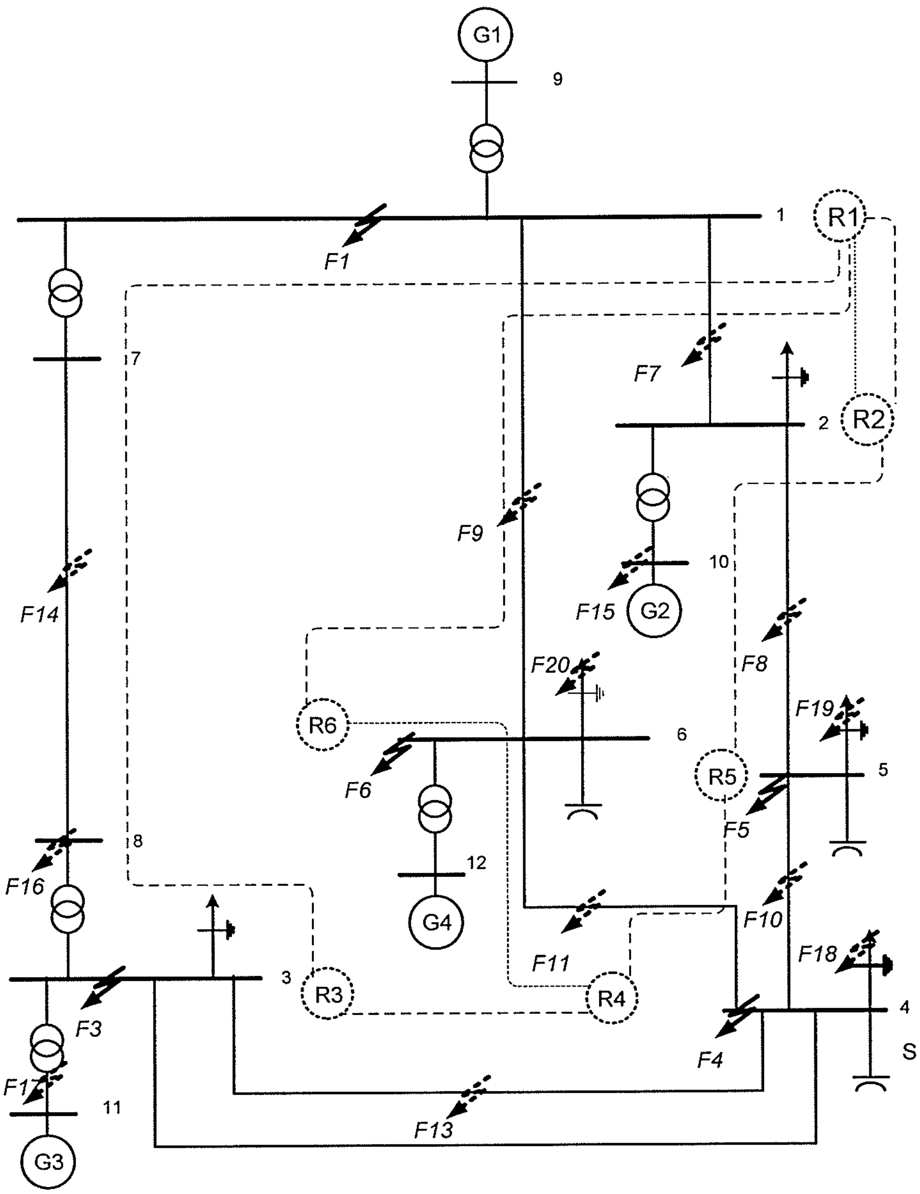

Figure 6.18: Faults simulated in HV network

6.4 Communication Failure

When a relay agent does not get the directional information form the neighboring relay agents within a pre-specified time, the relay agent assumes a communication failure and locate the faults based on the available information and overcurrent measurements observed in the direction of identified fault. To investigate this feature MV mesh network was simulated without the communication link between relay agents R2 and R4 . The fault categories and fault directions determined and information exchanged (using the available communication links) by the relay agents for a fault, F (ABC-G with 10 Ω fault impendence) simulated between the relay agents R2 and R4 are shown in Fig. 6.19.

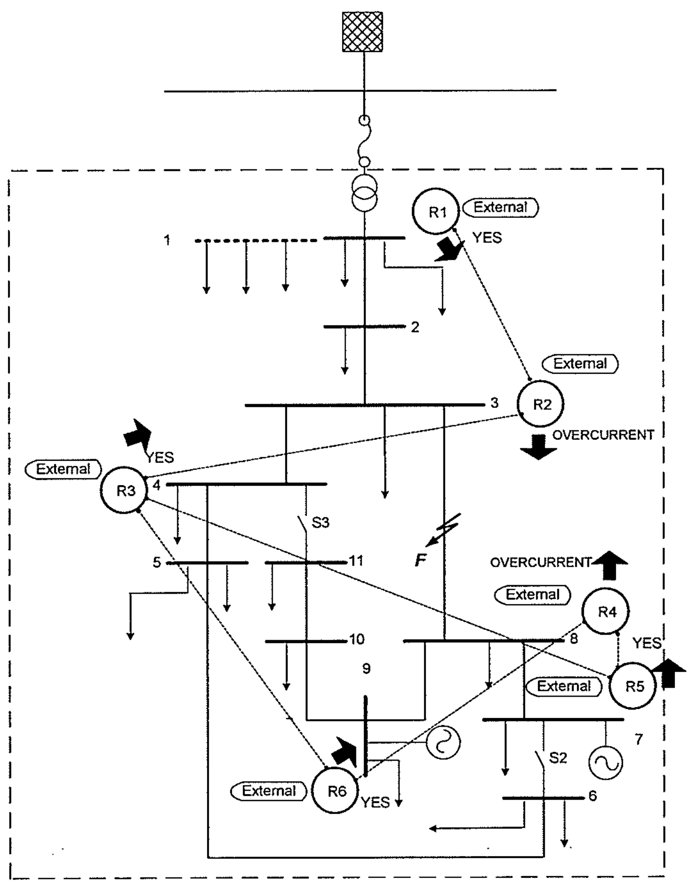

Figure 6.19: Fault identification during communication failure

The fault direction identified by R2 is in the direction of R4 whereas, the fault direction identified by R4 is in the direction of R2. Since there is a failure in the communication between R2 and R4, trip signals were generated based on the magnitude of the power frequency current observed in the relevant branches.

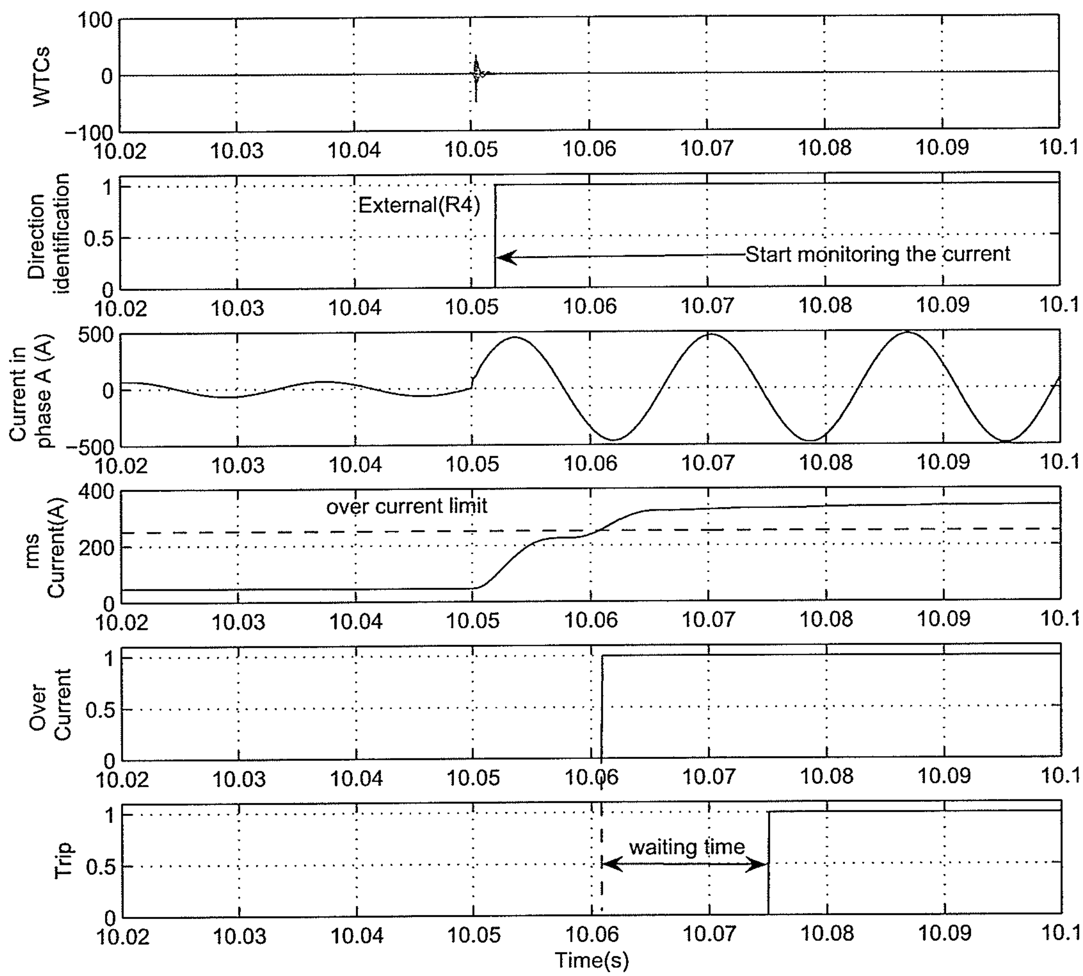

Figure 6.20: Operation of the relay agent R2 during communication failure, for fault F

Figure 6.20 shows the operation of relay R2 during this fault. The top most graph shows the observed WTCs during the fault. The fault direction was identified as R4 using WTCs. Since there is a failure in communication between R2 and R4, relay R2 started monitoring the rms current in the direction of R4. The variation of the current monitored in phase-A and the corresponding rms current are also shown in Fig. 6.20. Then the relay waited few cycles observing the over current, before sending the trip signal to isolate the fault. Similarly relay R4 determined the fault direction correctly and sent the trip signal to isolate the fault.

Simulations were carried out for 20 different types of faults simulated at different locations of the MV network with one communication link taken out. Simulation results show accurate faulty segment identification and isolation for all of the faults. Since the operation of the protection scheme during the communication failures is mainly depend on overcurrent measurements, sometimes a group of segments in addition to the faulty segment were isolated.

When there are more than one failed communication links many relays may operate based on the rms fault current, isolating unnecessarily large part of the network. However the network is still protected. The analogous situation in a conventional protection system is when a fault is identified and cleared by the backup protection scheme when the primary protection scheme fails.

6.5 Effects of Current Transformer Saturation

Current transformer saturation affects protection system operation depending on the type of relay used. For example electromechanical relays that develop an operating torque through internal phase-shifted fluxes can perform differently due to CT saturation. On the other hand, the response of digital relays depends on the relay operation software[41]. This section investigates the performance of the proposed protection scheme during CT saturation.

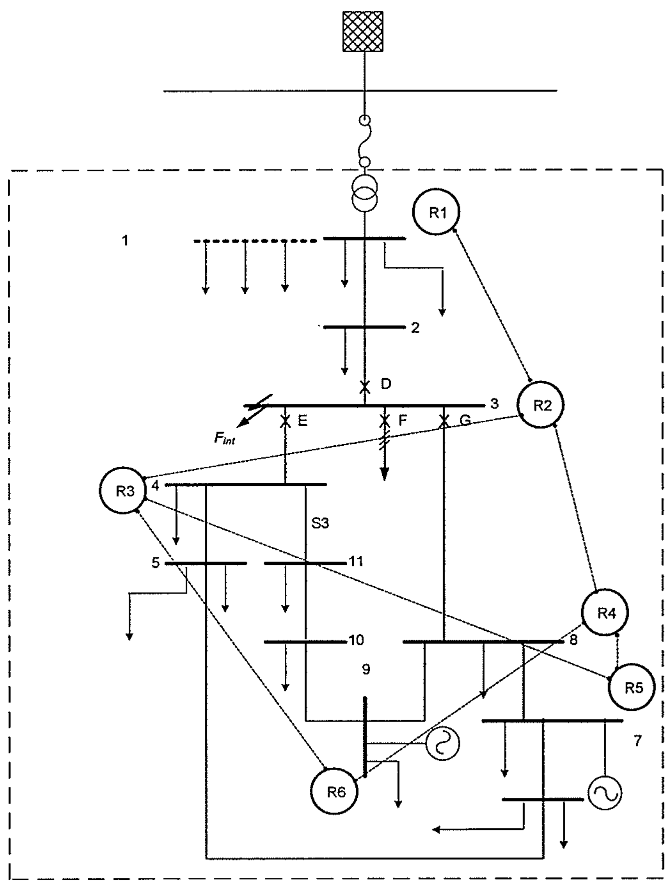

Figure 6.21: Internal fault simulated in radial network

MV radial network was used to study the effect of CT saturation on faulty segment identification. The set of CTs installed at D (which take current measurements for relay

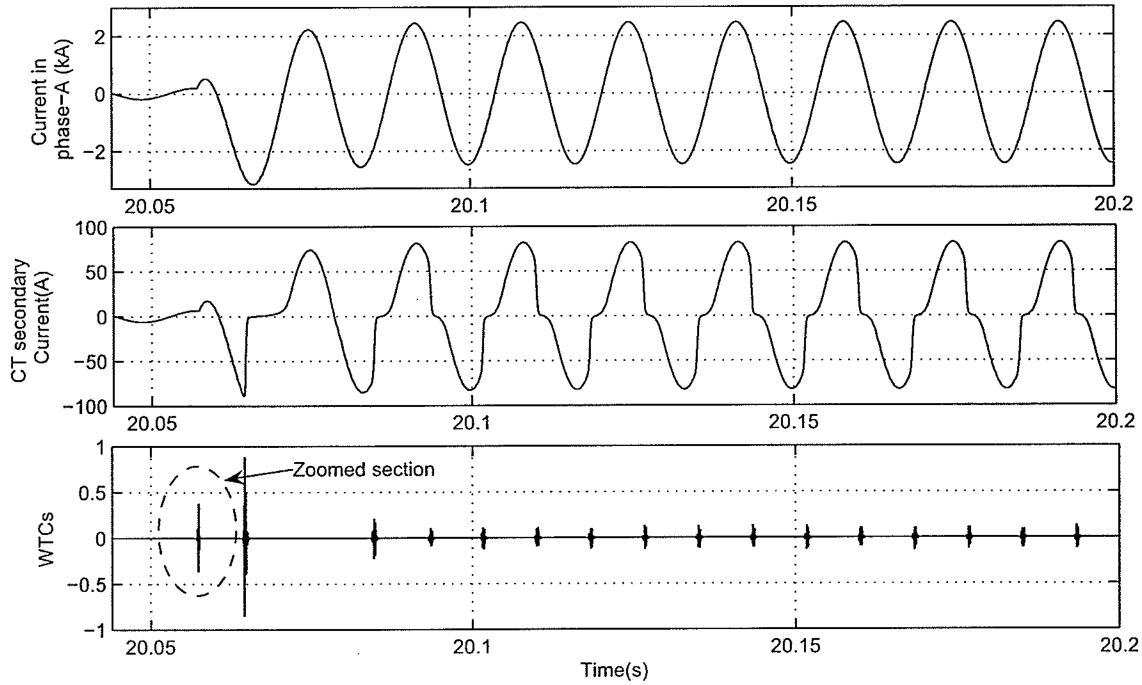

Figure 6.22: CT measurement for phase-a current at point D during a internal fault and WTCs observed at R2

agent R2) were made saturated under different internal and external fault situations. Simulation results are presented in Fig. 6.21 for the internal fault,F_{int}, which is a phase ABC-G, solid fault.

Figure 6.22 shows the variation of the phase-A current, corresponding saturated CT secondary waveform and the WTC observed at R2 for fault F_{int}. A zoomed view of the WTCs observed by relay agent R2 are shown in Fig. 6.23. All the WTCs observed at R2 including the WTCs obtained form saturated current measurement show positive correlation with each other. Faulty segment identification results shows correct fault category identification by relay agent R2 as an internal fault.

These simulation results shows accurate fault category and direction identification using the current measurements taken with the CT saturated. This is due to the fact that the proposed fault category and direction identification is based on high frequency transients initiated immediately after the fault. They are extracted at the point where there is a

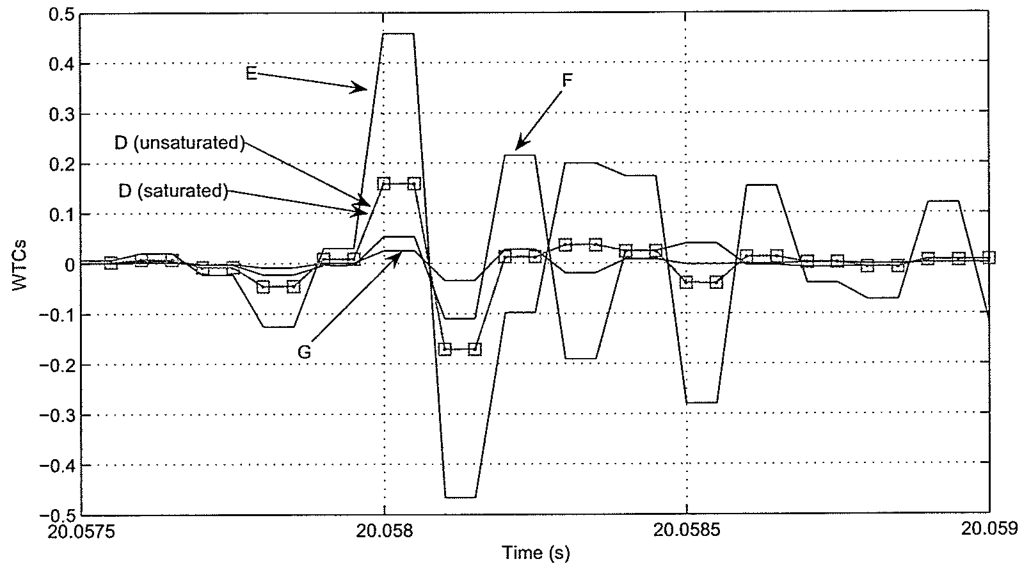

Figure 6.23: WTCs observed by R2 for fault F_{int}

sudden change in the current measurement. The the effect of CT saturation become visible only after a certain time (approximately in $\frac{1}{4}$ cycle). Thus the CT saturation effects do not affect the portion of waveform, when the proposed relay agents make the decision on fault direction.

However, when relay agents make the decision based on the steady state overcorrect measurements, for example during communication failures, CT saturation obviously affects the performance of the proposed protection scheme.

6.6 Effects of Fault Inception Angle

The fault currents can contain varying amounts of exponentially decaying DC offset, depending on the system X/R ratio and the fault inception angle. Since the proposed faulty segment location algorithm is purely based on transient currents, the fault inception angle can affects the operation of the relay. This section investigates the effects of fault inception angle on the performance of the faulty segment location algorithm.

Relay agent R2 was used for this study. Single phase A-G internal and external faults with respective to relay R2 were simulated at different inception angles as shown in Fig. 6.24. Figures 6.25 and 6.26 show two internal faults simulated with a DC offset and without

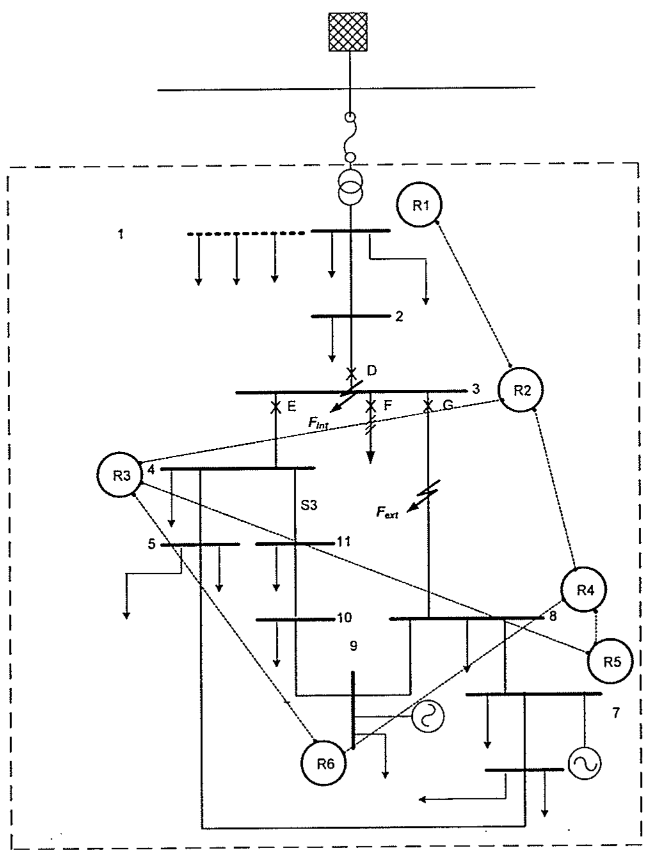

Figure 6.24: Internal and external fault simulated with respect to Relay Agent R2

a DC offset. The WTCs observed by the relay agent R2 are also shown for both cases in Figs. 6.25 and 6.26. For both cases irrespective of the DC offset, the relay agent has observed same signs in WTCs, which lead to the categorization of both faults as internal with respective to R2.

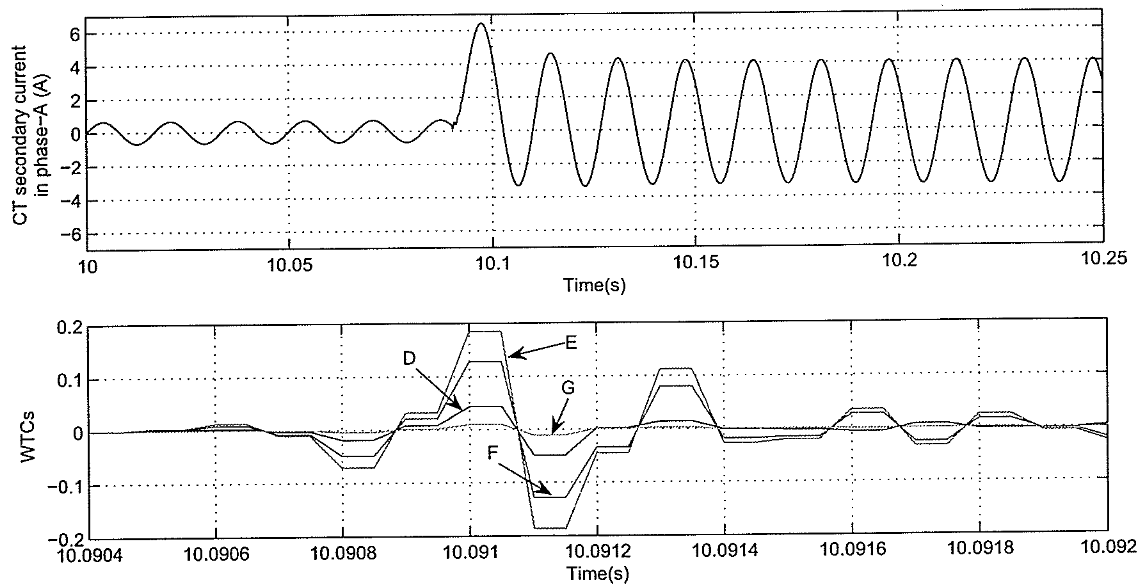

Figure 6.25: Phase-A current measurement with a DC offset and WTCs observed by R2 for fault F_{int}

Similarly the external fault F_{ext} on segment G shown in Fig. 6.24 was simulated with a DC offset and without (or negligible) a DC offset. The current signals in phase-A and corresponding WTCs observed by relay agents R2 during the faults are shown in Figs.6.27 and 6.28. In both cases, WTC observed in segment G showed opposite sign to those of the others as shown in Figs.6.27 and 6.28. Thus after feeding these WTCs into the fault locating algorithm, R2 determined the fault category as external and direction as G.

These simulation results show that the proposed faulty segment location algorithm can determine the fault categories and directions irrespective of the DC offsets in the measured currents. This is due to the fact that the proposed fault categorization and direction identification technique uses the detail-1 WTC, which is the highest frequency component

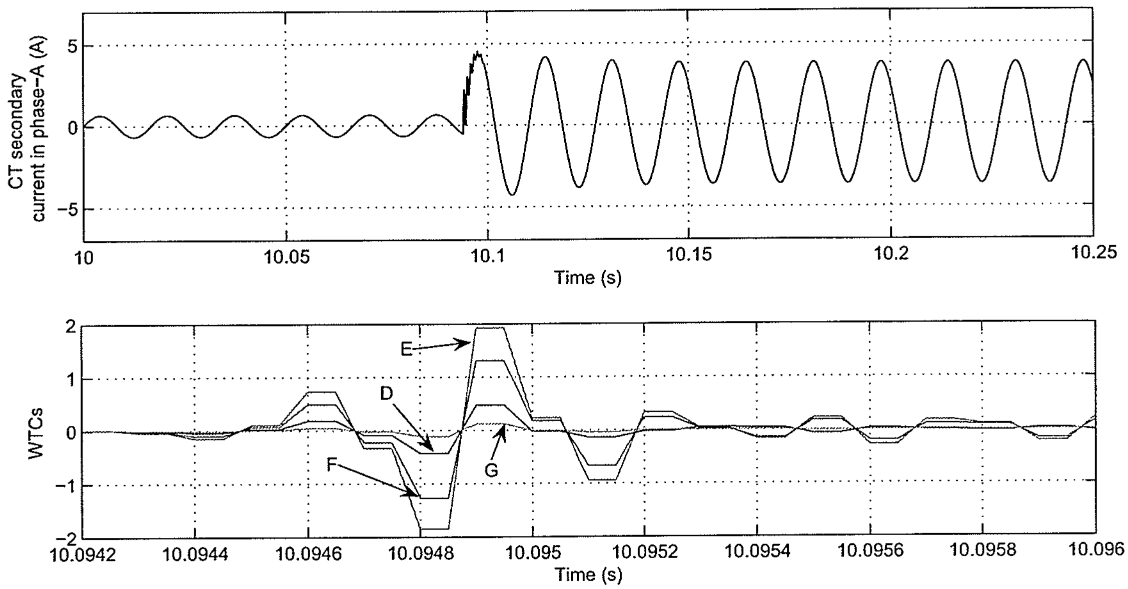

Figure 6.26: Phase-A current measurement without a DC offset and WTCs observed by R2 for fault F_{int}

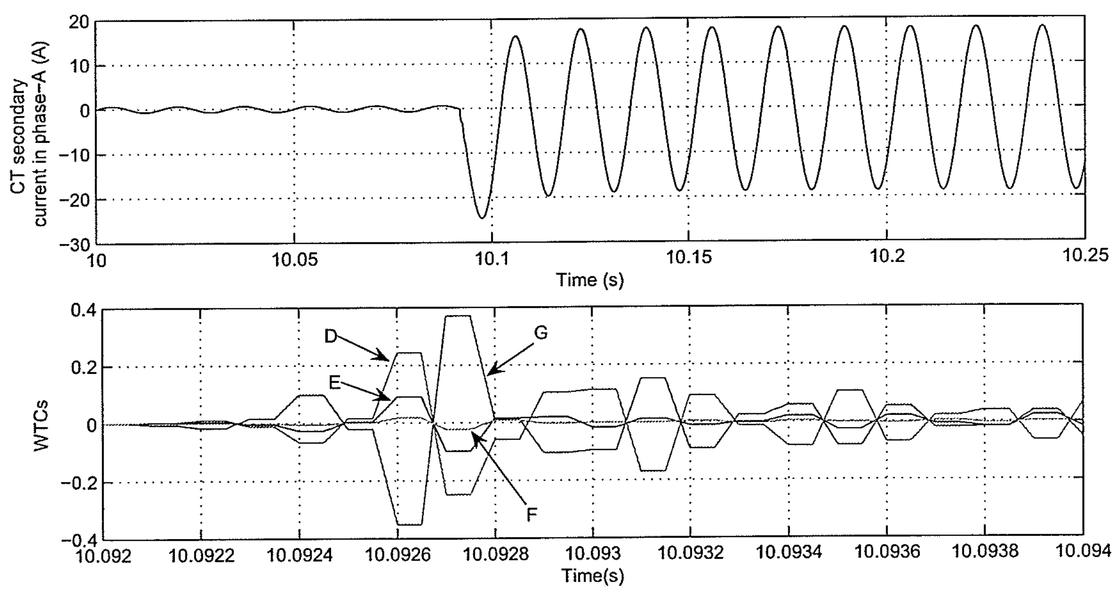

Figure 6.27: Phase-A current measurement with a DC offset and WTCs observed by R2 for fault F_{ext}

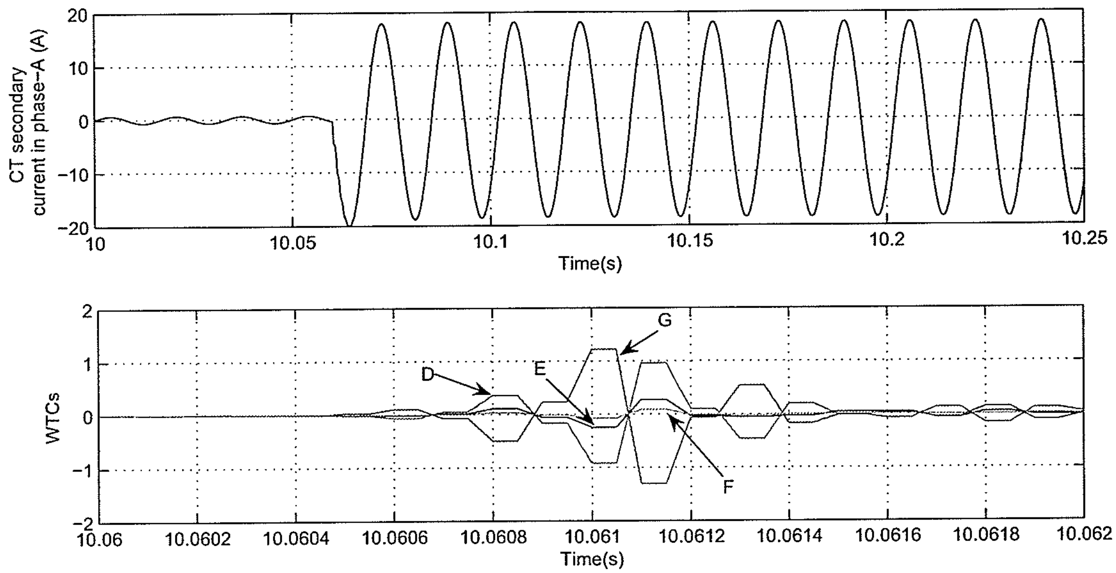

Figure 6.28: Phase-A current measurement without a DC offset and WTCs observed by R2 for fault F_{ext}

available in the current measurement. Thus the DC offset which is available at the power frequency does not affect the proposed faulty segment identification procedure.

6.7 Chapter Summary

This chapter investigated the operation of the proposed agent based faulty segment location and isolation scheme through extensive simulations. Simulation of two benchmark networks revealed that the proposed transient based isolation scheme works successfully at a signal sampling frequency as low as 10 kHz. Simulations indicated that in meshed networks, relay agents may fail to determine the fault directions when there are two parallel paths for the fault current. However it was shown that the majority of such situations can be rectified if a higher sampling frequency is used. Simulation also showed that the fault direction technique is not affected by CT saturation and fault inception angle.

Chapter 7

Conclusions and Recommendations

7.1 Conclusions

1. A component to perform online discrete wavelet transform in PSCAD/EMTDC environment was developed as the first step of this thesis. This component is capable of performing transformation for different types of mother wavelets at user specified sampling frequency.

2. A new fault direction identification technique using wavelet coefficients of the current signals was proposed. This technique is very fast: it can identify the fault direction within half cycle.

3. A protection scheme involving a set of cooperative relay agents was proposed for rapid isolation of faulty segments in a grid with distributed generators. The fault directions identified during a fault were exchanged between the relay agents to locate and isolate the faulty segment.

4. The performance of the relay agent algorithm was investigated through time domain simulations. Simulations were carried out using the proposed CIGRE, MV bench mark system showed that the proposed protection scheme is capable of locating the faulty segment accurately, for both radial and meshed network configurations.

5. Simulations were carried out using IEEE, HV bench mark system to investigate the applicability of the proposed protection scheme in transmission levels. Simulation results showed accurate faulty segment identification for most the simulated faults. Further, simulation results showed that the proposed agent based protection scheme can handle the network configurations with parallel lines.

6. During a failure in communication, relay agents can make the decisions based on the available information interchanged and the rms current measurements. Simulation results showed successful faulty segment identification and isolation capability during communication failures.

7. A decision tree-based method was proposed to detect faults using the wavelet coefficients of the current signals, derived from the one-cycle window. Successful results were obtained for the disturbances simulated in PSCAD/EMTDC.

8. In order to investigate the effects of CT saturation on proposed faulty segment location technique,simulations were carried out using saturated current measurements. The simulation results showed that CT saturation has no effect on fault category and direction identification.

9. Effect of the fault inception angle on faulty segment location was investigated through simulations. Faulty segment location algorithm gave correct faulty segment identification results irrespective of the DC current offset.

10. The use of current measurements only for fault identification, location and isolation avoids the installation of expensive voltage transformers. Hence the proposed techniques are economical in terms of implementation point of view.

7.2 Suggestions for Further Research

Further work is recommended as an extension of this thesis in the following areas:

1. The dependability of the proposed faulty segment location scheme is directly affected by the fault classification algorithm used to differentiate faults from other non-fault transits. In this thesis, investigations were carried out using transients simulated in PSCAD/EMTDC. As this is an important step in the algorithm, further research is necessary to develop 100 percent reliable transient classifier. Further it is essential to investigate the performance of such a transient classifier using real waveforms recorded by fault recorders.

2. Real-time implementation of the relay algorithm using appropriate hardware is suggested. This enables to perform further investigations on issues related to computational times and communication delays which are essential for successful implementation.

3. The performance of the proposed faulty segment location method is also dependent on the communication method used. Therefore further research should be carried out to investigate performances of the proposed method using realistic models for communication links.

Appendix A

Wavelet Transform

A.1 Computation of Wavelet Coefficients Using Mallat Algorithm

Consider the following matrix transformationA.1, which calculates level-1 approximate coefficients of a sampled signal. The transformation matrix consists of the low pass filter coefficients, h_0, h_1, h_2, h_3,....,h_n, arranged along the diagonal. The number of filter coefficients n depends on the selected type of the mother wavelet (see Tables 2-5 below). The signal vector $S = [s_1, s_2, s_3, ..., s_n]^T$ contains the m samples of the input signal. The multiplication of the signal vector by the transformation matrix gives the level one approximate coefficients vector $A1=[al_1, al_2, al_2, ..., al_l]^T$.

$$\begin{pmatrix} h_0 & h_1 & . & . & . & h_{n-1} & 0 & 0 & 0 & 0 \\ 0 & 0 & h_0 & h_1 & . & . & . & h_{n-1} & 0 & 0 \\ 0 & 0 & 0 & 0 & h_0 & h_1 & . & . & . & h_{n-1} \\ 0 & 0 & 0 & 0 & 0 & 0 & h_0 & h_1 & . & . \\ 0 & 0 & 0 & 0 & 0 & 0 & 0 & 0 & h_0 & h_1 \\ 0 & 0 & 0 & 0 & 0 & 0 & 0 & 0 & 0 & 0 \\ . & . & . & . & . & . & . & . & . & . \\ . & . & . & . & . & . & . & . & . & . \end{pmatrix} \begin{pmatrix} s_1 \\ s_2 \\ s_3 \\ . \\ . \\ . \\ . \\ s_m \end{pmatrix} = \begin{pmatrix} al_1 \\ al_2 \\ al_3 \\ . \\ . \\ . \\ . \\ al_l \end{pmatrix} \quad \text{(A.1)}$$

Similarly the corresponding level one detail wavelet coefficients vector $D1=[d1_1,d1_2,d1_2,...,d1_l]^T$ can be obtained as shown in A.2, where g_0, g_1, g_2, g_3,...,g_n in the transformation matrix represents the coefficients of the dual high pass filter corresponding to the low pass filter in A1.

$$\begin{pmatrix} g_0 & g_1 & . & . & . & g_{n-1} & 0 & 0 & 0 & 0 \\ 0 & 0 & g_0 & g_1 & . & . & . & g_{n-1} & 0 & 0 \\ 0 & 0 & 0 & 0 & g_0 & g_1 & . & . & . & g_{n-1} \\ 0 & 0 & 0 & 0 & 0 & 0 & g_0 & g_1 & . & . \\ 0 & 0 & 0 & 0 & 0 & 0 & 0 & 0 & g_0 & g_1 \\ 0 & 0 & 0 & 0 & 0 & 0 & 0 & 0 & 0 & 0 \\ . & . & . & . & . & . & . & . & . & . \\ . & . & . & . & . & . & . & . & . & . \end{pmatrix} \begin{pmatrix} s_1 \\ s_2 \\ s_3 \\ . \\ . \\ . \\ . \\ s_m \end{pmatrix} = \begin{pmatrix} d1_1 \\ d1_2 \\ d1_3 \\ . \\ . \\ . \\ . \\ d1_l \end{pmatrix} \quad \text{(A.2)}$$

The approximate and detail wavelet coefficients corresponding to level two, $A2=[a2_1, a2_2, a2_2,..., a2_l]^T$ and $D2=[d2_1,d2_2,d2_2,.., d2_l]^T$ respectively, can be determined by reapplying the transformations in A.1 and A.2 on the approximation coefficient vector A1. Equations A.3 and A.4 show this computation.

$$\begin{pmatrix} h_0 & h_1 & . & . & . & h_{n-1} & 0 & 0 & 0 & 0 \\ 0 & 0 & h_0 & h_1 & . & . & . & h_{n-1} & 0 & 0 \\ 0 & 0 & 0 & 0 & h_0 & h_1 & . & . & . & h_{n-1} \\ 0 & 0 & 0 & 0 & 0 & 0 & h_0 & h_1 & . & . \\ 0 & 0 & 0 & 0 & 0 & 0 & 0 & 0 & h_0 & h_1 \\ 0 & 0 & 0 & 0 & 0 & 0 & 0 & 0 & 0 & 0 \\ . & . & . & . & . & . & . & . & . & . \\ . & . & . & . & . & . & . & . & . & . \end{pmatrix} \begin{pmatrix} a1_1 \\ a1_2 \\ a1_3 \\ . \\ . \\ . \\ . \\ a1_m \end{pmatrix} = \begin{pmatrix} a2_1 \\ a2_2 \\ a2_3 \\ . \\ . \\ . \\ . \\ a2_l \end{pmatrix} \quad \text{(A.3)}$$

$$\begin{pmatrix} g_0 & g_1 & . & . & . & g_{n-1} & 0 & 0 & 0 & 0 \\ 0 & 0 & g_0 & g_1 & . & . & . & g_{n-1} & 0 & 0 \\ 0 & 0 & 0 & 0 & g_0 & g_1 & . & . & . & g_{n-1} \\ 0 & 0 & 0 & 0 & 0 & 0 & g_0 & g_1 & . & . \\ 0 & 0 & 0 & 0 & 0 & 0 & 0 & 0 & g_0 & g_1 \\ 0 & 0 & 0 & 0 & 0 & 0 & 0 & 0 & 0 & 0 \\ . & . & . & . & . & . & . & . & . & . \\ . & . & . & . & . & . & . & . & . & . \end{pmatrix} \begin{pmatrix} al_1 \\ al_2 \\ al_3 \\ . \\ . \\ . \\ . \\ al_m \end{pmatrix} = \begin{pmatrix} d2_1 \\ d2_2 \\ d2_3 \\ . \\ . \\ . \\ . \\ d2_l \end{pmatrix} \tag{A.4}$$

This calculation can be repeated to determine the approximate and detail wavelet coefficients up to the required level.

A.2 Computation of Reconstruction Wavelet Coefficients

According to A.1 and A.2, the computation of wavelet coefficients results in down sampling of input signal by a factor 2 at each level of calculation. Thus the calculated wavelet coefficients can not be used efficiently in time domain analysis. However, a time domain signal with the same sampling rate as the original signal can be reconstructed from a given wavelet coefficients vector. The resulting signal is known as reconstruction wavelet coefficients.

For example, to determine the reconstruction coefficients corresponding to level one approximate, the coefficient vector A1 is up-sampled (by adding zeros after each element) and multiplied by the inverse wavelet transformation matrix as shown in A.5. The inverse transformation matrix can be built using the low pass and high pass filter coefficients used in A.1 and A.2. The result of this transformation $A1r = [a1r_1, a1r_2, ...]^T$ contains the reconstruction wavelet coefficients.

$$\begin{pmatrix} h_0 & g_0 & . & . & . & h_{n-2} & g_{n-2} & 0 & 0 & 0 \\ h_1 & g_1 & . & . & . & g_{n-1} & h_{n-1} & 0 & 0 & 0 \\ 0 & 0 & h_0 & g_0 & . & . & . & h_{n-2} & g_{n-2} & 0 \\ 0 & 0 & h_1 & g_1 & . & . & . & g_{n-1} & h_{n-1} & 0 \\ 0 & 0 & 0 & 0 & h_0 & g_0 & . & . & . & h_{n-2} \\ 0 & 0 & 0 & 0 & h_1 & g_1 & . & . & . & g_{n-1} \\ 0 & 0 & 0 & 0 & 0 & 0 & h_0 & g_0 & . & . \\ 0 & 0 & 0 & 0 & 0 & 0 & h_1 & g_1 & . & . \\ 0 & 0 & 0 & 0 & 0 & 0 & 0 & 0 & h_0 & g_0 \\ . & . & . & . & . & . & . & . & . & . \end{pmatrix} \begin{pmatrix} a1_1 \\ 0 \\ a1_2 \\ 0 \\ a1_3 \\ 0 \\ . \\ . \\ . \\ . \\ a1_l \\ 0 \end{pmatrix} = \begin{pmatrix} a1r_1 \\ a1r_2 \\ a1r_3 \\ . \\ . \\ . \\ . \\ . \\ a1r_{m-1} \\ a1r_m \end{pmatrix} \tag{A.5}$$

When calculating the reconstruction wavelet coefficients for the details, for instance for level 1, the detail coefficient vector D1 is up sampled by adding a zero before each element. This is shown in A.6.

$$\begin{pmatrix} h_0 & g_0 & . & . & . & h_{n-2} & g_{n-2} & 0 & 0 & . \\ h_1 & g_1 & . & . & . & g_{n-1} & h_{n-1} & 0 & 0 & . \\ 0 & 0 & h_0 & g_0 & . & . & . & h_{n-2} & g_{n-2} & . \\ 0 & 0 & h_1 & g_1 & . & . & . & g_{n-1} & h_{n-1} & . \\ 0 & 0 & 0 & 0 & h_0 & g_0 & . & . & . & . \\ 0 & 0 & 0 & 0 & h_1 & g_1 & . & . & . & . \\ 0 & 0 & 0 & 0 & 0 & 0 & h_0 & g_0 & . & . \\ 0 & 0 & 0 & 0 & 0 & 0 & h_1 & g_1 & . & . \\ 0 & 0 & 0 & 0 & 0 & 0 & 0 & 0 & h_0 & . \\ . & . & . & . & . & . & . & . & . & . \end{pmatrix} \begin{pmatrix} 0 \\ a1_1 \\ 0 \\ a1_2 \\ 0 \\ a1_3 \\ 0 \\ . \\ . \\ . \\ . \\ a1_l \end{pmatrix} = \begin{pmatrix} d1r_1 \\ d1r_2 \\ d1r_3 \\ . \\ . \\ . \\ . \\ . \\ d1r_{m-1} \\ d1r_m \end{pmatrix} \tag{A.6}$$

For higher levels, up sampling and inverse transformations have to be applied several times.

A.3 Wavelet Filter Coefficients

Table A.1-A.3 give low pass filter coefficients for different the types of mother wavelets. The corresponding high pass filter coefficients can be simply derived using A.7.

$$g_k = (-1)^k h_{n-1-k} \tag{A.7}$$

where, k = 0 .... (n-1)

Table A.1: Haar filter coefficients[45]

n	h_n
0	0.70710678118655
1	0.70710678118655

Table A.2: DB filter coefficients[45]

db	n	h_n
1	0	0.70710678118655
	1	0.70710678118655
2	0	0.48296291314453
	1	0.83651630373781
	2	0.22414386804201
	3	-0.12940952255126
3	0	0.23037781330890
	1	0.71484657055292
	2	0.63088076792986
	3	-0.02798376941686
	4	-0.18703481171909
	5	0.03084138183556
	6	0.03288301166689
	7	-0.01059740178507
4	0	0.05441584224310
	1	0.31287159091430
	2	0.67563073629729
	3	0.58535468365421
	4	-0.01582910525635
	5	-0.28401554296155
	6	0.00047248457391
	7	0.12874742662048
	8	-0.01736930100181
	9	-0.04408825393079
	10	0.01398102791740
	11	0.00874609404741
	12	-0.00487035299345
	13	-0.00039174037338
	14	0.00067544940645
	15	-0.00011747678412

Table A.3: *sym* filter coefficients[45]

sym	n	h_n
1	0	0.70710678118655
	1	0.70710678118655
2	0	0.48296291314453
	1	0.83651630373781
	2	0.22414386804201
	3	-0.12940952255126
3	0	0.03222310060405
	1	-0.01260396726203
	2	-0.09921954357663
	3	0.29785779560530
	4	0.80373875180513
	5	0.49761866763278
	6	-0.02963552764600
	7	-0.07576571478950
4	0	0.00188995033277
	1	-0.00030292051472
	2	-0.01495225833706
	3	0.00380875201389
	4	0.04913717967373
	5	-0.02721902991710
	6	-0.05194583810788
	7	0.36444189483618
	8	0.77718575169963
	9	0.48135965125905
	10	-0.06127335906781
	11	-0.14329423835127
	12	0.00760748732498
	13	0.03169508781153
	14	-0.00054213233180
	15	-0.00338241595100

Table A.4: coif filter coefficients[45]

coif	n	h_n
1	0	-0.07273261951285
	1	0.33789766245781
	2	0.85257202021226
	3	0.38486484686420
	4	-0.07273261951285
	5	-0.01565572813546
2	0	0.01638733646360
	1	-0.04146493678197
	2	-0.06737255472230
	3	0.38611006682309
	4	0.81272363544961
	5	0.41700518442378
	6	-0.0764885990786 9
	7	-0.05943441864675
	8	0.02368017194645
	9	0.00561143481942
	10	-0.00182320887071
	11	-0.00072054944537

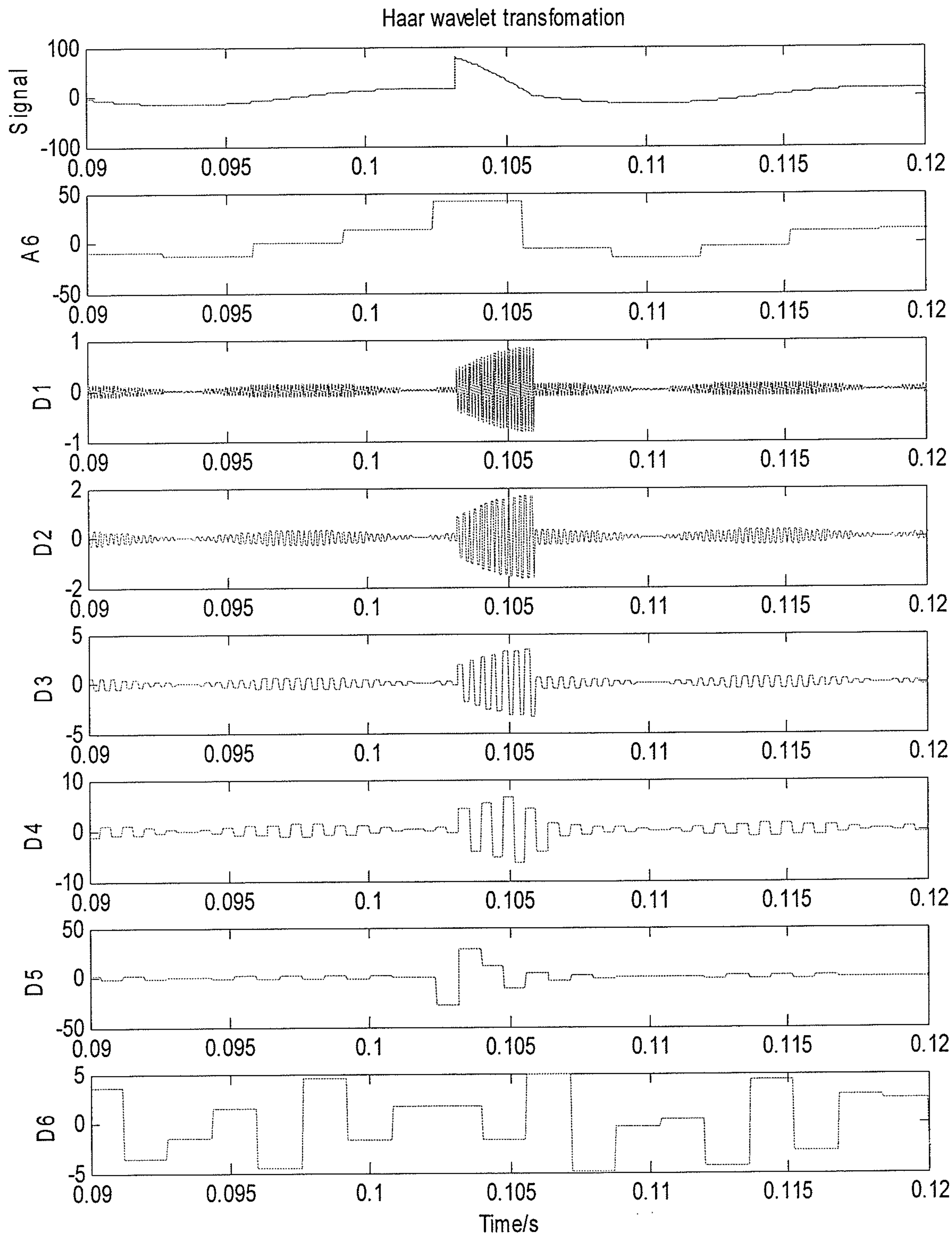

Figure A.1: Transient signal and its "haar" wavelet coefficients at level 6 using PSCAD and MATLAB

Difference between curves can't be observed as they are on top of each other.

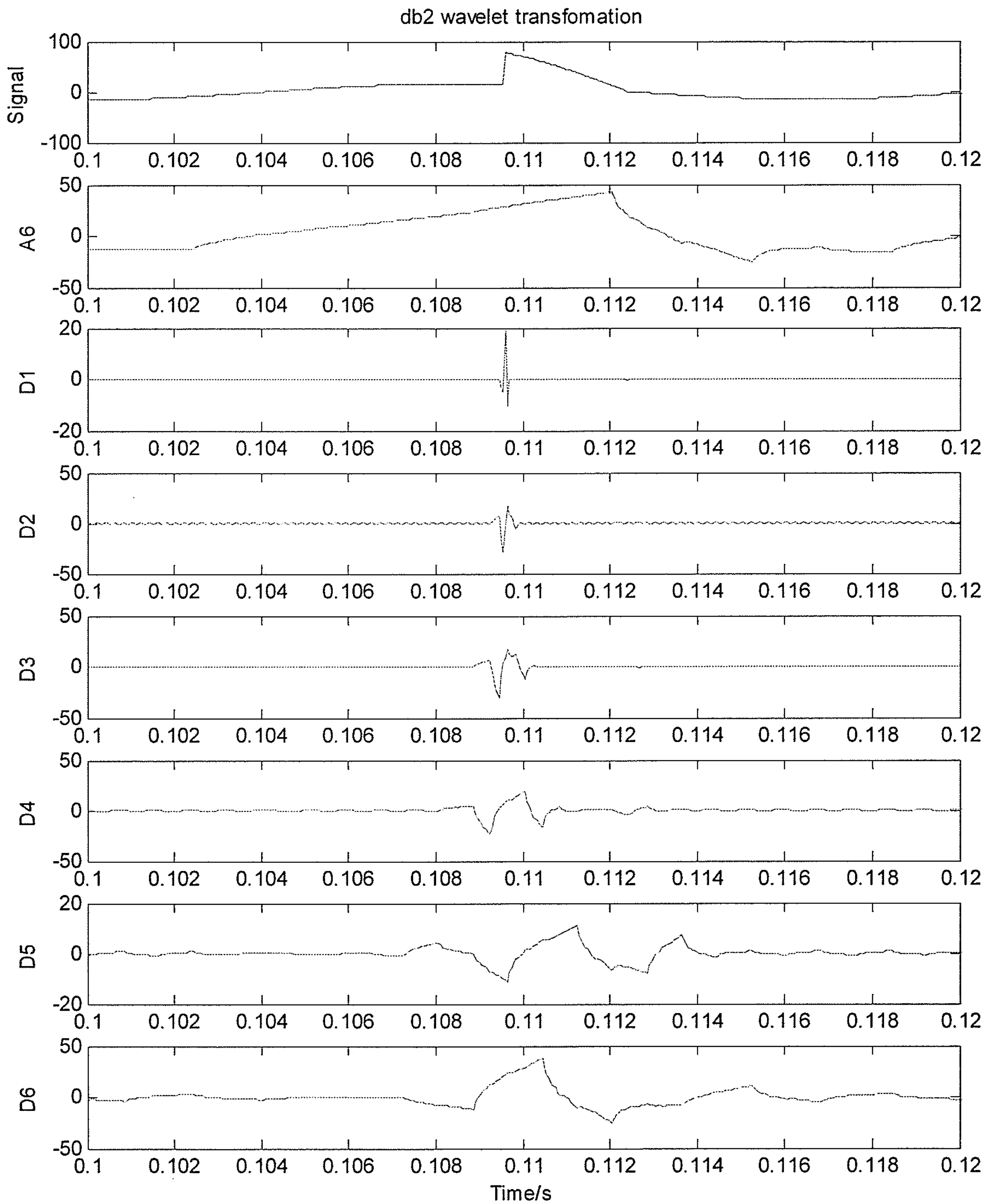

Figure A.2: Transient signal and its "db2" wavelet coefficients at level 6 using PSCAD and MATLAB

Difference between curves can't be observed as they are on top of each other.

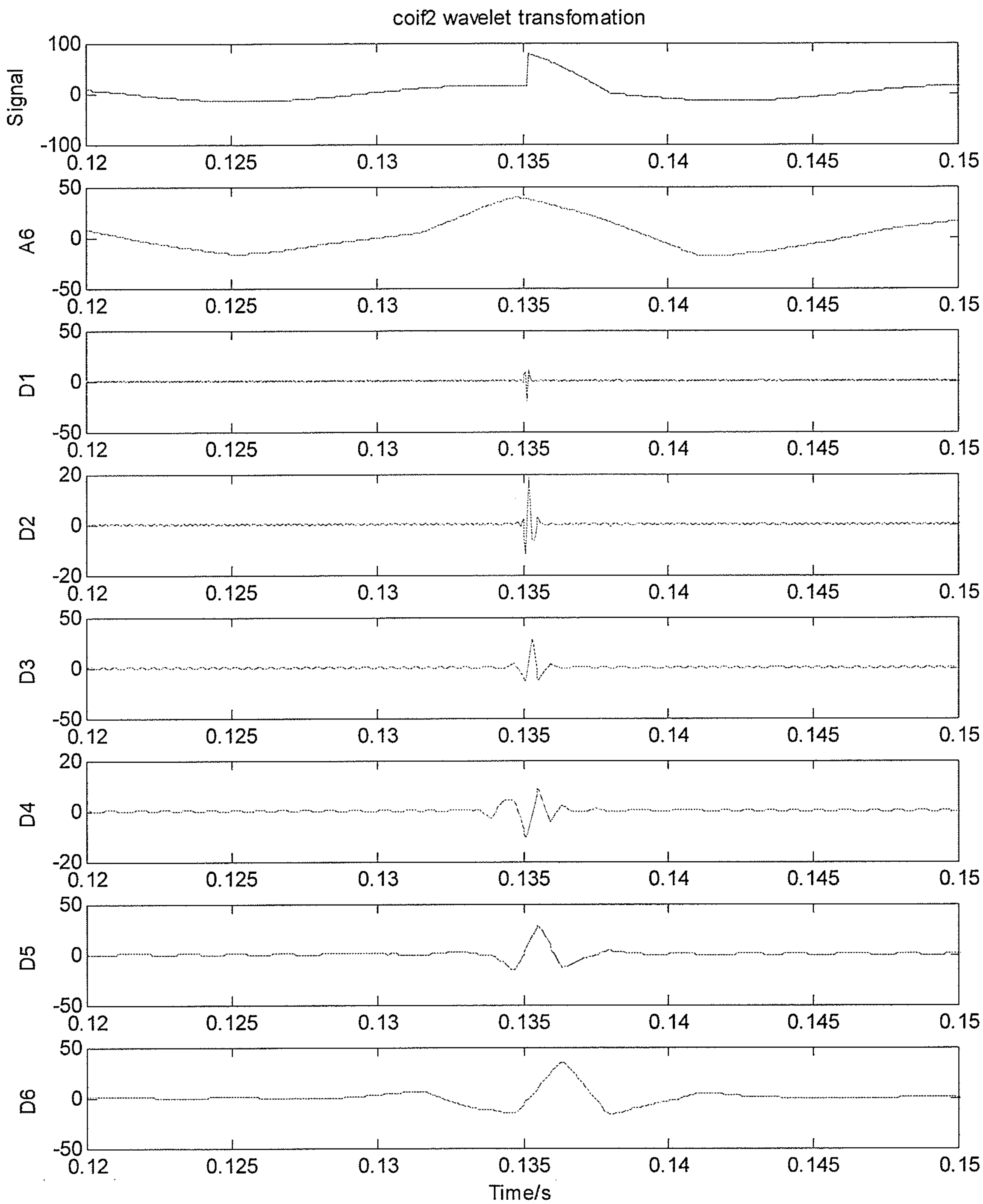

Figure A.3: Transient signal and its "coif2" wavelet coefficients at level 6 using PSCAD and MATLAB

Difference between curves can't be observed as they are on top of each other.

Appendix B

Relay Algorithm Implementation

B.1 Fault Categorization and Direction Identification Algorithm

Figure B.1 shows the implementation of fault categorization and fault direction identification algorithm in MATLAB. Variables i, j, k, l, m, p and z denotes various indices and n denotes the number of segments connected to the relay agent. *r(d)* represents the cross correlation of coefficients for a lag of d sampling intervals.

B.2 Fault Location Algorithm

Figure B.2 shows the algorithm developed in MATLAB for relay agents to locate the fault and determine the trip signals to isolate the faulty segments. Index i denotes segments number (i to n), info1(i) denotes the information sent in the direction of i^{th} segment and info2(i) denotes the information received in the direction of i^{th} segment. The values "1" and "0" are used to represent the fault direction. Trip(i) denotes the trip signal for CB on the i^{th} segment. Trip signal "1" causes CB to open.

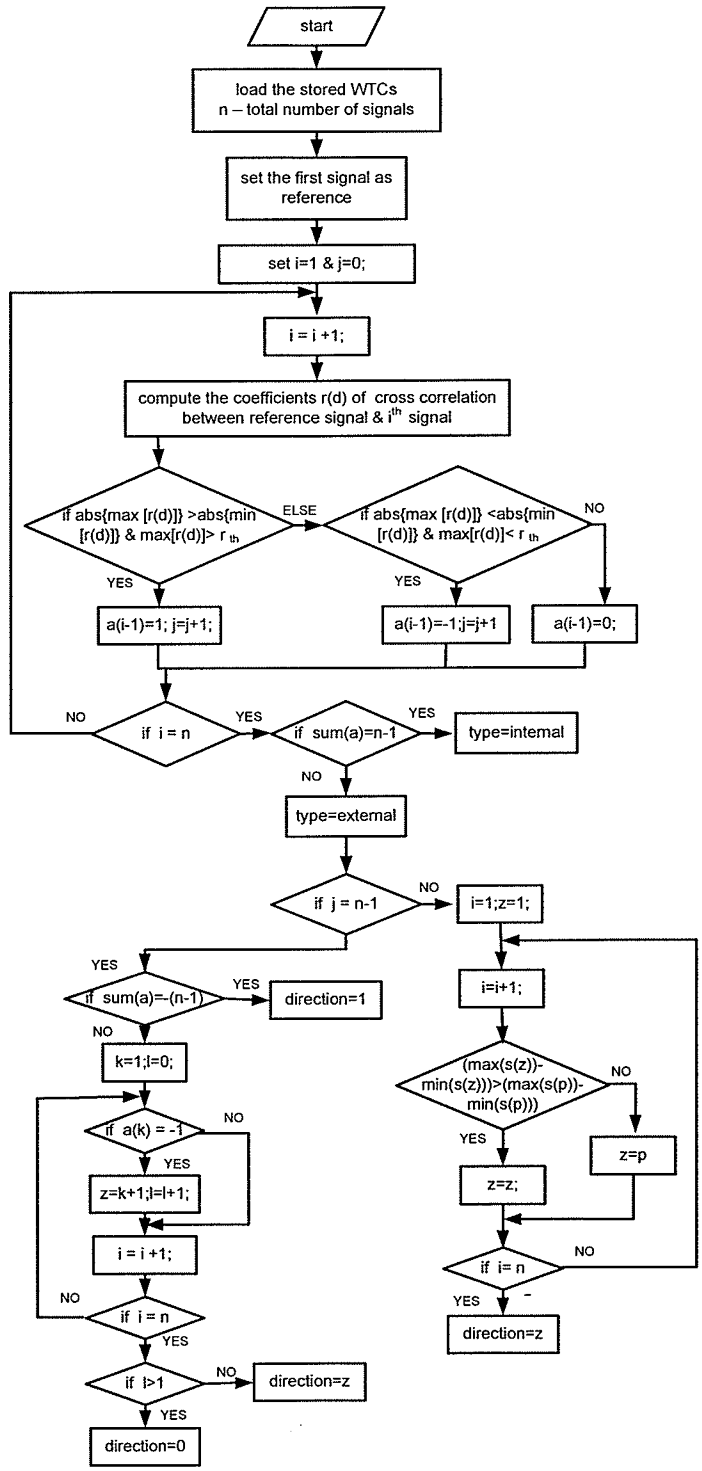

Figure B.1: Algorithm for fault direction identification

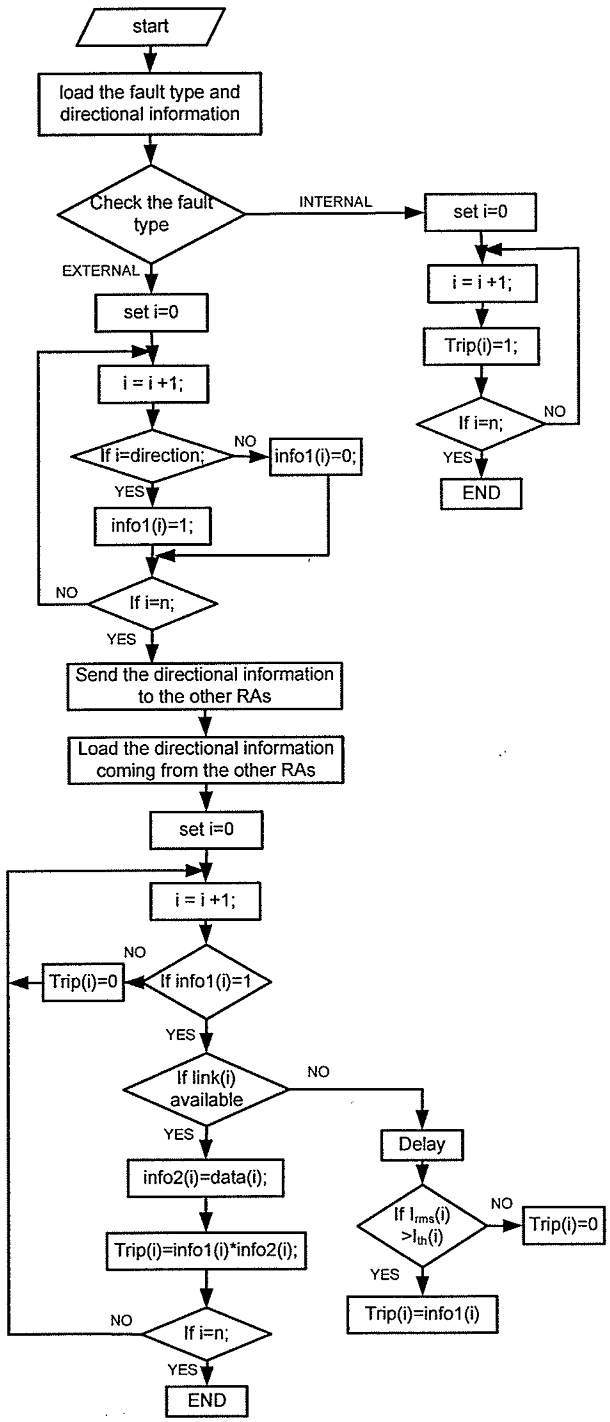

Figure B.2: Algorithm for faulty segment location

References

[1] N. Jenkins, R. Allan, P. Crossley, D. Kirschen and G. Strbac, "Embedded Generation", *IEE Power and Energy Series 13,* 2000.

[2] P. Barker and R.W. de Mello,"Determining the Impact of Distributed Generation on Power Systems: Part 1- Radial Power Systems", *Proc.IEEE Power Eng. Soc. Summer Meeting,* pp.1645-1658, July 2000.

[3] A.M. Borbely, J.F. Kreider,"Distributed Generation: The Power Paradigm for the New Millennium" *LLC: CRC Press*, 2000.

[4] R.C. Dugan and T.E. McDermott,"Distributed Generation", *IEEE Industry Application Magazine*, vol.8, issue: 2, pp.19-25, 2002.

[5] IEEE Std. 1547-2003, "IEEE Standard for Interconnecting Distributed Resources with Electric Power Systems", 2003.

[6] MicroPower Connect, "Interconnection Guidelines for Inverter Based Micro-distributed Resources (DR) systems connected to 600 V or less distribution systems - Version 8", July 2003.

[7] Baran M.E and l-Markabi I, "Adaptive over current protection for distribution feeders with distributed generators; IEEE PES 2004, vol.2, pp.715 - 719, Oct. 2004

[8] S.M. Brahma and A.A. Girgis,"Microprocessor-based Reclosing to Coordinate Fuse and Recloser in a System with High Penetration of Distributed Generation ", *IEEE Power Eng. Soc. Winter Meeting,* vol.1, pp.453 - 458, Jan. 2002.

[9] S.M. Brahma and A.A. Girgis, "Development of Adaptive Protection Scheme for Distribution System with High Penetration of Distribution Generation", *IEEE Trans. Power Del.*, vol. 19, no. 1, pp. 56-63, Jan. 2004.

[10] Z. Xiangjun, K.K. Li, W.L. Chan and S. Sheng, "Multi-agents Based Protection for Distributed Generation Systems", Electric Utility Deregulation, Restructuring and Power Technologies. *Proc. IEEE International Conference,* vol.1, pp.393-397, Apr. 2004.

[11] T. Ackermann and V. Knyazkin. "Interaction between distributed gen- eration and the distribution network operation aspects". IEEE PES Transmission and Distribution Conference and Exhibition Asia 2002, volume 2, pp 1357-1362, 2002.

[12] J.A.P. Lopes. "Integration of dispersed generation on distribution networks impact studies". In IEEE Power Engineering Society Winter Meeting, volume 1, pages 323328, 2002.

[13] C.J. Mozina. "Interconnection protection of IPP generators at commercial/industrial facilities", IEEE Transactions on Industry Applications, pp 681-688, 2001.

[14] W. El-Khattam,Y. Hegazy,M.M.A Salama,"Stochastic estimation of the contribution levels of customer operated distributed generation." Power Engineering Society General Meeting, 2004. IEEE Volume , Issue , 6-10 June 2004 Page(s) 2182 - 2186.

[15] Distributed Power Coalition of America (DPCA) (1998).

[16] Jan F. Kreider and P.E. Peter S. Curtiss,Distributed Electrical Generation Technologies and Methods for Their Economic Assessment.

[17] Smart Grids, European Technology Platform, European Commission, 2006.

[18] Y. Tomita, C. Fukui, H. Kudo, J. Koda and K. Yabe, "A Cooperative Protection System with an Agent Model" *IEEE Trans. Power Del.* vol.13, issue: 4, pp.1060-1066, Oct. 1998.

[19] S.W. Smith "Engineer's Guide to Digital Signal Processing ", California Technical Publishing,1997-2006.

[20] R. Moxley,K. Fodero, "High-speed distribution protection made easy: communications-assisted protection schemes for distribution applications", 58th Annual Conference for Protective Relay Engineers, pp.18- 26, April 2005.

[21] I. Daubechies, "Ten Lectures on Wavelets", *SIAM,Phladelphia*, 1992.

[22] D.C. Robertson, O. I. Camps, J.S. Mayer, and W.B. Gish, "Wavelets and Electromagnetic Power System Transients", *IEEE Transactions on Power Delivery*, Vol. 11, No. 2, April 1996.

[23] C.Y. Evrenosoglu and A. Abur, "Traveling Wave Based Fault Location for Teed Circuits", *IEEE Trans. Power Del.*, vol.20, pp. 1115- 1121, Apr. 2005.

[24] E. Clarke, "Circuit Analysis of AC Power Systems, Symmetrical and Related components", *New York, Wley*, 1943.

[25] L. M. Wedepohl, "Application of Matrix Methods to the Solution of Travelling wave Phenomena in Polyphase System", Proceedings IEE, vol 110, pp. 2200-2212. December, 1963.

[26] A. A. Hajar, M. M. Mansour and H. A. Talaat, "Travelling wave-based protection of six-phase transmission lines", The 4th Conference of Arab CIGRE National Committees, March 18-21, 2001, Tripoli Libya.

[27] H.Y. Li, P.A. Crossley and N. Jenkins,"Transient Directional Protection for Distribution Feeders with Embedded Generations", *PSSC, Sevilla*, 24-28, June 2002.

[28] M.H. Hassoun. "Fundamentals of Artificial Neural Networks", MIT Press, Cambridge (1995).

[29] P.F. Fantoni, A. Mazzola, "Multiple-failure signal validation in nuclear power plants using artificial neural networks", Nucl. Technol., March 1996.

[30] C. S. Myers and L. R. Rabiner. "A comparative study of several dynamic time-warping algorithms for connected word recognition", The Bell System Technical Journal, 60(7):1389-1409, September 1981.

[31] L. Breiman, Jerome H. Friedman, Richard A. Olshen and Charles J. Stone, "Classification and Regression Trees".

[32] O.D Richard ,Peter E. Hart and David G. Stork. "Pattern Classification".

[33] S.M. Halpin, R.F Burch,"Applicability of neural networks to industrial and commercial power systems: a tutorial overview", IEEE Transactions on Industry Applications, pp.1355-1361, Vol.33, Issue: 5, Sep/Oct 1997.

[34] A.M. Youssef,T.K. Abdel-Galil, E.F. El-Saadany,M.M.A. Salama,"Disturbance classification utilizing dynamic time warping classifier", IEEE Transactions on Power Delivery,Volume 19, Issue 1, Jan. 2004 Page(s):272 - 27.

[35] J. Ypsilantis,H. Yee, C.Y. Teo, "Adaptive, rule based fault diagnostician for power distribution networks" Generation,Transmission and Distribution, IEE Proceedings, Volume 139, Issue 6, Nov. 1992 Page(s):461 - 468.

[36] S.Rasoul Safavian and David Landgrebe, "A Survey of Decision Tree Classifier Methodology", School of Electrical Engineering, Purdue University, West Lafayette.

[37] L. Breiman, Jerome H. Friedman, R. A. Olshen and C. J. Stone, "Classification and Regression Trees".

[38] Y Sheng, S.M. Rovnyak, "Decision tree-based methodology for high impedance fault detection" , IEEE Transactions on Power Delivery Volume 19, Issue 2, April 2004 pp:533-536.

[39] S.M. Rovnyak, S.E. Kretsinger,J. S. Thorp,and D. E. Brown,"Decision trees for real time transient stability prediction", IEEE Trans on Power Systems, vol. 9, no. 3, pp: 1417-1426, Aug 1994.

[40] P. Bourke,*http://local.wasp.uwa.edu.au/ pbourke/other/correlate/*, University of Western Australia, Australia.

[41] IEEE Guide for the Application of Current Transformers Used for Protective Relaying Purposes.

[42] Benchmark Modeling and Simulation for Analysis, Design, and Validation of Distributed Energy Systems, CIGRE Task Force C6.04.02 September 2006.

[43] Shan Jiang, U. D. Annakkageand A. M. Gole, "A Platform for Validation of FACTS Models", IEEE Transactions on Power Delivery, Vol. 21, NO. 1, January 2006.

[44] Available: http://www.salford-systems.com.

[45] Pascal Getreuer,Filter Coefficients to Popular Wavelets, May 2006.